uOttawa

L'Université canadienne
Canada's university

FACULTÉ DES ÉTUDES SUPÉRIEURES ET POSTOCTORALES

uOttawa

L'Université canadienne
Canada's university

FACULTY OF GRADUATE AND POSDOCTORAL STUDIES

Jan Petrus Karel Reynhardt
AUTEUR DE LA THÈSE / AUTHOR OF THESIS

Ph.D. (Chemistry)
GRADE / DEGREE

Department of Chemistry
FACULTÉ, ÉCOLE, DÉPARTEMENT / FACULTY, SCHOOL, DEPARTMENT

Carbonylation Catalysis based on Metal Complexed PAMAM-Dendrimers Supported on Mesoporous and Periodic Mesoporous Silica supports

TITRE DE LA THÈSE / TITLE OF THESIS

Howard Alper
DIRECTEUR (DIRECTRICE) DE LA THÈSE / THESIS SUPERVISOR

CO-DIRECTEUR (CO-DIRECTRICE) DE LA THÈSE / THESIS CO-SUPERVISOR

EXAMINATEURS (EXAMINATRICES) DE LA THÈSE / THESIS EXAMINERS

Deryn Fogg

Jean Frechet

Marten Ternan

Abdel Savari

Gary W. Slater
LE DOYEN DE LA FACULTÉ DES ÉTUDES SUPÉRIEURES ET POSTDOCTORALES /
DEAN OF THE FACULTY OF GRADUATE AND POSTDOCORAL STUDIES

Carbonylation Catalysts based on Metal Complexed PAMAM-Dendrimers Supported on Mesoporous and Periodic Mesoporous Silica supports

by

Jan Petrus Karel Reynhardt

A Thesis Submitted to the Faculty of Graduate and Postdoctoral Studies
In Partial Fulfillment of the Requirements for the Degree of Doctor of Philosophy

Ottawa-Carleton Chemistry Institute
&
Centre for Catalysis Research and Innovation

Department of Chemistry
University of Ottawa
Ottawa, Ontario,
Canada

Ph.D Candidate

Jan Petrus Karel Reynhardt

Supervisor

Professor Howard Alper

THE UNIVERSITY OF OTTAWA

Your file Votre référence
ISBN: 0-494-11014-7
Our file Notre référence
ISBN: 0-494-11014-7

Vir

Kobie en Pappa,

Soli Deo Gloria

Acknowledgments

I would like to thank my supervisor Professor Howard Alper for his guidance and inspiration during the completion of this work. He has taught me that very little is impossible if you work hard and endure.

I would also like to thank the University of Ottawa for financial support.

Grateful acknowledgment is made to Professor Abdelhamid Sayari and his group for their contributions and collaboration during the last two years. I would especially like to thank Dr. Yong Yang for the preparation of the mesoporous materials, as well as for the collection of the nitrogen adsorption data and for his friendship over the last two years.

To the people of SASOL Technology R&D, a huge thank you, especially Dr. Mike Green, Dr. Anton Vosloo, Harriet Lubbe and Elize Bresser, not only for this opportunity but also for your support through difficult times. Also without the financial support of SASOL Technology R&D none of this would have been possible.

I would also like to sincerely thank the members of the Alper group, both past and present for their support and help over the years. I would especially like to thank Dr. Jong-Tae Lee, Christine Bourque, Pumza Zweni, Dr. Chune Dong and Ratana Chanthateyanonth for their friendship and motivation.

A special word of thanks to the professors and lecturers of the Chemistry Department, especially Professors Deryn Fogg, Sandro Gambarotta, Tony Durst, Prabhat Arya, Dr. Pam Arnold and Professor Martin Ternan of the Chemical Engineering Department.

I would like to thank the staff at the Chemistry Department, especially Lise Maisonnueve, Annette Campeau and Linda Baron for their help and service. I would also like to thank Don Hopkins, Andrew Zlotorzynski and Lee Sorensen, who always helped out with a smile and a joke.

I am grateful to Dr. Glenn Facey and Cheryl McDowell for the recording of the solid-state NMR spectra, and to Tamer El Bokl for teaching me about TGA and Egypt.

I would especially like to thank Dr. Thys Botha and his wife, Beverly Botha for their unwavering friendship and support.

I would also like to thank Inayath Mohamed for his friendship and support.

Finally, I would like to thank my family, especially my wife Giovanna, for her love and support, baby Isabelle, my mother Bets, Giovanna's mother Elsie Caricato, and the rest of the Caricatos: Enrico, Welma, Enrico and Ditto. This would not have been possible without your help, support and friendship and most importantly your love. I would also like to thank my father Jan Reynhardt, who recently passed away, for sowing the seed of science in me and for always loving and supporting all of us. He was a great man and will be terribly missed.

S.D.G.

Abstract

This thesis describes the synthesis and characterization of various polyamidoamine (PAMAM) dendrimer moieties supported on amorphous mesoporous and periodic mesoporous silica supports. The surface characteristics of the supports are investigated using various methods and found to be intricately involved in the success of the dendrimer synthesis. The dendrimers are phophinomethylated and complexed with either palladium or rhodium and used as catalysts for carbonylation reactions.

The palladium complexed C_6-PAMAM dendrimers supported on aminopropyl silica gel are recyclable catalysts for the hydroesterification of olefins and turnover numbers (TON) of up to 1200 are possible.

C_2-PAMAM dendrimers supported on LPMCM-41 and Davisil are complexed with rhodium and used as catalysts for the hydroformylation reaction of olefins. These catalysts show how the pore geometry influences the activity and recyclability of the catalysts. The dendrimer-rhodium complexes supported on LPMCM-41 exhibit very high activity and a TOF of up to 1800 h^{-1} are observed for the hydroformylaton of 1-octene. These catalysts can be recycled effectively by simple filtration. A negative dendrimer effect is observed with the higher generations exhibiting lower activity than the lower generations. The dendrimer-

rhodium complexes supported on Davisil also exhibit very high activity and a TOF of up to 1700 h^{-1} are observed for the hydroformylation of 1-octene. The activity of these catalysts are less dependent on the generation than the LPMCM-41 dendrimers, and excellent activity is observed up to the third generation for the hydroformylation reaction of 1-octene.

Abbreviations

%	Percent
Δ	heat
°C	Degree Celsius
a	unit cell dimension
Ac	Acetyl
APTES	3-Aminopropyltriethoxysilane
ATR	Attenuated total reflectance system
b	Pore wall thickness
B:L	Branched to linear ratio
S_{BET}	Brunauer, Emmet & Teller Surface area
CFMR	Continues flow membrane reactor
CH_2Cl_2	Dichloromethane
cod	1,5-cyclooctadiene
CP/MAS NMR	Cross-Polarization Magic Angle Spinning Nuclear Magnetic Resonance
CTAB	Cetyltrimethylammonium bromide
d_{100}	Interplanar spacing
dba	Dibenzylideneacetone
DMF	Dimethylformamide
DOP	Dioctyl phthalate

dppb	1,4-bis(diphenylphosphino)butane
DSC	Differential Scanning Calorimetry
DSC-TGA	Differential Scanning Calorimetry Thermal Gravimetric Analysis
EA	Elemental Analysis
equiv.	Equivalent
Et	Ethyl group
EtOH	Ethanol
FT-IR	Fourier-transform infra red spectroscopy
g	Grams
GC	Gas Chromatography
GPC	Gel Permeation Chromatography
h	Hours
H_z	Hertz
ICP-MS	Inductively coupled plasma-Mass spectroscopy
K	Degrees Kelvin
L	Ligand
L*	Chiral Ligand
M	Molar concentration, in mole/liter
MALDI-TOF	Matrix-Assisted Laser Desorption/Ionization - Time of Flight mass spectroscopy
MCM-41	Mobil Crystalline Material (LP- Large Pore, PE- Pore Expanded)

Me	Methyl group
MeOH	Methanol
mg	Milligram
min	Minute
ml	Milliliters
mmol	Millimole
mol	Mole
MS	Mass Spectrometry
Mt	Megaton
NaOAc	Sodium acetate
nm	Nanometer
NMP	N–methylpyrrolidone
NMR	Nuclear Magnetic Resonance
OAc	Acetate
PAMAM	Polyamidoamine dendrimer
Ph	Phenyl group
POSS	Polyhedral Oligomeric Silsesquioxanes
PPI	Pollypropyleneimine dendrimers
ppm	Parts per million
PSD	Pore size distribution
psi	Pounds per square inch
p-TsOH	*p*–Toluenesulphonic acid
r.t.	Room temperature

SASOL	South African Coal, Oil and Gas Company
STP	Standard temperature and pressure
TFA	Trifluoroacetic acid
TGA	Temperature Gravimetric Analysis
THF	Tetrahydrofuran
TMAOH	Tetramethylammonium hydroxide
TOF	Turnover frequency
TON	Turnover number
µmol	Micromole
V_m	Micropore volume
V_p	Total Pore volume
w	Pore diameter
X	Ionic non-labile ligand
XRD	X–Ray Diffraction Spectroscopy
δ	Chemical shift relative to tetramethylsilane

Contents

List of Schemes

Chapter 1. *Introduction*

Chapter 2. *Preparation of Palladium-Complexed C_6-PAMAM Dendrimers Immobilized on Silica as Catalysts for the Hydroesterification of Olefins*

Chapter 3. *Hydroesterification Reactions with Palladium-Complexed C_6-PAMAM Dendrimers Immobilized on Silica*

Chapter 4. *Preparation of Rhodium-Complexed C_2-PAMAM Dendrimers Immobilized on Mesoporous and Periodic Mesoporous Silica as Catalysts for the Hydroformylation of Olefins*

Chapter 5. *Hydroformylation Reactions with Rhodium-Complexed C_2-PAMAM Dendrimers Immobilized on Mesoporous and Periodic Mesoporous Silica supports*

List of Figures

Chapter 1. *Introduction*

Chapter 2. *Preparation of Palladium-Complexed C_6-PAMAM Dendrimers Immobilized on Silica as Catalysts for the Hydroesterification of Olefins.*

Chapter 3. *Hydroesterification Reactions with Palladium-Complexed C_6-PAMAM Dendrimers Immobilized on Silica*

Chapter 4. *Preparation of Rhodium-Complexed C_2-PAMAM Dendrimers Immobilized on Mesoporous and Periodic Mesoporous Silica as Catalysts for the Hydroformylation of Olefins*

Chapter 5. *Hydroformylation Reactions with Rhodium-Complexed C_2-PAMAM Dendrimers Immobilized on Mesoporous and Periodic Mesoporous Silica supports*

List of Tables

Chapter 1. *Introduction*

Chapter 2. *Preparation of Palladium-Complexed C_6-PAMAM Dendrimers Immobilized on Silica as Catalysts for the Hydroesterification of Olefins.*

Chapter 3. *Hydroesterification Reactions with Palladium-Complexed C_6-PAMAM Dendrimers Immobilized on Silica*

Chapter 4. *Preparation of Rhodium-Complexed C_2-PAMAM Dendrimers Immobilized on Mesoporous and Periodic Mesoporous Silica as Catalysts for the Hydroformylation of Olefins*

Chapter 5. *Hydroformylation Reactions with Rhodium-Complexed C_2-PAMAM Dendrimers Immobilized on Mesoporous and Periodic Mesoporous Silica supports*

Chapter 1 *Introduction:*

1.1 General introduction.

Catalysts are compounds and materials that give us control over chemical reactions. They allow us to lower the activation energy and increase the rate of reactions, thereby enabling the reactions to proceed at lower temperatures. In most cases they allow us to tailor reactions to specific needs. Catalyst technology has come a long way since the first bio-catalyzed fermentation gave our ancestors alcohol and cheese.[1] It could be argued that our lives are irreversibly influenced by catalysts e.g. even our bodies rely on bio-catalysts (enzymes) for energy production and countless other life sustaining processes. Enzymes control reactions with virtually perfect results leading to (in many cases) one product in high yield, unattainable by any "man-made" catalyst.[2] We are therefore only starting to discover and understand the advantages and utility of catalysis.

As with most human endeavors we are not satisfied by what nature provides, but are constantly trying to introduce new products, and probably the need for them also, into our lives. George Bernard Shaw said: "The reasonable man tries to adapt himself to the world. The unreasonable man tries to adapt the world to himself. It follows then, that all progress depends upon the unreasonable man." In this endeavor, scientists and chemists in particular are at the forefront leading unreasonable men and women towards great rewards.

Industrial catalysts are used to produce most chemical compounds that we use every day. Millions of tons of chemicals are produced annually and most of these by catalytic processes

Heterogeneous catalysts are preferred for large-scale production because they have the benefits of cost, robustness and ease of separation of products from reactants and catalysts. Although heterogeneous catalysts are used in 80 - 90% of chemical manufacturing processes these systems are often not well understood and an empirical approach is usually followed in their development, which leads to tedious and sometimes unnecessary experimentation.[3] Nonetheless, scientists are elucidating the intricacies of these processes and we are now even seeing enantioselective heterogeneous catalysts based on polymers with chiral substituents being developed.[4] This field may have significant impact and reward in the future.

On the other side of the spectrum lies homogeneous catalysis. This field has become increasingly important in industry. This is evident in the number of processes being developed and commercialized that rely wholly or in part on homogeneous catalysts.[5] Homogeneous catalysts allow almost total control over the reaction and due to their soluble nature, characterization is more facile, as is the elucidation of reaction mechanisms. It is one of the principles of science that if one can understand something one can change it. The defining characteristic of homogeneous catalysis, homogeneity, has made it possible for us to

understand many reactions and therefore to increase their rates and improve their utility. The main drawback of homogeneous catalysis ironically also stems from its homogeneous nature. Separations are often difficult and costly, but as process engineering improves we should see the utility of these systems increase.[6] However until we can cheaply separate homogeneous catalysts, without any loss of activity, and totally tailor heterogeneous catalysts to our needs, there exists a need for something else; a catalyst system that combines the utility of heterogeneous catalysis with the obvious control benefits of homogeneous catalysis. Industry dictates that the ultimate catalyst would be 100% selective, highly active, inexpensive to produce and operate, simple and infinitely robust. This is by all accounts impossible to attain, at least at present, but one should be capable of improving the characteristics of either homogeneous or heterogeneous catalysts to approach this goal. Our approach to addressing this problem is to tether traditional homogenous catalysts by means of organic linker molecules to traditional heterogeneous supports. This research therefore aims to identify and at the very least start to explain the challenges involved in approaching the almost unattainable goal of the "ultimate catalyst" system. We present here our attempts at taking advantage of the attributes of heterogeneous catalysts and the benefits of homogeneous catalysts. In an effort to guide the reader towards our research we first have to set the scene with some pertinent background information.

1.2 Heterogenizing homogenous catalysts.

1.2.1 Heterogeneous vs. homogeneous catalysis.

As stated before heterogeneous and homogeneous catalysis both offer benefits and present individual challenges. In this section both types will be discussed separately.

1.2.1.1 Heterogeneous catalysis.

Heterogeneous catalysis incorporates a huge variety of systems and processes, but they all share the same defining principle. The catalyst is either an insoluble material or a metal complex attached to an insoluble, rigid material. Reactions can be effected in the gas or the liquid phase depending on the nature of the process. Heterogeneous catalysts are used in 80- 90 % of industrial processes and some examples are catalytic cracking, hydrogenation and skeletal isomerization used in the petrochemical industry. (Scheme 1-1.)

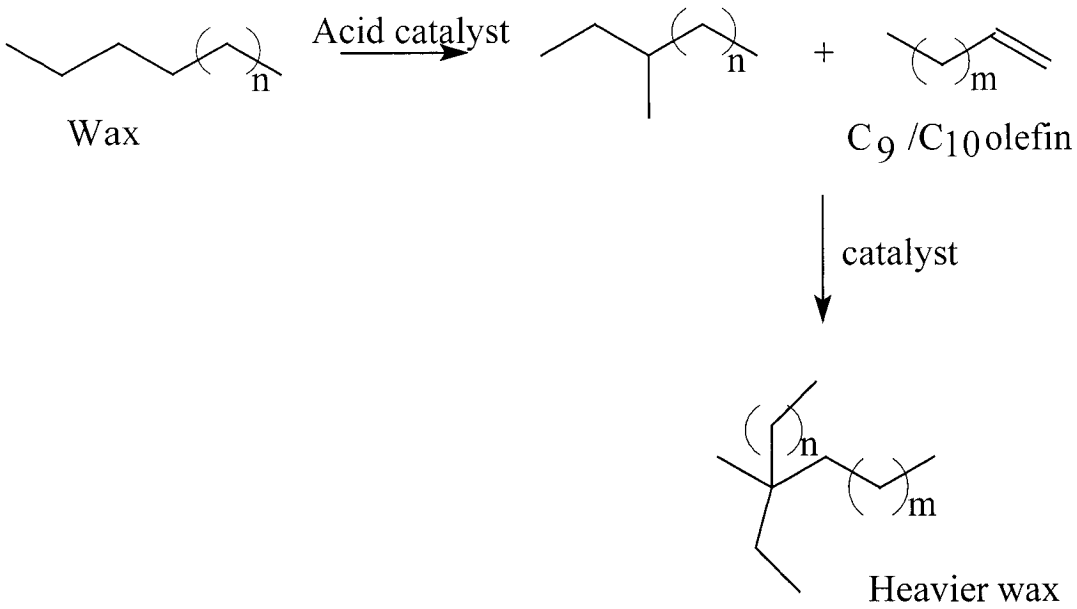

Scheme 1-1. Skeletal isomerization of paraffins used in industry.

Reactions can be carried out in different vessels including fixed bed, stirred tank, fluidized bed and riser reactors. The variations of the reactor systems are almost as numerous as the catalysts used, and fall outside the focus area of this thesis.[1,3]

All heterogeneous catalysts share the benefit of ease of separation from the product stream, which is usually accomplished by trapping the catalyst in the reactor (like in fixed bed reactors) or simple filtration e.g. in some stirred tank and fluidized bed reactors. The catalyst can then be reused (directly or after being subjected to oxidation, reduction or activation). The development of these catalysts usually relies on empirical optimization and the active site is generally difficult to identify. Another problem is that the activity and selectivity of the

catalyst systems rely on the characteristics of the solid supports and parameters like acidity, basicity, surface area, porosity, and particle dimensions are important. Control of the exact surface characteristics are often impossible and reactions like skeletal isomerization that rely on specific anomalous reaction sites on the surface can be catalyzed by various types of sites, leading to side reactions and loss of control. Well defined supports are being developed but even in these the catalytically active sites are not necessarily homogeneous in nature, and therefore selectivity is a very elusive goal in heterogeneous catalysis and is usually a function of activity. Elaborate optimization methods have been developed with great success and any heterogeneous catalysis laboratory now routinely employ software programs to reduce the number of reactions that have to be performed in an optimization regime. These programs usually work on the principle of comparing interrelated parameters to identify optimum reaction conditions. Although these are valuable tools, their success is still limited by the nature of the catalyst and the whole process often has to be repeated, even for a slight variation in the catalyst composition. This, in combination with high throughput methodology specifically tailored to heterogeneous catalysis, has been helpful in demystifying the process of catalyst development.[7] Although there has been great progress over the last 50 years toward understanding heterogeneous catalysts and processes, a large part is still art rather than science.

1.2.1.2 Homogeneous catalysis.

Homogeneous catalysis offers the benefit that the catalyst and the reagents are in the same phase (mostly liquid) during the reaction. This leads to the benefits of control, not only of the pre-catalyst loaded into the reactor, but also of the active catalyst which can usually be identified by careful experimentation. By understanding the catalytic cycle more intimately, the rate-limiting step can be identified and the catalyst can, in theory at least, be tailored to speed up this step and improve the overall rate of the reaction. Side reactions (or undesired reactions) can also be identified and in principle be suppressed or eliminated by improving the catalyst design and controlling the reaction conditions. This does not mean that homogeneous processes are simple and easily optimized, and it usually takes much longer to commercialize homogeneous processes than heterogeneous processes. This is due to the fact that there are so many factors to consider and permutations of ligand and metal combinations that are possible that economically feasible homogeneous processes are formidable achievements. Nonetheless, homogeneous processes do offer control, the ultimate requirement of an excellent catalyst system, but it is not coincidental that the vast majority of industrial processes are still heterogeneously catalyzed. The biggest challenge with commercializing homogeneous processes is cost. Cost of separation, voluminous reactor setups, metal and ligand systems and of solvents are essential components in evaluating the economic feasibility of a process. It is therefore important to develop other more economic means of separation. The "holy grail" of catalysis is to combine the selectivity and activity of homogeneous

catalysis with the stability and separation capabilities of heterogeneous catalysis. A direct comparison is given in Table 1-1.

Table 1-1. Advantages and disadvantages of homogeneous and heterogeneous catalytic processes.

	Batch homogeneous process	**Fixed Bed heterogeneous process**
Conversion	High	Low
Separation	Filtration of residue Distillation Extraction	No, catalyst immobilized in reactor
Additional equipment required	Yes	No
Catalyst recycle	Difficult	Easy regeneration
Cost of Catalyst	High	Low
Catalysts in product	Low	Usually not

1.2.2 Methods of supporting homogeneous catalysts

Supporting homogeneous catalysts has become increasingly prevalent in recent years. The four main methods for supporting homogeneous catalysts are 1. Covalent bonding to a support 2. Adsorption on a support. 3. Ion pair formation between a charged metal complex and a charged species on a support. 4.

Entrapment inside the structure of a support (The so called ship in a bottle approach). (Figure 1-1.)

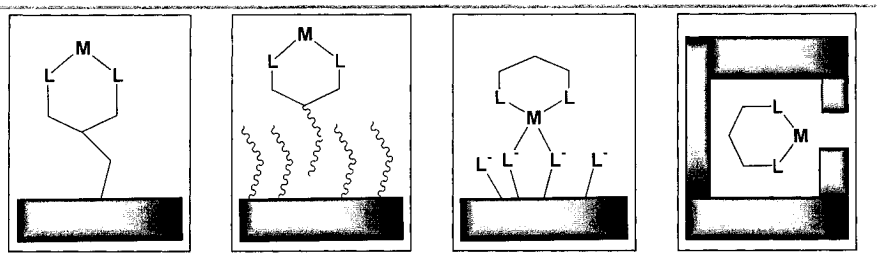

Immobilization method	**Covalent binding**	**Adsorption**	**Ion pair formation**	**"Ship in a bottle"**
Applicability	Broad	Restricted	Restricted	Restricted
Problems	Preparation	Competition with solvents, substrate	Competition with ionic substrates, salts	Size of substrate, diffusion.

Figure 1-1. Heterogenization of homogeneous catalysts.

These constitute the vast majority of the support methods but many others have also been developed. In this brief introduction we will focus on the covalently bonded supporting approach, as this is the field that most closely relates to our approach.

The advantages and disadvantages of supporting homogeneous catalysts. [8]

Advantages

1. Ease of catalyst separation and recycle.
2. Homogeneous catalysts with unique ligand surroundings can be stabilized.
3. Multifunctional catalysts are possible by supporting various complexes on the same support.
4. Immobilization and stabilization of uniform active species (single site catalysts).

Disadvantages

1. Leaching of metal and/or ligand from the support.
2. Catalyst deactivation in subsequent cycles.

As we will be using dendrimers to attach catalysts covalently to supports we need to consider the background literature on dendrimers, and their use as catalysts for homogeneous processes.

1.3 Dendrimers.

The word dendrimer is derived from the Greek word *"dendra"* for tree and is usually used in the chemical context for highly branched, monodisperse (or close to) macromolecular compounds.[9] Some research groups also refer to their highly branched molecules as arborols which is derived from the Greek word *"arbor"* meaning branch.[10]

The monodispersity of these molecules should be understood in context. For perfect dendrimer molecules with perfect branching the polydispersity should be 1 (monodisperse) but for large dendrimers prepared by sequential reactions there could be a wider molecular weight distribution and therefore a polydisperse mixture of macromolecules. This is due to the statistical probability of inefficient reactions taking place.

P. J. Flory, wa the first to statistically predict the formation of highly branched polymers by the polymerization of AB_2 type monomers. Flory proposed a model for the calculation of molecular size distributions and other physical properties of these polymers.[11] Although these hyperbranched polymers are significantly different from dendrimers it is believed that Flory's theoretical study contributed to the development of dendrimers. This work was published in the fifties, but no dendrimers were synthesized until the late seventies.

1.3.1 Historical view of dendrimers.

The word dendrimer was first coined by Tomalia in 1985, although the first synthesis can be attributed to Vögtle *et al*, who in their 1978 paper described the first true synthesis of a dendrimer.[12] Vögtle *et al* described a cascade synthesis of poly(propyleneimine) (PPI) dendrimers. The synthesis (Scheme 1-2) was based on a two-step process. Exhaustive Michael addition of acrylonitrile to an amine gives a bisnitrile (**1**) followed by a catalytic reduction of the nitrile to give a bis-amine (**2**). The repetition of these two steps leads to higher generations (**4**).

The reduction step was however fraught with difficulties and in the first synthesis the two steps were only repeated twice to give the second generation PPI dendrimer. The problem is that the growing dendrimer has very efficient metal complexing ability, making isolation of higher generations from the reduction catalyst problematic.

De Brabander-van den Berg and Meijer later succeeded in preparing higher generations efficiently by using Raney-Cobalt as reduction catalysts [13] and these PPI dendrimers were commercially available for a few years as DAB-$(NH_2)_x$ dendrimers.[14]

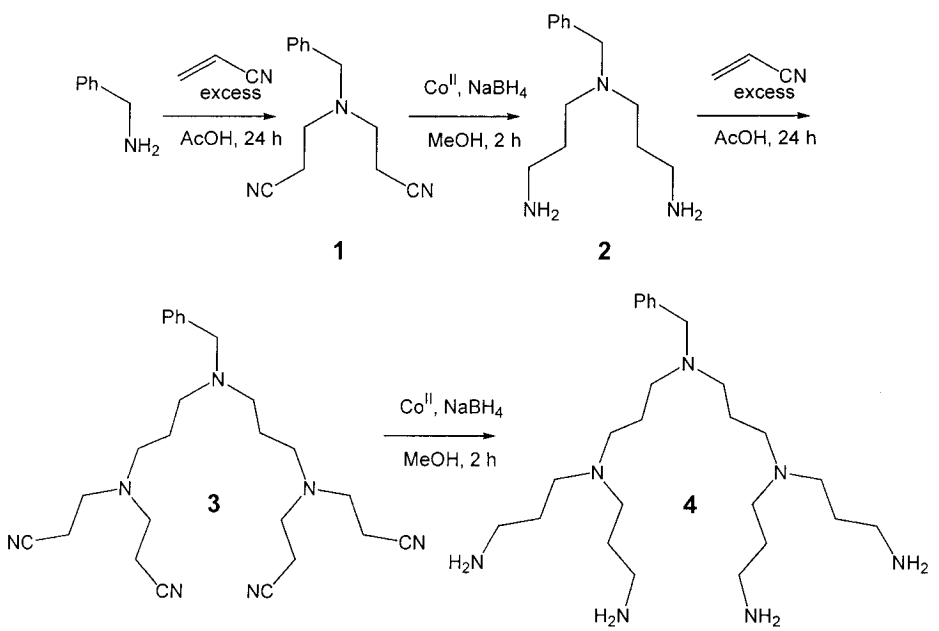

Scheme 1-2. The first preparation of dendrimers (PPI/DAB) reported by Vögtle *et al.*[12]

Tomalia and his group first synthesized polyamidoamine (PAMAM) dendrimers by a stepwise synthesis. The homogeneous synthesis of these dendrimers gave

fairly good polydispersity, and dendrimers up to the tenth generation could be synthesized in this manner. Again exhaustive Michael addition of methyl acrylate with ammonia followed by amidation with a large excess of ethylenediamine (15-250 molar eq.) leads to the first generation. (Scheme 1-3). Repetition of these two reactions gives higher generations in excellent yields of 98-100% per step. These dendrimers are sold under the trademark Starburst® by the DNT and Dendritech.[15]

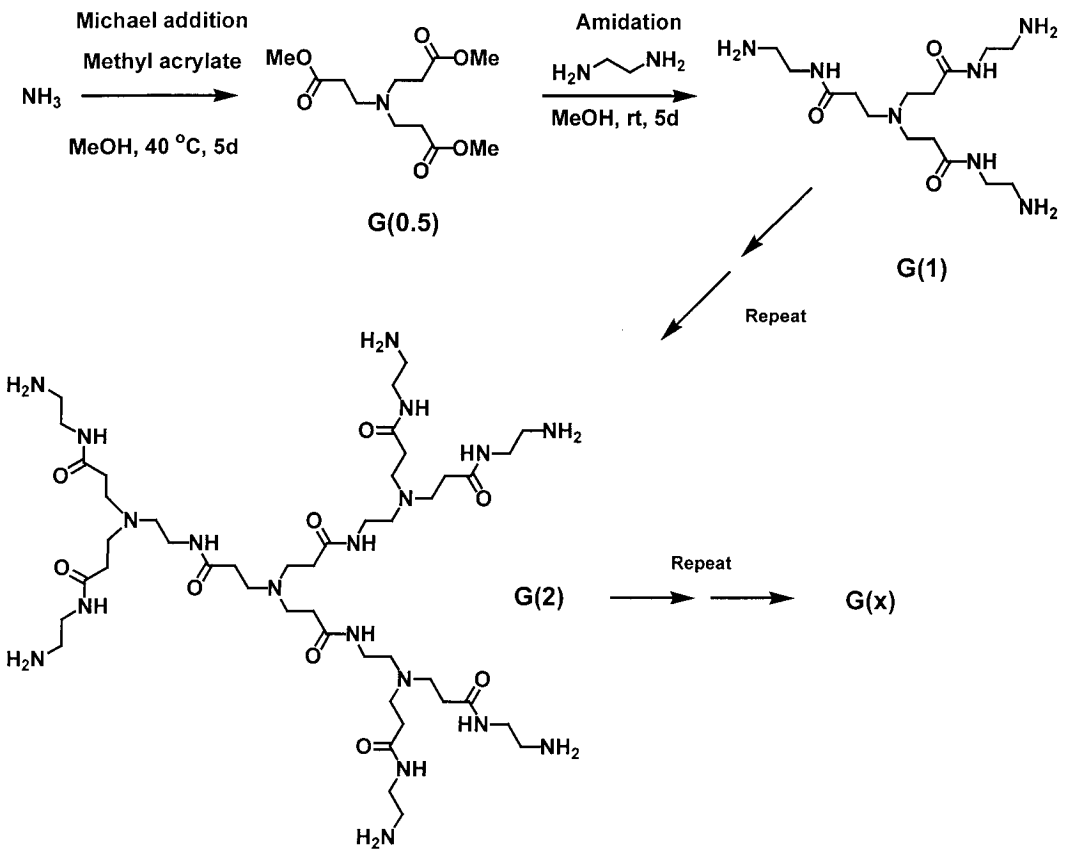

Scheme 1-3. Tomalia's preparation of PAMAM dendrimers.

In an effort to increase branching Newkome *et al* started developing highly branched dendrimers using tetrahedral carbons as branching units. Molecules like pentaerythritol have been used as branching units and very compact, highly branched macromolecules were prepared. The surface of these dendrimers were functionalized with polar surface groups and investigated as micelle analogs and supramolecular building blocks. [16]

These three groups paved the way for others to join the field of dendrimer synthesis. One of the most prolific and well-known groups deserves a mention. Fréchet *et al*[17] used the convergent synthesis approach to synthesize poly-aryl ether dendrimers up to the sixth generation (Scheme 1-4).

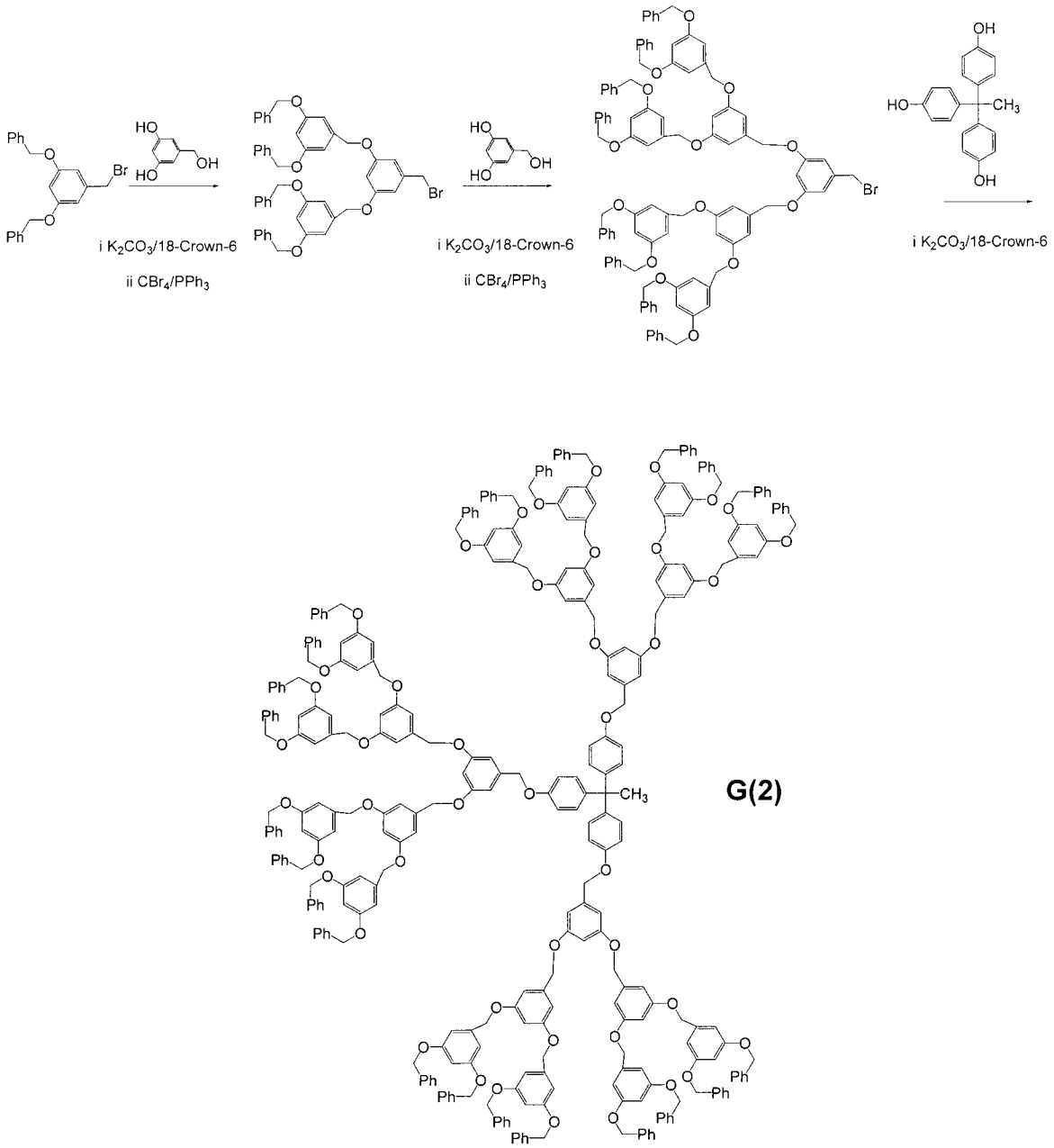

Scheme 1-4. Poly-aryl ether dendrimers prepared by Fréchet *et al.*[17]

The convergent approach has some benefits when compared to the divergent synthesis. First the large excess of reagents often employed in the divergent approach can be avoided and secondly purification at each step is, although

cumbersome, in principle possible due to the smaller size of the dendritic wedges. The main disadvantage of this approach is that the yields of the higher generations are negatively affected by steric hindrance and a threshold is reached quickly depending on the flexibility of the dendritic wedges. Fréchet *et al* also substituted the original core of the dendrimer for a more flexible core leading to flexible spherical dendrimers. [17]

Majoral *et al* developed a unique type of dendrimer with phosphorus atoms at the branching points, and have been successful in preparing very large dendrimers with varied endgroups.[18] These dendrimers were functionalized with phosphines at the periphery and various well-characterized metal complexes were prepared.[19] (Scheme 1-5.)

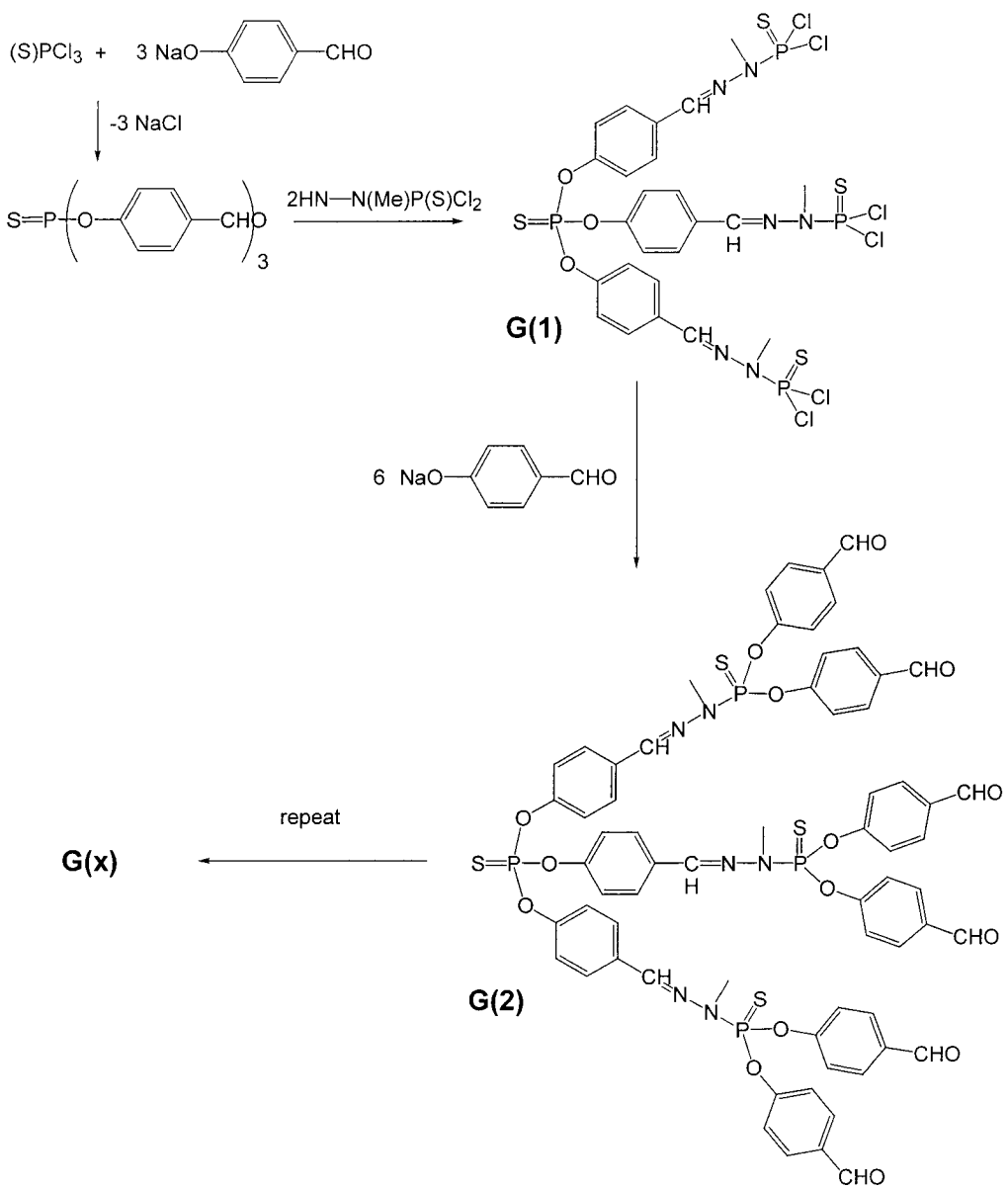

Scheme 1-5. Preparation of Majoral's phosphorus containing dendrimers.

Several other groups have also synthesized dendrimers with other motifs based on silicone,[20] aminoacids,[21] aryl esters[22] and saccharides.[23] Metallodendrimers (where the branching points consist of metal atoms) have also become more common. [24]

Dendrimers have found widespread application in host-guest chemistry[25], catalysis[26], liquid crystals, layers and films[27], analytical chemistry[28] and in biology and medicine.[29]

Before we can however look at the applications of dendrimers it is important to spend some time on the characterization and physical properties of dendrimers.

1.3.2 Characterization of dendrimers.

Dendrimer characterization has always been problematic. Because of the size of these molecules, traditional characterization methods are usually only partly successful. For instance, as most dendrimers are prepared by synthetic organic chemistry, ^{13}C, ^{1}H NMR and mass spectroscopy methods were originally employed for characterization. These methods are unfortunately inadequate because the dendrimer molecules are typically constructed from repeating units and ^{13}C and ^{1}H NMR does therefore not differ substantially between generations. For phosphorus and nitrogen containing dendrimers ^{15}N and ^{31}P NMR are helpful in their characterization.[18] The mass spectroscopic methods usually employed for organic molecules are also inadequate as these methods are not very useful for

large molecules. Soft ionization methods like matrix-assisted laser desorption/ionization-time of flight (MALDI-TOF) mass spectroscopy originally developed for bio-macromolecules is valuable for the characterization of dendrimers.[30] X-ray diffraction is of course the ultimate tool for structurural elucidation, but unfortunately this method is not especially useful for dendrimer characterization as even the most rigid dendrimers lack sufficient long-range uniformity necessary for XRD.

Traditional polymer characterization methods have improved the structure elucidation of dendrimers, including gel permeation chromatography (GPC). Dendrimers synthesized by convergent synthesis techniques can often be purified from side products by GPC (or sometimes by column chromatography). Divergently synthesized dendrimers can also be separated from low-molecular weight impurities by GPC. GPC is therefore also the preferred method for determining the polydispersity. As perfect dendrimers have polydispersity indices of 1 (monodisperse), this is the goal when synthesizing them.

Some dendrimers have been synthesized with polydispersity values very close to 1, but for large dendrimers synthesized by the divergent approach like PAMAM dendrimers and PPI dendrimers, polydispersities other than 1 are reported, but dendrimers are significantly closer to monodisperse than linear polymers.[30] This is probably due to reaction by-products that are inseparable from the pure dendrimers. We will discuss the statistics of dendrimer synthesis in later chapters

to address this problem further.

1.3.3 Dendrimers as Catalysts.

As we saw in the previous sections, the development of dendrimers from the late 70 s until the early 90 s was confined to synthesis, characterization and theoretical studies. Only in the last ten years have there been considerable development of applications for this unique class of molecules. Specific characteristics of dendrimers like their size, the control over structure and properties like solubility combined with the ease of functionalization, has inspired many research groups to use dendrimer molecules as "supports" for transition metals and therefore also in catalysis. Various reviews on the subject have already appeared[26], and the volume of papers published using dendrimer based catalysts has increased tremendously since the first dendrimer based catalytic process appeared in 1991 in a Shell patent where a hexaphosphine catalyst containing a benzene core was used for the palladium catalyzed alternating CO-olefin copolymerization reaction. The dendritic catalyst reduced reactor fouling (caused by the polymer sticking to the wall of the reactor) when compared with the mononuclear catalyst. [31]

The group of van Leeuwen in conjunction with the van Koten group reported the first true use of dendrimers in catalysis. They used G(0) and G(1) carbosilane dendrimers with up to 12 pincer type NCN-nickel(II) groups at the periphery. (Figure 1-2.) These dendrimers were used to catalyze the Kharash addition of

tetrachloromethane to methylmethacrylate. (Scheme 1-6.)

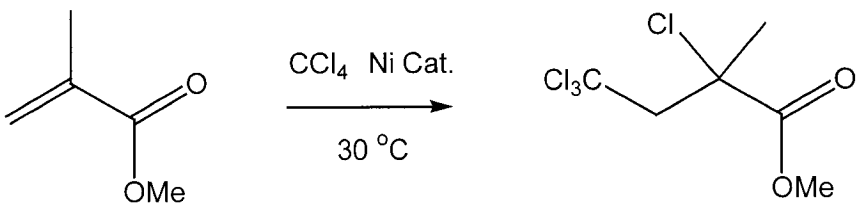

Scheme 1-6. Kharash addition with X = Halogen; Y = H, Halogen or CF_3.

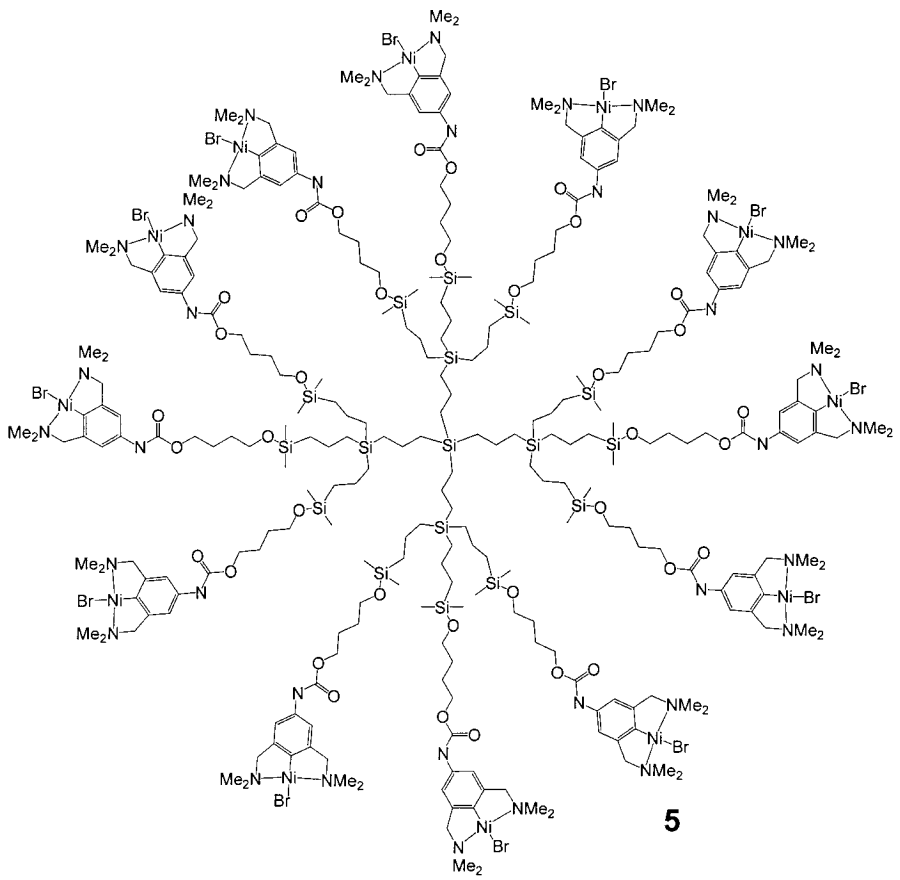

Figure 1-2. The first carbosilane dendrimers used by van Koten and van Leeuwen.

This seminal paper also represent the first occurrence of a dendrimer effect, albeit negative. The activity of the tested catalysts decreased from the parent complex to the G(0) complex (4 Ni centers) followed by the G(1) complex (12 Ni

centers). The explanation given was that the dendrimers posses high localized concentration of Ni(II) centers at the periphery. As the dendrimers become larger the metal centers come closer together, thereby allowing neighboring Ni(II)/Ni(III) species to interact and accelerate the 2 metal center deactivation mechanism. The higher generations are therefore less active than the parent complex due to higher local metal concentrations.[32] This hypothesis was tested by using flexible spacers in the dendrimers. (Figure 1-3.) The more flexible complex **7** was significantly more active than the rigid complex **6**.

Complex **5** decomposed during the reaction due to the hydrolysis of the Si-O bond causing leaching of the metal. All catalysts were subsequently tested in a CFMR (continues flow membrane reactor) and B gave a retention of 99.75% in the reactor indicating that it is large enough for CFMR applications without significant catalyst loss over 100 cycles. The catalyst unfortunately lost virtually all activity after 45 cycles and because leaching was eliminated as a cause of the activity loss, the loss in activity was attributed to the deactivation mechanism.[33]

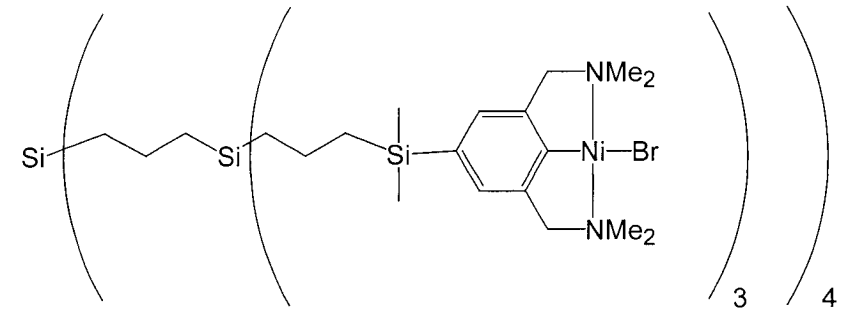

6

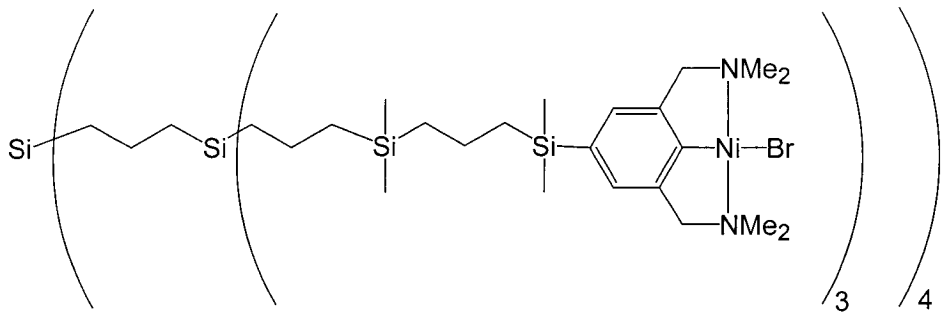

7

Figure 1-3. Stable carbosilane dendrimers used by van Koten and van Leeuwen in the CFMR. [33]

van Koten *et al* recently showed that amino acid based dendrimers could be used as supports for the NCN-pincer ligands. The dendrimers showed comparable reactivity to the parent complex, the carbosilane dendrimer based catalysts and polymer bound catalysts in the Kharash addition.[34]

van Leeuwen and co-workers synthesized a series of core-functionalized dendrimers based on a 1, 1-bis(diphenylphosphino)ferrocene core. They

attached carbosilane dendrimer wedges of different generations to the para position of the P-Aryl groups.

After complexation with $Pd(MeCN)_2Cl_2$ these ferrocene centered chelate complexes were shown to be efficient in palladium-catalyzed allylic alkylation reactions.

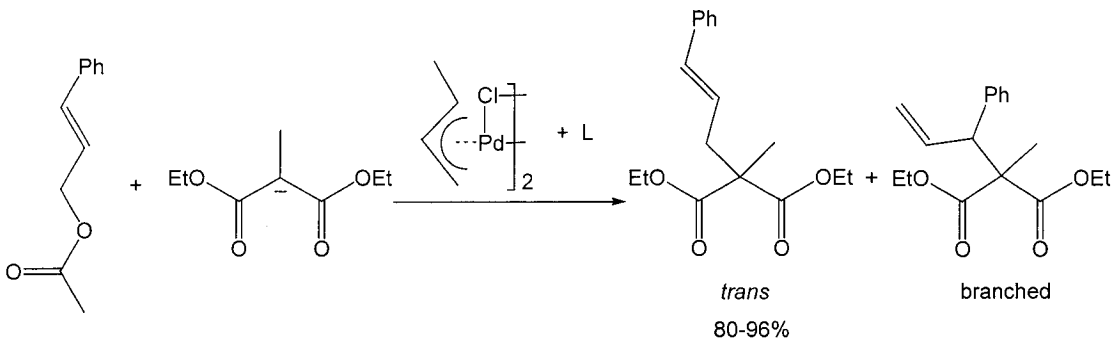

Scheme 1-7. Allylic alkylation reaction tested by van Leeuwen *et al.*[35]

The rate of the allylic alkylation reaction decreased with increasing dendrimer generation. The rationale was that more difficult mass transport comes into play in the larger dendrimers due to the steric bulk of these complexes. (Scheme 1-7.) The largest difference was observed between G(2) and G(3). Interestingly the size of the dendrimers also affected the selectivity of the reaction with a slight shift to the branched products observed for the G(3) dendrimer. This might be due to the increased steric bulk of the larger dendrimer interfering with the attack of the nucleophile on the Pd-allyl complex.[35]

Reetz *et al* pioneered the use of the phosphomethylation reaction for the

synthesis of dendrimer-based catalysts. They phosphomethylated a commercial DAB (PPI) dendrimer with eight terminal amine groups leading to a phosphine terminated dendrimer that could be used to form bidentate complexes of transition metals. The PNP ligand terminated dendrimers were used to prepare palladium (**8**, **9**), rhodium (**11**) and iridium (**10**) complexes and a mixed metal functionalized dendrimer was also prepared with alternating nickel and palladium centers on the periphery of the dendrimer (**12**). (Scheme 1-10) The palladium complexed dendrimer (**9**) efficiently catalyzes the Heck reaction of bromobenzene and styrene with the formation of stilbene. (Scheme 1-8) The rhodium complexed dendrimer (**11**) was used as a catalyst for the hydroformylation of styrene (Scheme 1-9), but although the potential of recycling was addressed, no procedure was available at the time for the effective recycle of small dendrimers.[36]

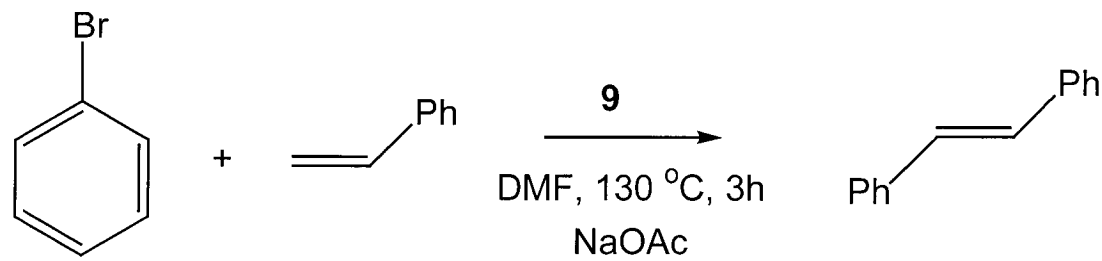

Scheme 1-8. Heck reaction of bromobenzene and styrene with the formation of stilbene.[36]

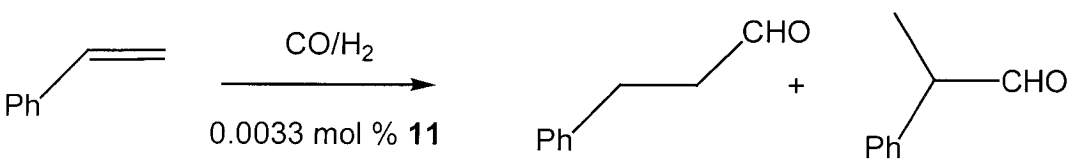

Scheme 1-9. The hydroformylation reaction of styrene.[36]

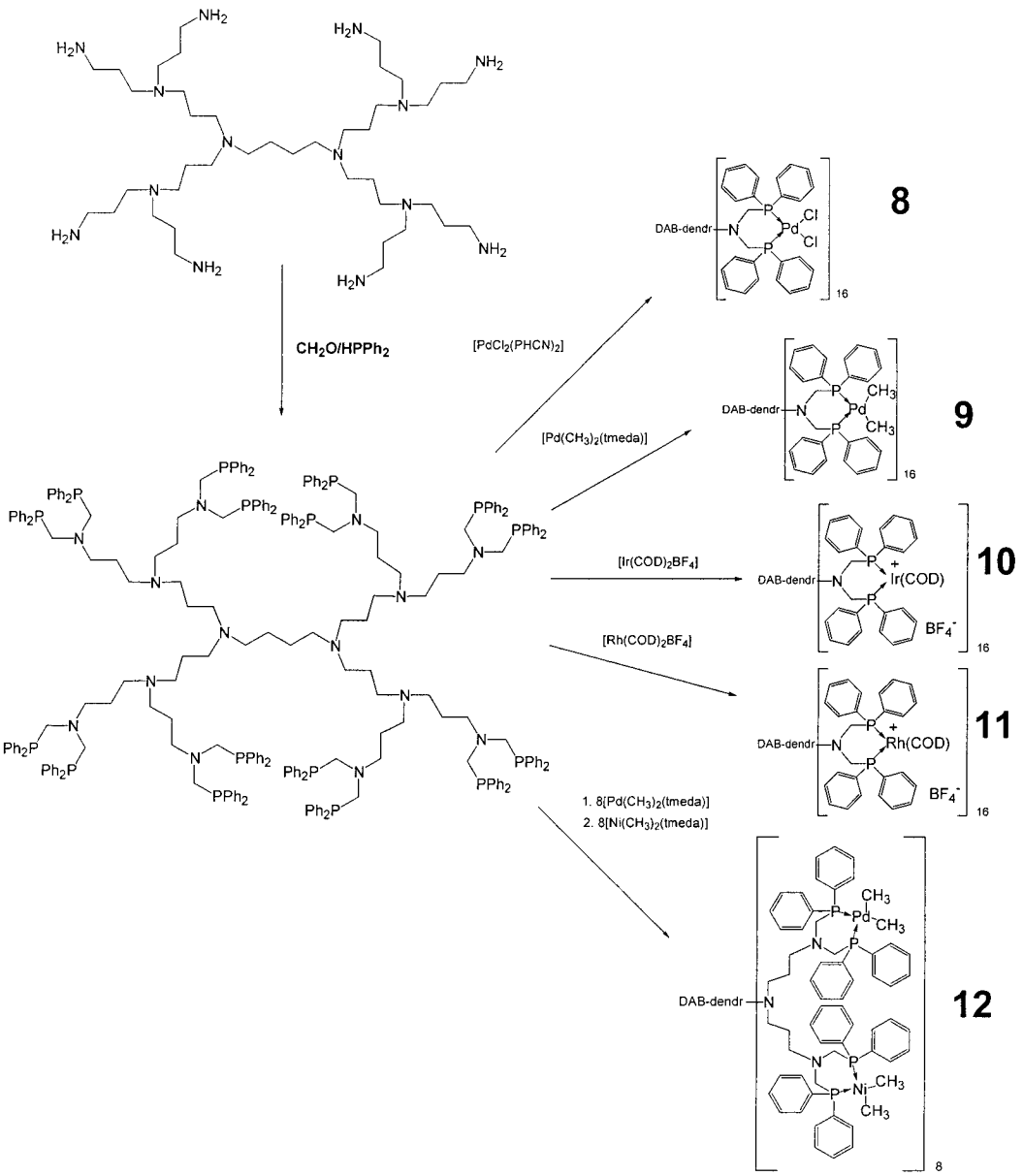

Scheme 1-10. Reetz's polyphosphonated DAB dendrimer and complexes thereof. [36]

Cole-Hamilton *et al* described dendrimer-based catalysts that exhibited increased selectivity for the hydroformylation reaction. They prepared carbosilane dendrimers based on polyhedral oligomeric silsesquioxanes (POSS) cores. Dendrimers with 16 diphenylphosphine end groups at the periphery gave much higher linear selectivity (14:1) than their parent complexes (3-4:1) for the hydroformylation of 1-octene. This positive dendrimer effect was explained on the basis that the increased steric crowding at the periphery of the dendrimer aids in the formation of the linear aldehyde over the branched aldehyde.

They also noted that due to steric congestion at the periphery complex **13** had between 12 and 15 phosphine groups as opposed to the theoretical 16 groups. (Scheme1-11.) [37]

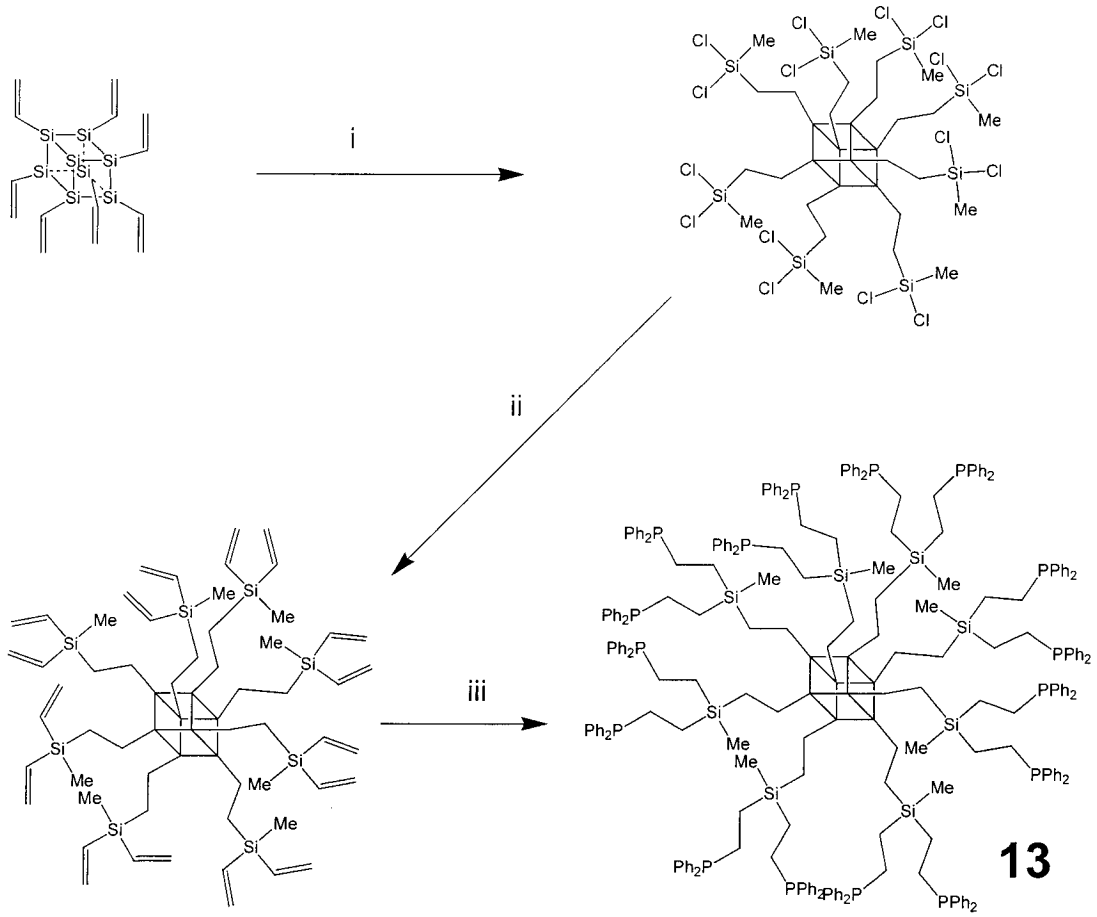

Scheme 1-11. Cole-Hamilton's[37] silsesquioxane core carbosilane dendrimers. Reagents i. $MeSiHCl_2$, H_2PtCl_6 (Catalyst); ii. (vinyl)MgBr; iii Ph_2PH, azodi(isobutyryl)nitrile. Each edge of the cube in the POSS core represents Si-O-Si.

Hoveyda *et al* recently reported two highly active recyclable olefin metathesis catalysts based on functionalized carbosilane dendrimers. (Figure 1-4.)

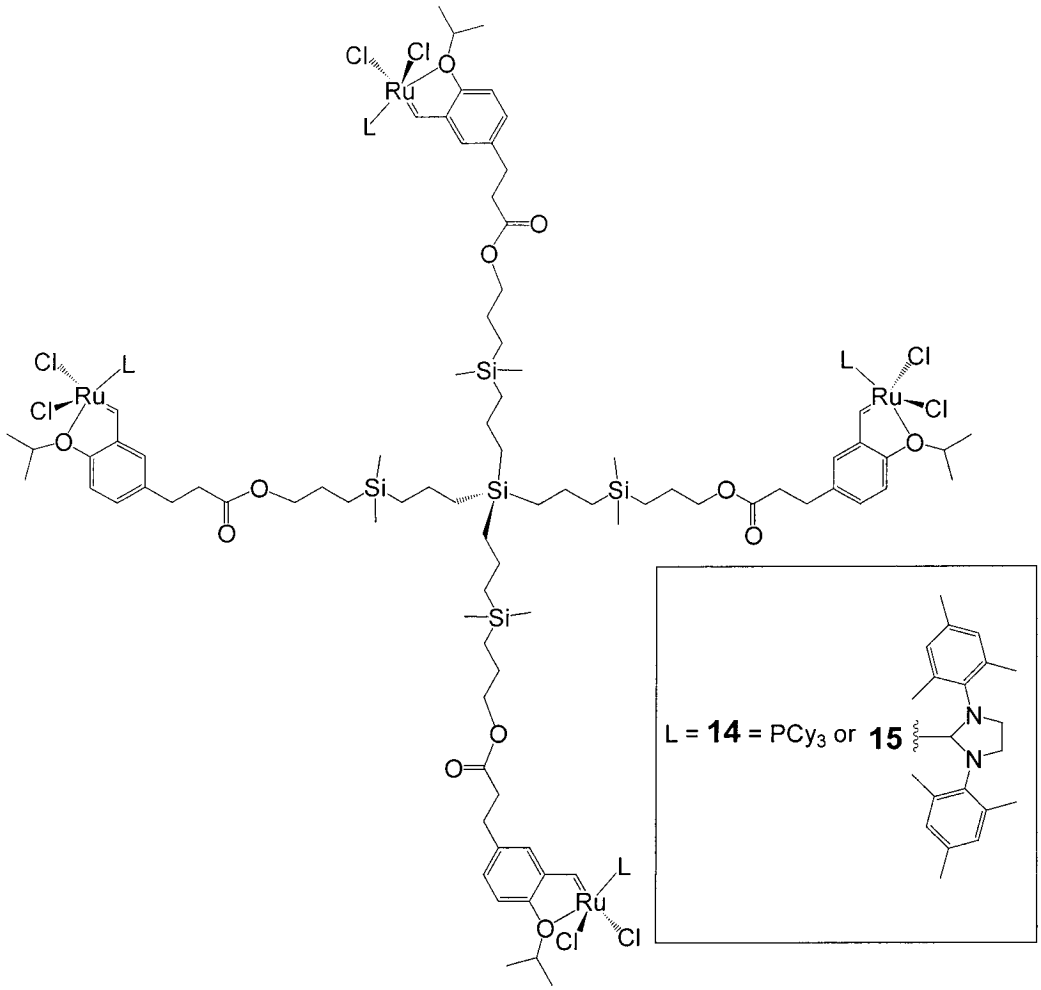

Figure 1-4. Hoveyda's[38] carbosilane dendrimer-based ruthenium functionalized metathesis catalysts.

The catalysts (**14**,**15**) were highly active for the ring closing metathesis of various dienes. Hoveyda *et al* proposed a "release and return" mechanism whereby a metal center in the catalytic cycle actually leaves the dendrimer support only to return at another point in the cycle. This did not however affect the recyclability of the catalyst, which could be separated from the reaction mixture by means of silica chromatography.[38]

Fréchet *et al* [39] found an interesting microenvironmental effect of their polyethers on polymerization. The dendrimers were used as macroinitiators for anionic ring opening polymerization of ε-caprolactone. (Scheme 1-12) The dendrimers showed a significant effect on the degrees of polymerization and polydispersities of the polymers obtained. This was accomplished by anchoring the growing tip of the polymer inside a cavity of the dendrimer and thereby avoiding termination by reaction with another chain. Because of the large void space inside these dendrimers the monomers are free to diffuse into the dendrimer to reach the growing tip thus allowing the polymerization to proceed, but the growing end of the polymer is shielded from the polymer by the size of the dendrimer, and no backbiting occurs. This leads to polymers with better linearity and polydispersity, with less branching. In this case the dendrimer morphology and structure are pivotal for the success of the polymerization and the dendrimer is not merely a large scaffold for the attachment of an active catalyst. This serves as the first real application in catalysis where the dendrimer itself is vital for the reaction and sets the stage for similar approaches in the future

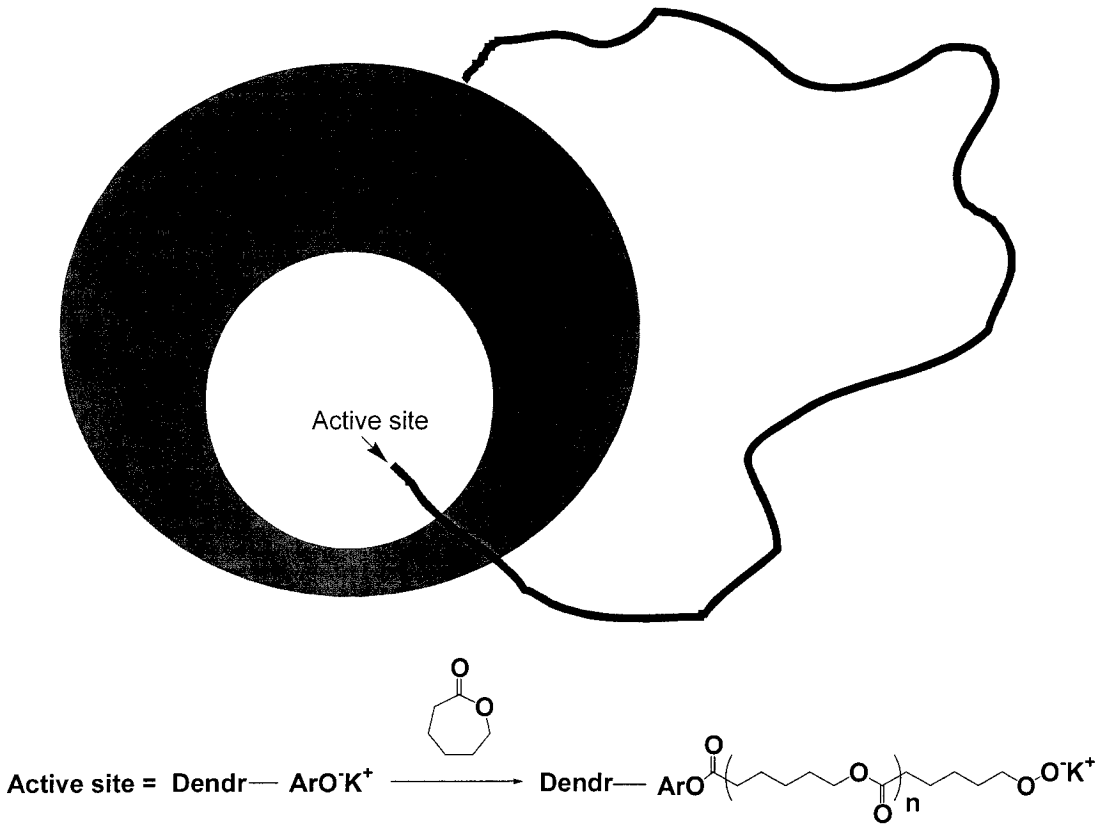

Scheme 1-12. Fréchet's polymerization experiment.

These examples are by no means comprehensive and only serve to represent a varied selection of the processes where dendrimer based catalysts have been used.

1.3.4 Supporting dendrimer-based catalysts on solid supports.

Why would one want to anchor dendrimers on solid supports? This is an interesting question and one that will be addressed in this section. The ultimate goal of dendrimer-based catalysis is twofold: First the catalysts can be tailored

like homogenous single site catalysts and therefore the activity and selectivity of these systems becomes important. Second, the separation of macromolecular catalysts is in principle possible.

The separation of dendrimers from the feedstock is not trivial. Very complex membrane reactors have to be used in most cases, and this technology is limited in its application. Many groups have attempted reactions catalyzed by dendrimer-based catalysts in membrane reactors with limited success. If one were however able to bind the dendrimer to a support of some sort (either polymer beads or silica), the separation problem is instantly solved, without interfering with the attributes of the dendrimer based catalyst. This represents a continuation on the heterogenization of homogeneous catalysts. The organic dendrimer is solvated by the solvent or the substrate, and the metal complex attached to the dendrimer can react like a homogeneous catalyst, with the core of the dendrimer attached to the surface of an insoluble support thereby affecting easy separation by filtration. This approach raises the possibility of the use of these catalysts in fixed bed reactors (a significant cost improvement over membrane reactors).

The use of solid supports for dendrimers also present a new set of challenges not least of these being the characterization of the dendrimer species and the catalyst. One can circumvent this problem by synthesizing the dendrimer homogeneously before attaching it to the support, but this approach is also

limited. For instance, not all dendrimers can be synthesized and attached this way, and even the dendrimers that can be suffer from limitations. The greatest drawback is the increasing size of the dendrimer wedges interfering with the attachment due to steric congestion at the focal point of the attaching group. The support, although not directly evident, can play a significant role in the performance of the dendrimers and the catalysts. Some of the points to consider are the size of the dendrimer vs. the void space available inside the pores of the support, the surface area of the support, the distribution of the active sites, and finally the effect of the support on the success of the growth of the dendrimers. But the most crucial questions are related to the characterization of these unique complexes.

Metal complexed dendrimers immobilized on silica have been used previously by Alper *et al* as catalysts for the hydroformylation of olefins[40], the Heck reaction[41] and for the carbonylation of aryl iodides.[42] In all these systems polyamidoamine (PAMAM) dendrimers were supported on silica by means of a divergent synthetic approach. Phosphinomethylation of the terminal amine groups of the dendrimers was achieved by reacting the dendrimers with diphenylphosphinomethanol prepared in situ from diphenylphosphine and paraformaldehyde and the resulting phosphine terminated dendrimers were functionalized with various metals including palladium and rhodium and these dendrimer complexes were used as catalysts.

The rhodium complexed dendrimers used for the hydroformylation of olefins showed significant activity, but the most valuable observation was the selectivity that these catalysts afforded. The G(2) catalyst gave 30:1 branched to linear selectivity at room temperature and 1000 psi CO/H_2 pressure. For the higher generations the phosphomethylation and complexation reactions did not go to completion as determined by ICP-MS analysis. This was attributed, at least in part, to steric congestion at the periphery. To address this PAMAM dendrimers with longer spacer groups i.e. 1,4-diaminobutane, 1,6-diaminohexane and 1,12-diaminododecane was prepared. The C_6 and C_{12} linkers proved to be most active and could be recycled most efficiently. Low levels of rhodium leaching were reported in all cases.

C_2-Diamine linkers were used for the preparation of dendrimers up to G(3), and then applied to the carbonylation of iodoarenes. The dendrimers were complexed with palladium and proved to be quite active for the carbonylation reactions. The catalysts could be recycled 4-5 times without significant loss of activity. The catalysts were inactive for bromo- or chloroarenes.[42] (Scheme 1-13)

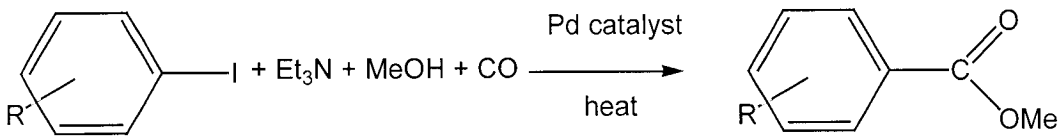

R = H, 4-NO_2, 4-Me, 2-MeO, 4-MeO, 4-CF_3, 4-I, 4-Br, 4-OH, 4-CH_3CO, 4-I-C_6H_4-

Scheme 1-13. Carbonylation of iodoarenes.

Alper *et al* also synthesized amino acid-based dendrimers (**16** Figure 1-5.) by a divergent synthesis. These dendrimers were attached to a Rink-amide resin and after phosphomethylation and complexation with rhodium, used as catalysts for the hydroformylation of olefins. These dendrimer-based catalysts were found to be very efficient for this reaction. In some cases the dendrimers were active for several cycles and excellent regioselctivity was observed. For instance the hydroformylation of styrene gave aldehydes in a branched to linear ratio of up to 35:1 (25 °C, 35% conversion). At elevated temperatures the B:L ratio decreased to around 16 but the reactions went essentially to completion. The activity observed was higher than expected for heterogeneous systems and it was speculated that the activity might be due to the highly exposed nature of the metal complexes, or to a cooperative effect between the metal centers. [43]

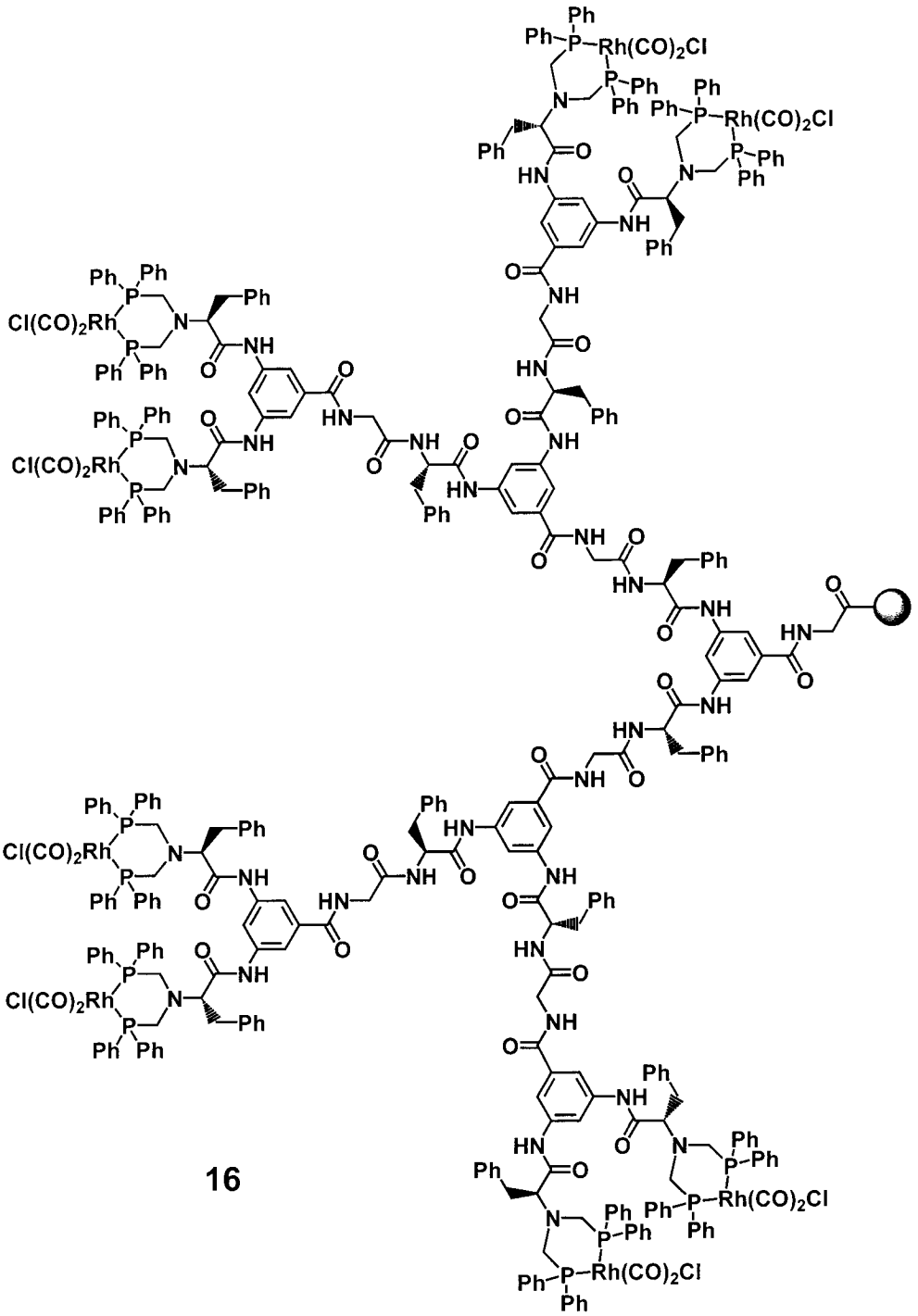

Figure 1-5. The G(3) octavalent dendrimer ligand supported on resin beads.[43]

After the initial work Alper *et al* followed a biomimetic approach and prepared dendrimers **17** and **18** (Figure 1-6.) to investigate if the metal centers could be protected in the inner core of the dendrimer. This was compared to proteins and enzymes where the active centers are often protected in the inner core of the molecule. It was thought that the architecture of **18** would protect the active center leading to higher catalyst robustness and therefore better recyclability. This robustness would be preferred even if the catalyst had lower activity, an attribute also predicted due to steric hindrance. Complex **18** had enhanced recyclability for the hydroformylation of *p*-methoxystyrene and vinyl benzoate. For the hydroformylation of *p*-methoxystyrene, **18** was more active in the fifth cycle (>85% conversion, B:L 30:1) than **17** (56% conversion, B:L 30:1). This was also observed for the hydroformylation of vinyl benzoate. Complex **17** gave only 43% conversion (B:L 30:1) in the fourth cycle and activity also reduced significantly in the fifth cycle (20% conversion, B:L 30:1). Complex **18** was however much more active in the fourth (91% conversion, B:L 20:1) and fifth cycles (83% conversion, B:L 19:1). Both catalysts gave excellent branched to linear ratio's for the hydroformylation of styrene with values around 18:1 at 45°C and with 5 recycles as the norm. [44]

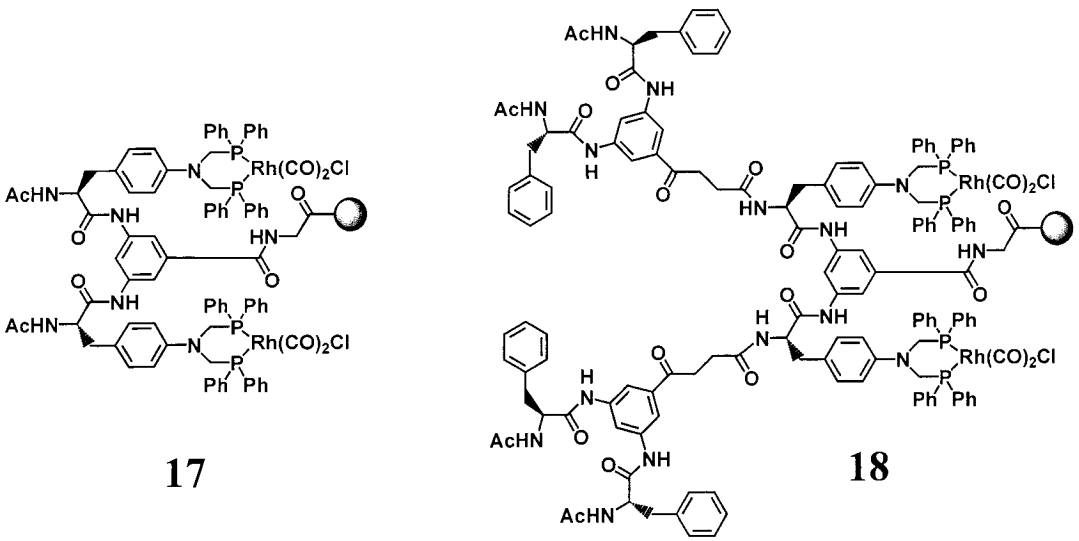

Figure 1-6. Alper, Arya *et al's* dendrimer ligands supported on resin beads for the biomimetic study.

Lu and Alper[45] continued this approach by supporting glycine based dendrimers on resin beads. The purpose of glycine as a structural unit was to give access to unique dendrimers with inside and outside (protected and unprotected) metal centers and to obviously increase the amount of active sites in the dendrimer (**19** Figure 1-7.).

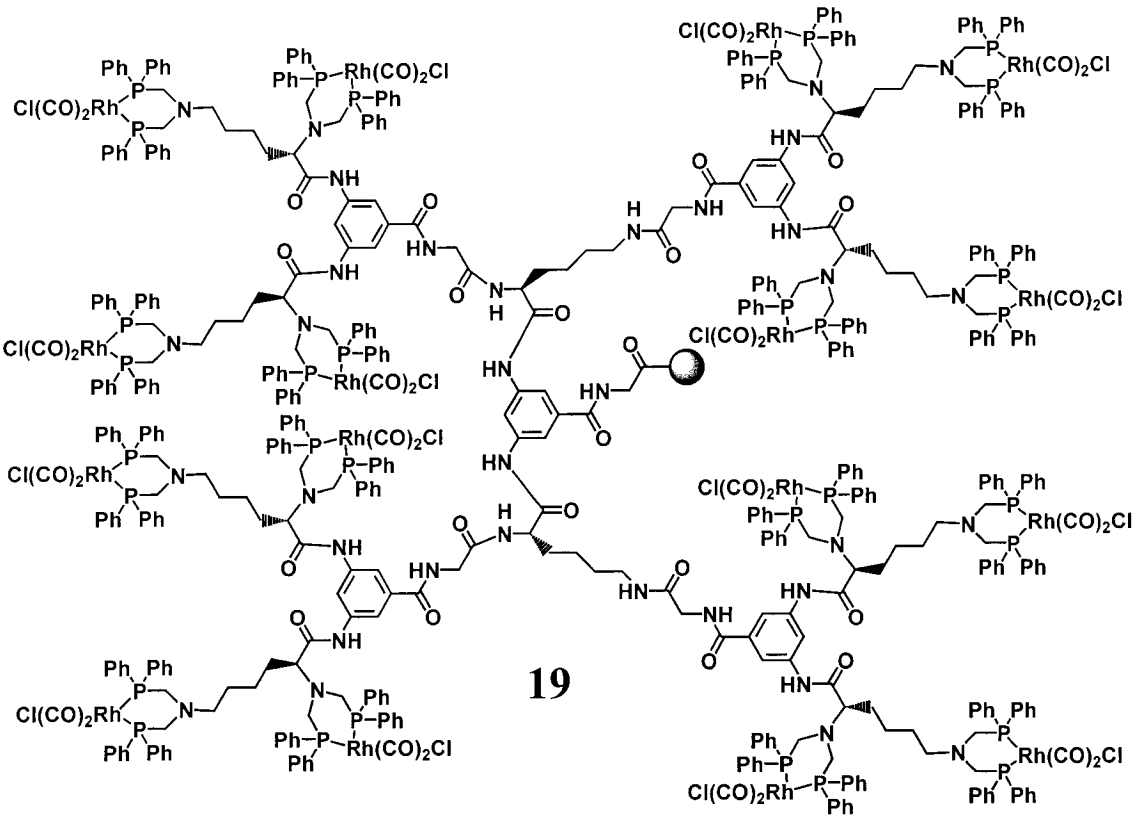

Figure 1-7. The G(2) glycine based dendrimer ligand supported on resin beads.[45]

These dendrimers constituted a significant improvement over the previous attempts with respect to activity, selectivity and recyclability. For the hydroformylation of styrene the G3 dendrimer (**19**) gave branched to linear ratios of 39:1 and could be recycled ten times at 25 °C without loss of activity. The catalysts were also tested with a variety of olefins and gave good activity and selectivity. The reaction conditions are remarkably mild for hydroformylation reactions.[45]

Lu and Alper also applied the glycine-based dendrimers to the carbonylative ring expansion of aziridines to form β-lactams. (Scheme 1-14.)

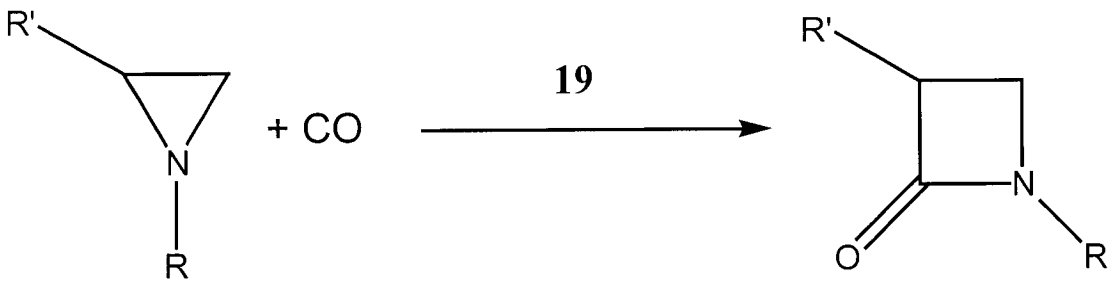

Scheme 1-14. Carbonylative ring expansion of aziridines with rhodium complexed dendrimers.[46]

The catalysts showed comparable activity with homogeneous equivalents, but the catalysts could be recycled effectively without significant loss of activity.[46]

In these first projects the utility of supported dendrimers as catalysts were clearly demonstrated. A lot of challenges were identified in using supported dendrimers.

1.4 Research objectives.

The research presented in this thesis is based on the assumption that supported dendrimer catalysts have immense potential as recyclable catalysts, but that the challenges intrinsic to these complexes must be addressed. The first and most important challenge was to develop a reliable measure of the growth of the dendrimers, as GPC and MS are not feasible techniques for supported species, a different approach had to be developed to determine reaction yields. This would allow quantification of the organic phase and give better insight into the structure and properties of these systems. Also the effect of the support was not understood and this will be addressed. The use of a multi-tier approach to the characterization was developed using methods from heterogeneous catalysis as our guide. We will present our effort towards understanding these systems chronologically by means of the development of characterization methods for specific catalytic processes.

The catalytic processes selected for this research is based on carbonylation chemistry. Carbonylation is immensely important, as synthesis gas (CO/H_2) is the principal feedstock for many catalytic operations. For example, the company SASOL produces millions of tons of synthesis gas annually and most is used to produce liquid fuels by the Fischer-Tropsch process. Significant amounts of olefins are also produced as side products of the FT process and these are separated and purified for use in polymer manufacture and other applications.

The dendrimer-metal complexes presented in this thesis were used as catalysts for carbonylation reactions of olefins.

1.4.1 Carbonylation chemistry.

Carbonylation chemistry involves using carbon monoxide as a synthon for the introduction of an extra carbon atom into the substrate. Carbonylation is considered an atom efficient process as the whole CO molecule is incorporated into the substrate.[47] Because of the rich chemistry of carbonyl complexes a multitude of variations exist on the theme and in this thesis we have already seen at least three. Two of the most important processes involving carbon monoxide are hydroesterification (scheme 15) and hydroformylation (scheme 16).

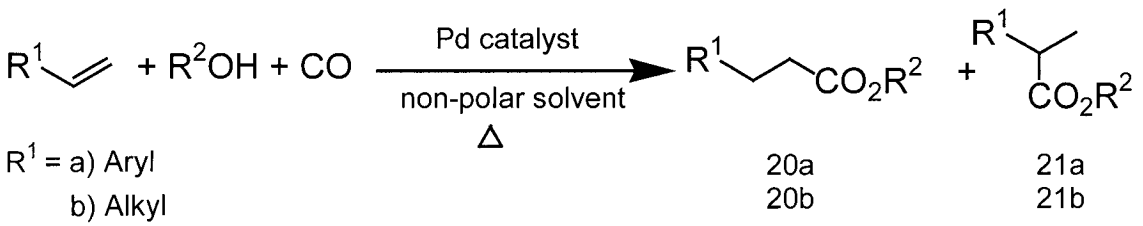

R1 = a) Aryl
b) Alkyl

20a
20b

21a
21b

Scheme 1-15. The hydroesterification reaction.

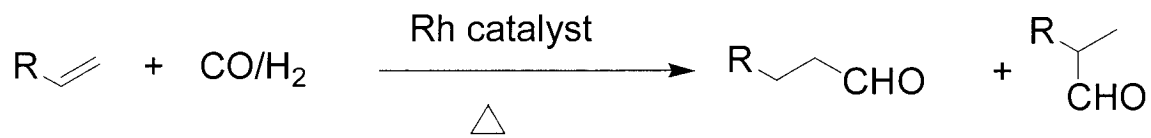

R = a) Aryl
b) Alkyl

22a
22b

23a
23b

Scheme 1-16. The hydroformylation reaction.

Hydroesterification is an important transformation as it adds significant value to olefins. The value lies in the fact that it introduces an extra carbon in the form of a useful ester functionality. On replacement of the alcohol with water the reaction is called hydrocarboxylation and introduces a carboxylic acid functional group into the olefin. The long chain aliphatic esters (**20a**, Scheme 1-15) are of particular interest for the petrochemical industry as these compounds can be used as lubricants and plasticizers.[48] The branched aromatic esters (**21b,** Scheme 1-15.) are of importance to the pharmaceutical industry as these compounds can be hydrolyzed to form nonsteroidal anti-inflammatory agents like Naproxen® and Ibuprofen®. Depending on the reaction conditions the target products can also be produced directly by hydrocarboxylation (Scheme 1-17.)[49]

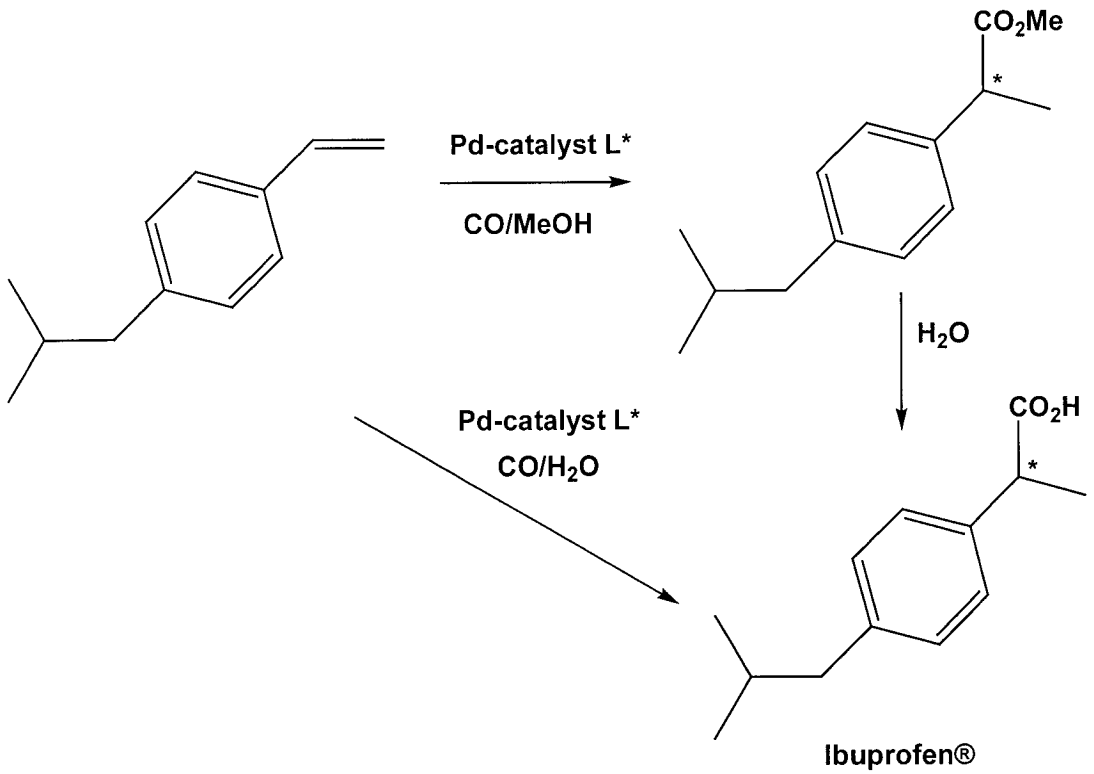

Scheme 1-17. Preparation of Ibuprofen® by hydroesterification followed by hydrolysis.

Palladium catalysts are the preferred catalysts for this reaction. The mechanism will be discussed later in the text when it becomes important to describe the optimization regime that was followed.

Hydroformylation (Scheme 1-16. oxo-synthesis) is closely related to hydroesterification, but the products are either aldehydes (usually) or alcohols depending on the catalyst system used. Otto Roelen detected the reaction for the first time in 1938 while working on heterogeneous cobalt based FT catalysts. The

catalyst was later determined to be homogeneous and the reaction came to be known as the OXO-synthesis.[50] Today this reaction is one of the most important industrial processes involving homogeneous catalysts. The reactions are usually conducted at temperatures between 40 and 120 °C and at total pressures between 10 and 100 atm in the presence of a catalytic amount of rhodium, cobalt or platinum. The importance of this reaction has increased significantly over the past 20 years or so. In 1980 5.2 Mt of oxo-aldehydes were produced and by 1995 this had increased to 6.6 Mt.[51] The value of this reaction lies in the utility of the aldehydes produced. The largest fraction of the products are directly reduced to alcohols (for instance n-butanol for solvent applications) or subjected to aldol condensation followed by reduction (to form 2-ethylhexanol for dioctyl phthalate (DOP) production).[52] The long chain alcohols, mainly C_{13}-C_{15}, are used as detergent alcohols.[53] Recently the reaction has spurred significant interest in the pharmaceutical industry for the preparation of valuable intermediates. Rhodium catalysts are usually favored due to the fact that rhodium has an activity of approximately 10^4 times that of cobalt.

The first hydroformylation plant was operated in Germany after the Second World War, but was not successful and it was dismantled. Exxon in the United States put a commercial plant on stream in 1948. This process used $Co_2(CO)_8$ as a precatalyst for the active species $HCo(CO)_4$. The process was operated at high pressures (200-300 atm) to stabilize the catalyst. Shell developed the first modified cobalt based process in the '60s. This process utilized phosphine ligand

modified cobalt catalysts and could be used at lower pressures. In the '70s Union Carbide and Celanese introduced phosphine modified rhodium catalysts for commercial processes. These catalysts were based on Wilkinson's catalyst ($RhCl(PPh_3)_3$). Various modified systems have been commercialized based on alkyl- and aryl phosphine modified rhodium catalysts. Ruhrchemie commercialized a biphasic system where the catalyst is immobilized in the water phase by using sulphonated phosphine ligands. This process is mainly used for the production of butanol, and is not suited to higher olefins.

As most of the modern hydroformylation plants rely on rhodium based catalysts we consider the mechanism of rhodium based hydroformylation.

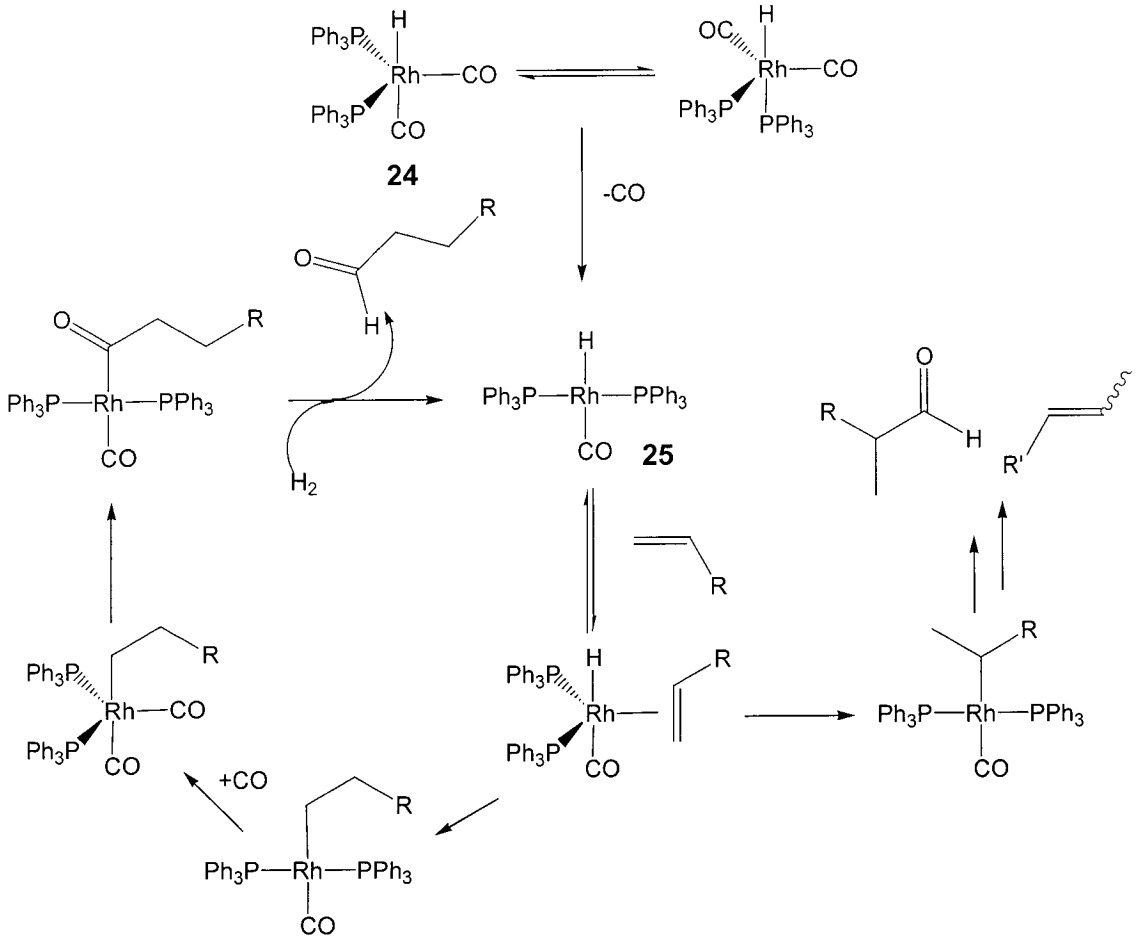

Scheme 1-18. Dissociative mechanism for the hydroformylation reaction.

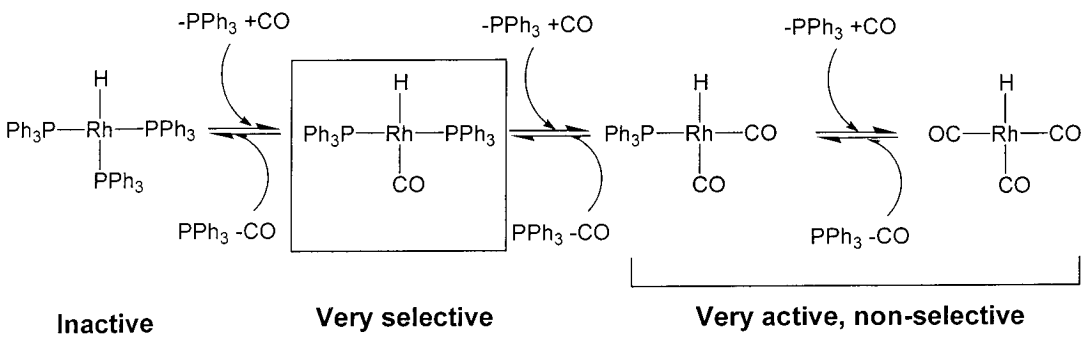

Scheme 1-19. The facile Rh-PPh_3 dissociation equilibrium in solution.

In the dissociative mechanism Complex **24** loses CO to form the key 16 e^- intermediate complex **25**. This is followed by alkene complexation to the metal center and olefin insertion into the Rh-H bond. CO binds to the metal center and inserts into the Rh-C bond. This is followed by reductive elimination on reaction with H_2. The high regioselectivity of the PPh_3-Rh system then arises not due to the 20 e- species as originally proposed[54] but by an equilibrium that exists due the facile Rh-PPh_3 bond. The dissociation of the Rh-PPh_3 bond leads to very active Rh-species in solution, but at the expense of regioselectivity. Therefore by increasing the molar concentration of PPh_3 and lowering the partial pressure of CO the highly selective catalyst is stabilized. (Scheme 1-19.)[55]

1.5 Thesis organization.

This thesis is organized both chronologically and by project. The rest of the thesis is subdivided into Section A and Section B, followed by the general experimental and concluding chapters.

Section A will cover the first project: Hydroesterification of olefins with C_6-PAMAM-dendrimers supported on silica. Section B will cover the second project: Hydroformylation of olefins with C_2-PAMAM dendrimers supported on mesoporous, and periodic mesoporous silica. Both sections are subdivided into two chapters; one covering the synthesis and characterization of the dendrimers and catalysts and the second covering the catalytic testing.

References for Chapter 1.

1. Moulijn J. A., van Leeuwen P. W. N. M., van Santen R. A., *Catalysis. An Integrated Approach to Homogeneous, Heterogeneous and Industrial Catalysis.* Elsevier Science Publishers B.V., Amsterdam, **1993**.
2. General biocatalysis references: (a). Burington J. D., Clark D. S., *Biocatalysis and Biomimetics*, ACS Symposium Series, Toronto, **1989**. (b) Abramowicz D. A., *Biocatalysis*, Van Nostrand Reinhold catalysis series, New York, **1990**. (c) Cabrel J M S., Best D., Boross L., Tramper J., *Applied Biocatalysis*, Harwood Academic Publishers, Chur, **1993**.(d) Schoemaker H.E., Mink D., Wubbolts M. G., *Science*, **2003**, 299, 1694.
3. Thomas J. M., Thomas W. J., *Principles and Practice of Heterogeneous Catalysis*, Wiley-VCH, Weinheim, **1997.**
4. (a) Bergbreiter D. E., *Chem. Rev.,* **2002**, 102 3345. (b) Saluzzo C., Lemaire M., *Adv. Synth. Catal.,* **2002**, 344, 915.
5. According to ACS Scifinder 539 patents on homogeneous catalysts were filed between 1982 and 1992 and 718 between 1993 and 2003 this constitutes an increase of 33 %.
6. Kakkar A. K., *Chem. Rev.,* **2002**, 102, 3579.
7. (a) Bromley S. T., Catlow C. R A., Maschmeyer T., *Cattech*, **2003**, 7, 164. (b) Isabel B. M., Collado M., Garcia-Verdugo E., Vincent M. J., Luis S. V., Graf von Keyserling N., Martens J., *Tetrahedron*, **2003**, 59, 1797. (c) Thomson S., Hoffmann C., Ruthe S., Schmidt H.-W., Schuth F., *Applied Catalysis, A: General*, **2001**, 220, 253. (d) Senkan, S. M., Ozturk S., *Angew. Chem. Int.*

Ed., **1999**, 38, 791.

8. (a) Keim W., *Green Chem.,* **2003**, 5, 105. (b) Park E. D., Lee K. H., Lee J. S., *Catalysis today,* **2000**, 63, 147. (c) Gao H., Angelici R. J., *J. Mol Cat. A: Chemical,* **1999**, 145, 83. (d) de Miguel Y. R., Brúle E., Margue R. G., *J. Chem. Soc., Perkin Trans. 1,* **2001**, 3085. (e) Yang H., Gao H., Angelici R. J., *Organometallics,* **2000**, 19, 622. (f) Davies I. W., Matty L., Hughes D. L., Reider P. J., *J. Am. Chem. Soc.,* **2001**, 123, 10139. (g) Li B., Li X., Asami K., Fujimoto K., *Energy & Fuels*, **2003**, 17, 810.
9. Mekelburger H., Jaworek W., Vögtle F., *Angew. Chem. Int. Ed. Engl.*, **1992**, 31,1571.
10. (a) Newkome G. R., Yao Z., Baker G. R., Gupta V. K., J. Org. Chem., **1985**, 50, 2003. (b) Newkome G. R., Baker G. R., Saunders M. J., Russo P. S., Gupta V. K., Yao Z., Miller J. E., Bouillion K., *J. Chem. Soc. Chem. Commun.*, **1986**, 752. (c) Newkome G. R., Yao Z., Baker G. R., Gupta V. K., Russo P. S., Saunders M. J., *J. Am. Chem. Soc.*, **1986**, 108, 849.
11. Flory P. J., *J. Am. Chem. Soc.*, **1952**, 74, 2718.
12. Buhleier E., Wehner W.,Vögtle F., *Synthesis*, **1978**,155.
13. (a) De Brabander-van den Berg E. M. M., Meijer E. W., *Angew. Chem. Int. Ed. Engl.*, **1993**, 32, 1308. (b) De Brabander-van den Berg E. M. M., Nijenhuis A., Mure M., Keulen J., Reintjens R., Vandenbooren F., Bosman B., de Raat R., Frijns T., v. d. Wal S., Castelijns M., Put J., Meijer E. W., *Macromol. Symp.*, **1994**, 77, 51.
14. Available from DSM Fine Chemicals as DAB- dendr.-$(NH_2)_x$ where x denotes

the number of end groups.

15. Tomalia D. A., Naylor A. M., Goddard III W. A., *Angew. Chem. Int. Ed. Engl.*, **1990**, 29, 138.

16. (a) Newkome G. R., Moorefield C. N., Baker G.R., Johnson A. L., Behera R. K., *Angew. Chem. Int. Ed. Engl.*, **1991**, 30, 1176. (b) Newkome G. R., Moorefield C. N., Baker G.R., Saunders M. J., Grossman S. H., *Angew. Chem. Int. Ed. Engl.*, **1991**, 30, 1178. (c) Newkome G. R., Moorefield C. N., Baker G.R., Behera R. K., Escamillia, G. H., Saunders M. J., *Angew. Chem. Int. Ed. Engl.*, **1992**, 31, 917.

17. (a) Hawker C. J., Fréchet J. M. J., *J. Am. Chem. Soc.*, **1990**, 112, 7638. (b) Gitsov I., Wooley K. L., Fréchet J. M. J., *Angew. Chem. Int. Ed. Engl.*, **1992**, 31, 1200.(c) Wooley K. L., Hawker C. J., Fréchet J. M. J. *J. Am. Chem. Soc.*, **1991**, 113, 4252. (d) Uhrich K. E., Fréchet J. M. J. *J. Chem. Soc. Perkin Trans 1*, **1992**, 1623.

18. Slaney M., Bardají M., Casanove M., Caminade A., Majoral J., Chaudret B., *J. Am. Chem. Soc.*, **1995**, 117, 9764.

19. (a) Bardají M., Kustos M., Caminade A., Majoral J., Chaudret B., *Organometallics*, **1997**, 16, 403. (b) Slaney M., Bardají M., Casanove M., Caminade A., Chaudret B., Majoral J., *Inorg. Chem.*, **1997**, 36, 1939. (c) Maraval V., Laurent R., Caminade A., Majoral J., *Organometallics*, **2000**, 19, 4025. (d) Caminade A., Laurent R., Chaudret B., Majoral J., *Coordination Chemistry Reviews*, **1998**, 178-180, 793.

20. Seyferth D., Son D. Y., Rhengold A. L., Ostrander R. L., *Organometallics*,

1994, 13, 2682.

21. (a) Denkewalter R. G., Kolch J., Lukasavage W. J., US Patent no 4 289 872, **1981**. (b) Twyman L., Beezer A., Mitchell J. C., *Tetrahedron Lett.*, **1994**, 35, 4423. (c) Gossage R. A., Jastrezbski J. T. B. H., van Ameijde J., Mulders S. J. E., Brouwer A. J., Liskamp R. M. J., van Koten G.,*Tetraherdron Lett.*, **1999**, 40, 1413.

22. Nagasaki T., Ukon M., Arimori S., Shinkai S., *J Chem. Soc., Chem. Commun.*, **1992**, 608.

23. (a) Roy R., Polymer News, **1996**, 21, 226. (b) Roy R., Kim J. M., *Tetrahedron*, **2003**, 59, 3881. (c) Colonna B., Harding V. D., Nepogodiv S. A., Raymo F. M., Spencer N., Stoddart J. F.,*Chemistry. Eur. J.,* **1998**, 1244.

24. (a) Achar S., Puddephatt R. J., *J Chem. Soc., Chem. Commun.*, **1994**, 1895. (b) Achar S., Puddephatt R. J., *Organometallics*, **1995**, 14, 1681.

25. (a) Jansen J. F. G. A., de Brabander-van den Berg E. M. M., Meijer E. W., Science, **1994**, 266, 1226. (b) Jansen J. F. G. A., Meijer E. W., de Brabander-van den Berg E. M. M., *J. Am. Chem. Soc.*, **1995**, 117, 4417.

26. General reviews of dendrimers in catalysis: (a) Matthews O. A., Shipway A. N., Stoddard J.E., Progress in Polymer Sci., **1998**, 23, 1. (b) Oosterom G. E., Reek J. N. H., Kamer P. C. J., van Leeuwen P. W. N. M., *Angew. Chem. Int. Ed.,* **2001**, 40, 1828. (c) Astruc D., Chardac F., *Chem. Rev.*, **2001**, 101, 2991. (d) Kreiter R., Kleij A. W., Klein Gebbink R. J. M., van Koten G., *Topics in Current Chemistry*, Vol. 217, Springer-Verlag, Berlin, Heidelberg, **2001**, 164. (e) van Heerbeek R., Kamer P. C. J., van Leeuwen P. W. N. M Reek J. N. H.,

Chem. Rev., **2002**, 102, 2991.

27. (a) Percec V., Kawasumi M., *Macromolecules,* **1992**, 25, 3843. (b) Percec V., Chu P., Kawasumi M., *Macromolecules,* **1994**, 27, 4441. (c) Kwon Y. K., Chvalun S. N., Blackwell J., Percec V., Heck J. A., *Macromolecules,***1995**, 28, 1552. (d) Percec V., Chu P., Ungar G., Zhou J., *J. Am. Chem. Soc.*, **1995**, 117, 11441. (e) Stebani U., Lattermann G., Wittenberg M., Wendorff H., *Angew. Chem. Int. Ed. Engl.,* **1996**, 35, 1858. (f) Watanabe S., Regen S. L., *J. Am. Chem. Soc.*, **1994**, 116, 8855. (g) Bar G., Cutts R. W., Taylor T. N., Zawodzinski T. A., *Langmuir*, **1996**, 12, 1172.

28. (a) Kuzdzal S. A., Monnig C. A., Newkome G. R., Moorefield C. N., *J Chem. Soc., Chem. Commun.*, **1994**, 2139. (b) Singh P., Moll F III, Lin S. H., Ferzli C., Yu K. S., Saul R. G., Cronin P., *Clin Chem.,* **1994**, 40, 1845. (c) Ispasoiu R. G., Balogh L., Varnvski O. P., Tomalia D. A., Goodson T., III, *J. Am. Chem. Soc.,* **2000**, 122, 11005.

29. (a) Roberts J. C., Bhalgat M. K., Zera R. T., *J. Biomed. Mater. Res.,***1996**, 30, 53. (b) Weiner E. C., Auteri F. P., Chen J. W., Brechbiel M. W., Gansow O. A., Schneider D. S., Belford R. L., Clarkson R. B., Lauterbur P. C., *J. Am. Chem. Soc.*, **1996**, 118, 7774. (c) Hawthorne M. F., *Angew. Chem. Int. Ed. Engl.,* **1993**, 32, 950.

30. Zhou L., Russell D. H., Zhao M., Crooks R. M., *Macromolecules*, **2001**, 34, 3567-3573.

31. Keijsper J. J., van Leeuwen P. W. N. M., van der Made A. W., *European Patent*, EP 0456317, **1991**.

32. Knapen J. W. J., van der Made A. W., de Wilde J.C., van Leeuwen P. W. N. M., Wijkens P., Grove D. M., van Koten G., *Nature*, **1994**, 372, 659.

33. Kleij A.W., Gossage R.A., Jastrzebski J. T. B. H., Boersa J., van Koten G., *Angew. Chem Int. Ed.*, **2000**, 39, 176.

34. Gossage R.A., Jastrzebski J. T. B. H., van Ameijde J., Mulders S. J. E., Brouwer A. J., Liskamp R. M. J., van Koten G.,*Tetrahedron Lett.*, **1999**, 40, 1413.

35. Oosterom G. E., van Haaren R. J., Reek J. N., Kamer P. C. J., van Leeuwen P. W. N. M., *Chem, Commun.*, **1999**, 1119.

36. Reetz M. T., Lohmer G., Schwickardi R., *Angew. Chem Int. Ed.*, **1997**, 36, 1526.

37. Ropartz L., Morris R. E., Foster D. F., Cole-Hamilton D. J., *Chem, Commun.*, **2001**, 361.

38. Garber S. B., Kingsbury J. S., Gray B L., Hoveyda A. H., *J. Am. Chem. Soc.*, **2000**, 122, 8168.

39. Gitsov I., Ivanova P. T., Frechét J. M. J., *Macromol. Rapid Commun.*, **1994**, 15, 387.

40. Bourque S. C., Maltais F., Xiao W., Tardif O., Alper H., Arya P., Manzer L.E., *J. Am. Chem. Soc.*, **1999**, 121, 3035-3038.

41. Alper H., Arya P., Bourque S. C., Jefferson G.R., Manzer L.E., *Can. J. Chem.*, 2000, 78, 920-924.

42. Antebi S., Arya P., Manzer L.E., Alper H., *J. Org Chem.*, **2002**, 67, 6623-6631.

43. Arya P., Rao N. V., Singkhonrat J., Alper H., Bourque S. C., Manzer L. E., *J. Org. Chem.*, **2000**, 65, 1881.

44. Arya P., Panda G., Rao N. V., Alper H., Bourque S. C., Manzer L. E., *J. Am. Chem. Soc.*, **2001**, 123, 2889.

45. Lu S.-M., Alper H., *J. Am. Chem. Soc.*, **2003**, 125, 13126.

46. Lu S.-M., Alper H., *J. Org. Chem.*, **2004**, 69,3558.

47. El Ali B., Alper H. in Beller M., Bolm C., *Transition Metals for Organic Synthesis,* Vol 1, Wiley-VCH, **1998**, 49.

48. Cole-Hamilton D. J., *Science*, **2003**, 299, 1702.

49. (a) Alper, H., Hamel, N., *J. Am. Chem. Soc.,* **1990**, *112*, 2803. (b) Alper, H., *Aldrichchimica Acta*, **1991**, *24*, 3.

50. (a) O. Roelen, German Patent 849,548, **1938**. (b) O. Roelen, U. S. Patent 2,327,066, **1943**. (3) Adkins H., Kresek, *J. Am. Chem. Soc.,* **1949**, 71, 3051.

51. Botteghi C., Marchetti M., Paganelli S., in Beller M., Bolm C., *Transition Metals for Organic Synthesis Volume 1*, Wiley-VCH, Weinheim, **1998**, p 25.

52. (a) Green C. R., U. S. Patent 3,278,612, **1966**. (b) Hughes O.R., Hillman M., U. S. Patent 3,821,311, **1974**.

53. Pruett R. L., *Advances in Organometallic Chemistry*, **1979**, Vol. 17, 1.

54. Cotton F. A., Wilkinson G., Gaus P. L., *Basic Inorganic Chemistry 3rd Ed.,* John Wiley & Sons, 1995, 718.

55. Pruett R. L., Smith J. A., *J. Org. Chem.*, **1969**,34, 327.

Section A:

Hydroesterification of olefins catalyzed by Palladium-Complexed C_6-PAMAM dendrimers supported on silica

Chapter 2. *Preparation of Palladium-Complexed C_6-PAMAM Dendrimers Immobilized on Silica as Catalysts for the Hydroesterification of Olefins*

2.1 Introduction:

The hydroesterification reaction is usually catalyzed by homogeneous palladium catalyst systems. These systems generally are composed of palladium (II) centers in conjunction with phosphine ligands in an acidic media. We therefore focused on preparing palladium complexed dendrimers. From previous work it is clear that phosphomethylated PAMAM dendrimers supported on silica could be used for the complexation of various metals including palladium. The system developed here is based on this idea.

Work in our laboratory demonstrated that the best recyclable PAMAM dendrimer based catalysts for the hydroformylation were prepared using 1,6-diaminohexane (C_6) linkers.[1] We therefore set out to prepare dendrimers on silica with C_6 linkers as a starting point. Before complexation could be attempted various questions arose. The development of dendrimers on supports were at an early stage and although many dendrimers had been synthesized before, the only characterization methods available were solid state NMR and metal ICP-MS. The objective of this work was therefore to elucidate the structure of the support and the dendrimers so as to secure more evidence for the structure of these

molecules, and to attempt to address some of the issues that arose previously. For example, it was noted that higher dendrimers essentially suffer reduced activity in the phosphomethylation step (and therefore also in the complexation and catalytic steps). It was speculated that this was due to steric interactions exacerbated by the increasing bulk of the dendrimer, but no concrete evidence for this existed. The only measure of the activity of the catalysts was inductively coupled plasma mass spectroscopy (ICP-MS) analysis of the metal but no information was available on the extent of phosphomethylation or complexation of the dendrimer ligands.[2] The heterogenization of catalysts for hydroesterification is further complicated by the fact that there exist different proposals for the mechanism of this reaction. Various palladium complexes were prepared and tested. In this chapter the preparation of silica supported C_6-PAMAM dendrimers and palladium catalysts based on supported C_6-PAMAM dendrimers will be presented, with catalyst evaluation being presented in the next chapter.

2.2 Results and Discussion:

As with any catalytic system the complex loaded into the reactor usually represents only the pre-catalyst. The active catalyst can be significantly different. After normal deactivation the active catalyst is transformed into a resting state, which can be reactivated under the right conditions to regenerate the active species. With supported dendrimer catalysts the situation becomes more complicated. In conventional heterogeneous catalysis the deactivated catalyst

must be reactivated by some external process like calcination, reduction or oxidation. Some catalysts must be treated with an activating substance before the reaction[3]. In the case of the supported dendrimer catalyst with highly active metals like rhodium, this problem does not seem to be a significant factor. As soon as more complex reactions with less active metals are attempted, like the hydroesterification reaction with palladium for instance, the resting state becomes very important. It is essential that the resting state of the catalyst be reactivated under the reaction conditions, to assure high catalytic activity in subsequent cycles.

Palladium catalysts are difficult to characterize due in part to the fact that palladium is not NMR active. Previous attempts to elucidate the mechanism of this reaction have been hindered by this fact. However by studying the accepted proposed mechanisms it is possible to predict what possible resting states the catalyst would form. [4,5,6] The greater part of this research was devoted to the search for a pre-catalyst and reaction conditions, under which a resting state that could be reactivated in subsequent cycles is generated.

2.3 Preparation and characterization of palladium complexed-PAMAM-SiO_2 dendrimers.

Polyamidoamine (PAMAM) dendrimers, up to the 4th generation (Figure 2-1.), on commercial aminopropyl silica gel (0.9 mmol $\pm$0.1 amine groups/g), were prepared using a modified literature method.[1] The preparation involves two

steps: 1. Exhaustive Michael addition of methylacrylate to the aminopropyl silica gel. 2. Amidation of the methylester groups with 1,6-diaminohexane. Both reactions are performed in methanol under a nitrogen atmosphere at 50 °C. The two steps are repeated to yield the higher generation dendrimers. (Scheme 2-1.) With every repeat reaction the reagent is increased to compensate for the increasing functional groups on the dendrimer that are available to react.

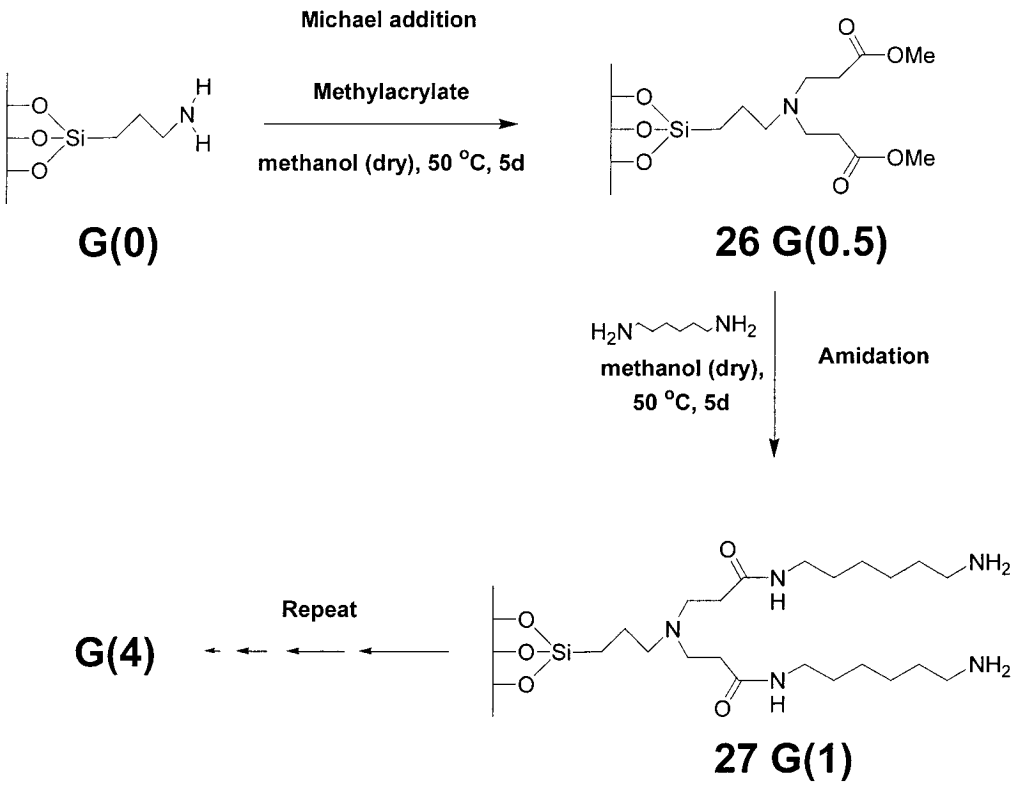

Scheme 2-1. Synthesis of C_6-PAMAM dendrimers on silica.

The dendrimers were phosphinomethylated using diphenylphosphine and paraformaldehyde by modification of literature methods.[7] The double

phosphinomethylation of the terminal amine groups of the dendrimers was achieved by reacting the dendrimers with diphenylphosphinomethanol prepared in situ from diphenylphosphine and paraformaldehyde in toluene (110 °C, 48 h). The resulting phosphinomethylated dendrimers were characterized by solid state ^{31}P and ^{13}C NMR, e g a chemical shift of –27.5 ppm in the ^{31}P NMR spectrum compares well with previously reported systems.[1] The phosphinomethylated dendrimers were readily complexed on treatment with the appropriate palladium complexes in toluene (rt., 1-2h under argon). The silica turns deep orange to blood red, and decolorization of the supernatant solvent was used as an indication of the extent of complexation (Scheme 2-2.).

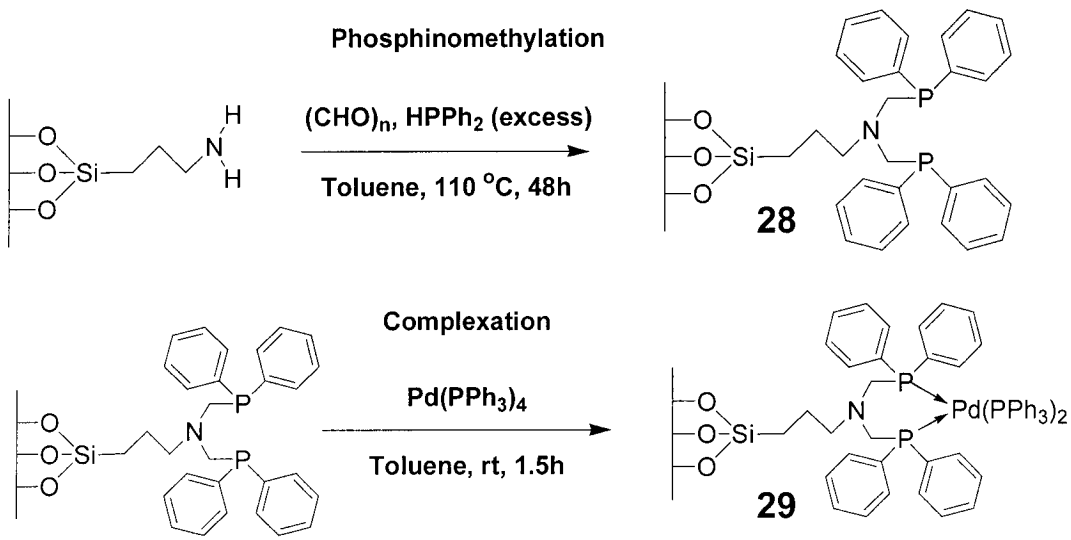

Scheme 2-2. Phosphinomethylation and complexation of G(0) aminopropyl silica gel.

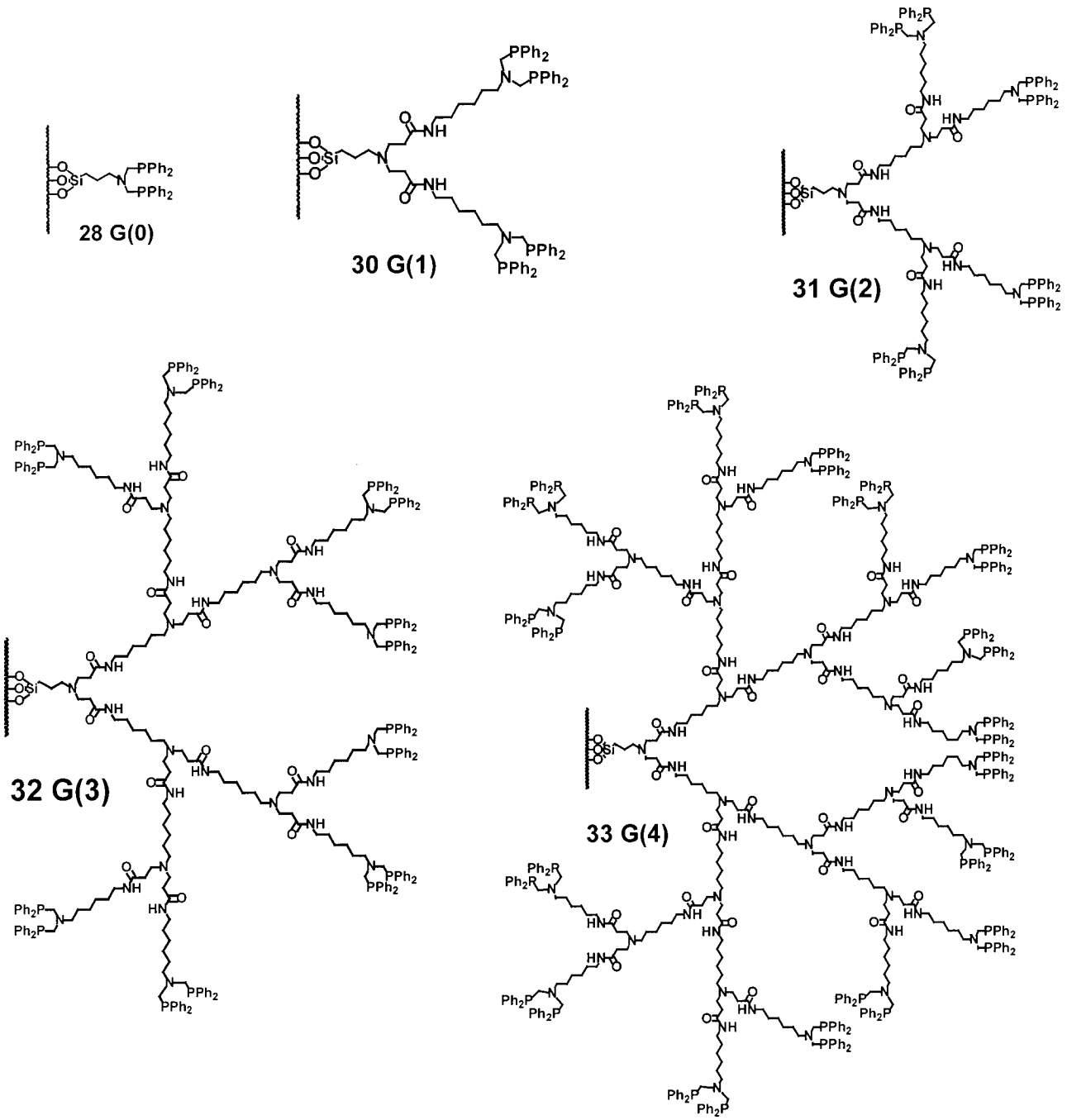

Figure 2-1. Proposed structure of the phosphonated generation zero through four PAMAM-silica dendrimer ligands (C6-linker).

2.4 The characterization of dendrimers on silica.

Due to the heterogeneous nature of the catalysts, usual dendrimer characterization methods like MS and GPC could not be employed. For this reason we developed new methods. We also used established methods like ^{13}C and ^{31}P NMR spectroscopy.

2.4.1 NMR and ICP-MS analysis.

^{13}C and ^{31}P NMR were used to elucidate the structure, and palladium and phosphorus ICP-MS analysis was done to quantify the amount of palladium and the extent of phosphinomethylation of the catalysts. A solid state NMR internal standard method (methyltriphenylphosphonium bromide as the internal standard) for the rapid quantification of the extent of phosphinomethylation was also developed. This proved essential in estimating the amount of palladium to be used for the complexation. (Table 2-1.).

The internal standard NMR method was developed to assist in the rapid determination of the extent of phosphinomethylation as the ICP-MS analysis could not be done in-house and takes several weeks.

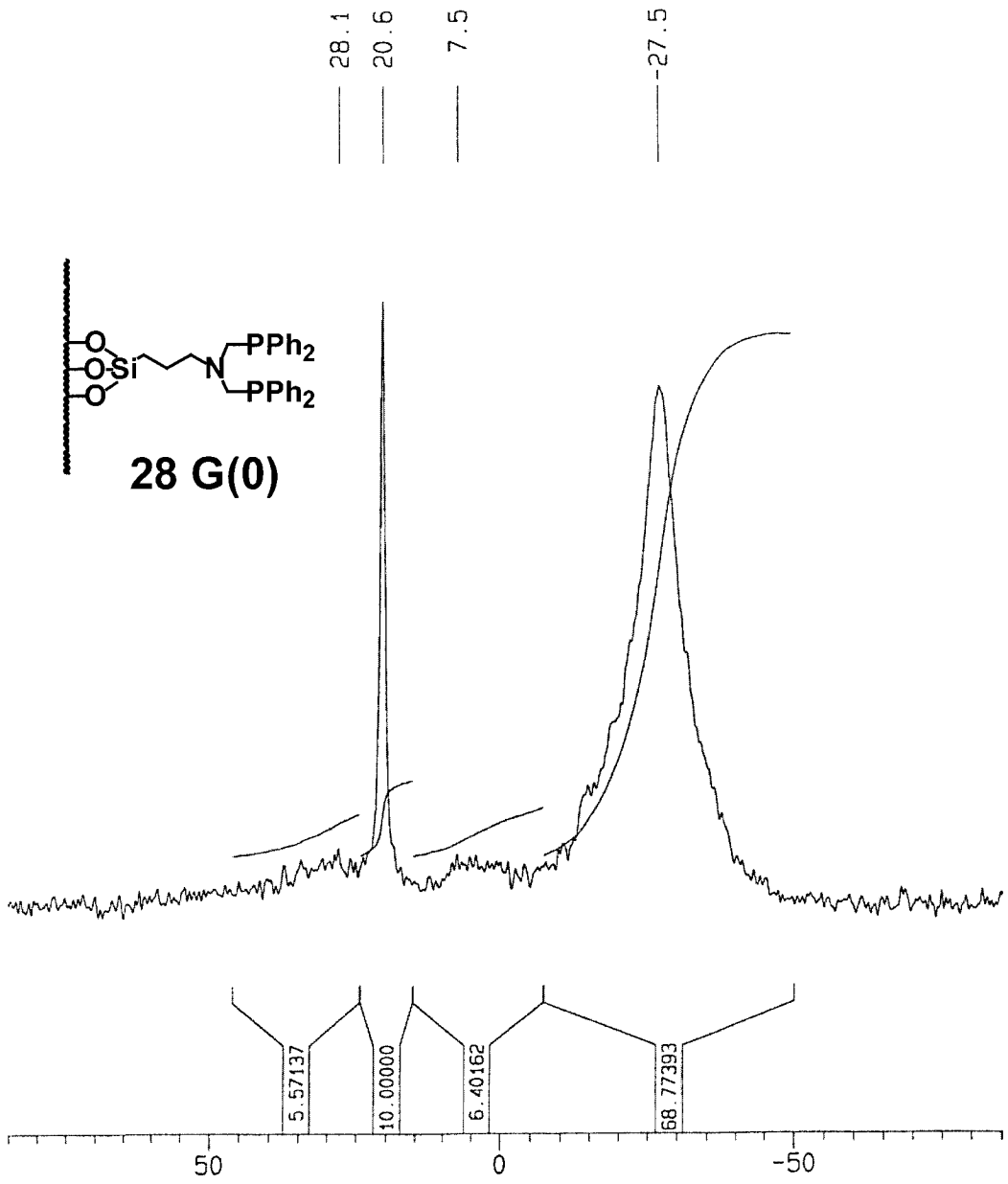

Figure 2-2. ^{31}P NMR spectrum of the phosphinomethylated G(0) complex (28) showing the internal standard methyltriphenylphosphonium bromide.

Methyltriphenylphosphonium bromide was selected as the internal standard for the NMR experiments, because it is readily available, relatively cheap and quite stable.

The ^{31}P signal for methyltriphenylphosphonium bromide (+20.6 ppm) is significantly different from the ^{31}P signal for the phosphinomethylated dendrimers (-27.5 ppm, Figure 2-2.). In order to operate an NMR spectrometer in quantitative mode, T_1-relaxation times of all the phosphorus atoms in the matrix had to be determined, after this the recycle delay in the pulse sequence has to be set to at least 5 times the value of the largest T_1-relaxation time. This ensures that all phosphorus magnetization returns to its equilibrium and that all the contributions to the signal are recorded. When applying this method to liquid NMR samples very few analytical methods are as accurate, but with solid samples one has to be very vigilant in ensuring that a proper homogeneous mixture of the substrate and the standard is achieved. Nonetheless this method worked beautifully, except for one problem. The acquisition times for these experiments were exceedingly long (a few days) and as the substrate phosphines are very air sensitive, great care had to be taken to ensure that the phosphine does not oxidize during the acquisition period. In solid state MAS-NMR, cross polarization is often employed to circumvent this problem. Cross polarization involves the excitation of abundant protons, and then the proton magnetization is transferred to the ^{31}P atoms. The detector of the spectrometer is set to detect the principal atom's magnetization (^{31}P in this case), which is enhanced by the ^{1}H-^{31}P

magnetization transfer, the data collection time is significantly decreased compared to direct excitation. The only problem is that cross polarization cannot be run quantitatively because different atoms cross polarize at different rates. Thus the only way to correct for this is to determine both quantitative spectra and CP-spectra and calculate the difference. This process can be likened to the determination of retention factors in GC-quantification, where the detector sensitivity is a function of the molecule being detected. As long as one knows the difference factor, and the substrates being tested, any detector can be used for quantitative analysis. We therefore determined the difference, and to our surprise the substrate and the standard had very similar CP-characteristics, with the difference being less than 5 %. We were then able to use the CP-method directly for a quick estimation of the phosphine-groups. The ^{31}P quantitative NMR method could not be used for the determination of the amount of phosphine in the complexed species due to the fact that the ^{31}P signal for the standard falls in the region of the phosphine groups attached to palladium centers. For these samples the phosphorus ICP-MS method was used exclusively. ICP-MS is the most accurate method. Both values for the various dendrimers are represented in Table 2-1.

It is clear from Table 2-1 that the extent of phosphomethylation differed from the theoretical expectations, and several reasons for this are plausible: 1. Some of the amino groups on the aminopropyl silica gel used for the synthesis of the dendrimers might reside in the pores of the support and would therefore lead to

ineffective growth of the dendrimers due to steric hindrance and would then lead to ineffective phosphinomethylation. 2. It is statistically probable that the growth of the dendrimers (whether inside the pores or outside) is not complete[8] and therefore more than likely resemble highly branched polymers instead of dendrimers. This in turn leads to a smaller amount of free amines available for phosphinomethylation. 3. Higher generations of dendrimers grafted to the silica surface should be subject to crowding at the periphery leading to further steric congestion and possible back folding making fewer free amines available for phosphinomethylation.[9]

Table 2-1. ICP-MS and quantitative ^{31}P NMR analysis of different generations of the $Pd(PPh_3)_2$ -PAMAM-silica catalysts.

Entry	Generation	P_{ICP-MS} (mass %)	P_{NMR} (mass %)	P_{Theory} (mass %)	P_{ICP-MS} / P_{Theory}	Pd_{ICP-MS} (mass %)	Pd_{used} (mass %)
1	G(0)	1.11	1.19-1.44	4.1	0.27	-	-
2	G(0) $_b$	-	-			0.96	1.29
3	G(1)	1.57	0.691-0.993	5.5	0.28	-	-
4	G(1) $_b$	-	-			0.74	0.79
5	G(2)	1.38	1.13-1.25	4.15	0.33	-	-
6	G(2) $_b$	-	-			0.96	1.32
7	G(3)	1.96	0.562-0.870	4.43	0.44	-	-
8	G(3) $_b$	-	-			0.99	1.31
9	G(4)	1.90	0.75	4.59	0.41		
10	G(4)$_b$	-	-			0.88	1.29
11[a]	G(0)	1.74	1.70-1.997	4.1	0.42		
12[a]	G(4)	1.37	0.951-1.43	4.59	0.298		

Note: a) refers to previously prepared dendrimer samples b) refers to Pd-complexed dendrimers.

A solid-state ^{13}C NMR method was developed to assess the extent of growth of the dendrimers. The process is quite straightforward, and is derived from a method developed by Mayoral[18] for his phosphorus containing dendrimers. If the dendrimer grows perfectly, the ratio of the integral of the aliphatic carbons to the integral of the carbonyl carbon in the PAMAM backbone will be a function of the generation, with the ratio declining over the generations. As we cannot determine the absolute value of the aliphatic carbons associated with the aminopropyl silica gel alone (there is no carbonyl carbon in the structure of aminopropyl silica gel), we have to correct the theoretical value for G(1), with the experimental values of G(1). The method indicates a trend for the growth of the G(2) –G(4) dendrimers. The correction factor was determined to be 13.6. This is most likely due to the methyl capping of the aminopropylsilica gel. Data for the higher generations was then calculated with this value as a correction in the G(1) theoretical value.

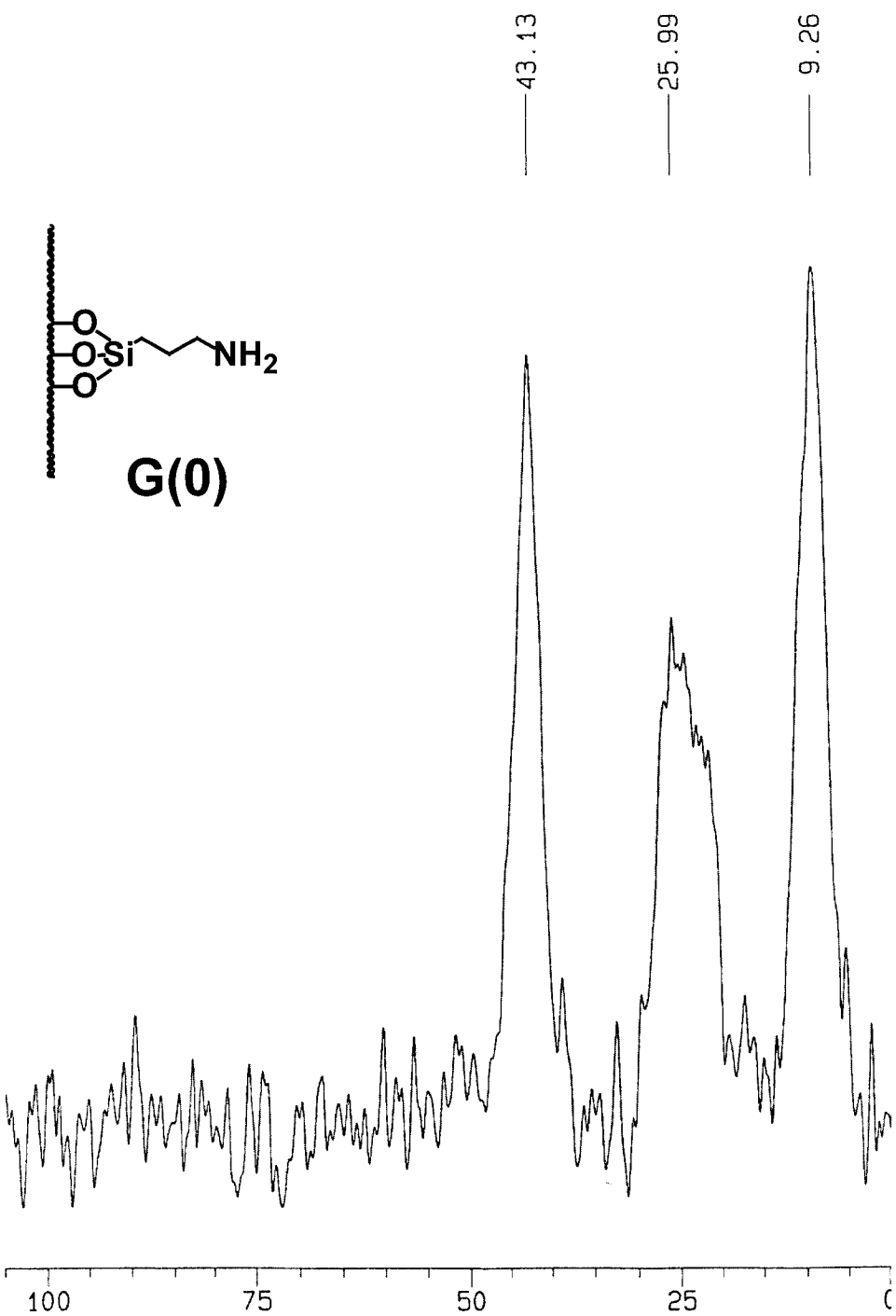

Figure 2-3. ^{13}C CP/MAS NMR spectrum of aminopropyl silica gel (G(0)).

To clarify the results further we also calculated a 50 % growth column based on the assumption that only one branch grows for each branching point (and not two as in the perfect dendrimer). The results can be seen in Table 2-2.

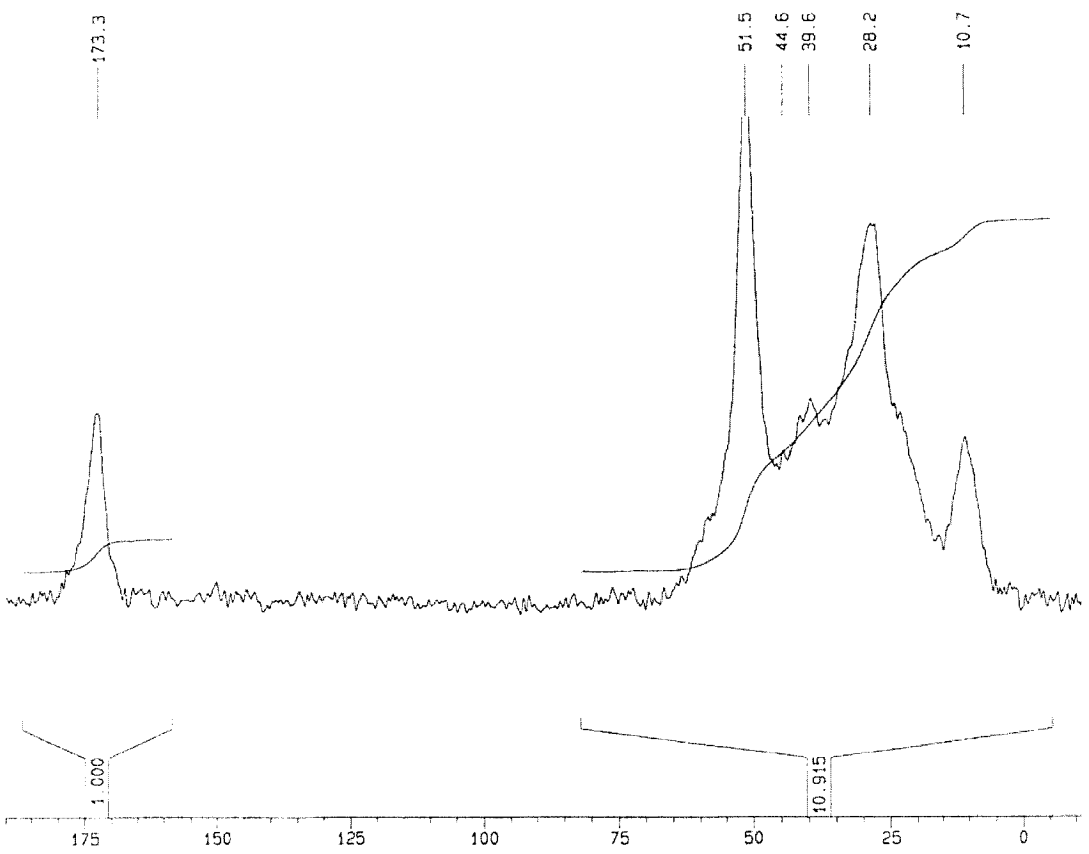

Figure 2-4. ^{13}C CP/MAS NMR spectrum of G(4)C_6 PAMAM dendrimer supported on silica gel.

Cross-polarized magic angle spinning (CP/MAS) ^{13}C NMR was used in this study for the identification of functional groups. Representative ^{13}C NMR spectra are shown in Figure 2-3 and 2-4. Figure 2-3 is the ^{13}C NMR for the aminopropylsilica gel (G(0)). In this case, three signals were obtained at 9.26 ppm, 25.99 ppm and 43.13 ppm. They were attributed to the three carbons between the Si atom and the nitrogen, with increasing distance from the Si atom leading to a higher ppm value. Figure 2-4 is the ^{13}C NMR spectrum of the G(4) dendrimer species on silica. The signal at 50.5 ppm corresponds to carbons attached directly to nitrogen in the hexamethylenediamine species, with the broadening of the aliphatic region corresponding to the other carbons in the hexamethylenediamine moiety at 28.2 and 39.6 ppm. The signals for the two remaining carbons from the aminopropylsilane are now much smaller at 10.7 and 44.6 ppm. This spectrum shows that the amide signal at 173.3 ppm, although clearly visible and large, is subject to considerable line broadening and therefore does not allow for clear distinction between amide and ester groups in the molecule. This is a limitation of the ^{13}C NMR technique because the full generations were prepared by changing ester groups into amide groups and should therefore only contain amides. It is thus impossible to ascertain from ^{13}C NMR if full conversion between half generations and full generations was accomplished. The ratios used in the quantitative ^{13}C calculations can also be seen in Figure 2-4.

Table 2-2. Quantitative ^{13}C NMR study of PAMAM-silica dendrimers.

Generation	Integral (aliphatic)	Integral (carbonyl)	Ratio	Theoretical Ratio	Difference[a]	Corrected theoretical	50% growth[b]
1	23.138	1	23.138	9.5	13.6	23.138	23.138
2	14.869	1	14.869	8.5	-	10.771	13.55
3	14.186	1	14.186	8.2	-	9.188	11.32
4	10.915	1	10.915	8.1	-	8.550	9.84

a) Excess carbon due to methyl capping of the silanol groups on the surface of the support.

b) Determined based on the assumption that only one branch, instead of two, grows at each branching point (thus 50 % growth).

This table demonstrates also that lower than expected growth of dendrimers is observed.

As the growth of the dendrimers was not complete another characterization method was required to verify the ICP-MS and NMR results.

2.4.2 Degree of growth as determined by TGA.

To quantitatively determine the degree of growth of the dendrimer, a function D, defined as follows, is proposed.

$$D = M(d)/ M_t(d)$$

Where D is the degree of growth of the dendrimer,

M(d) is the mass of the dendrimer per gram of silica and $M_t(d)$ is the theoretical mass of the dendrimer per gram of silica.

To assess D a Thermal Gravimetric Analysis (TGA) study was undertaken. The results are summarized in Table 2-3.

Table 2-3. Degree of growth as determined by TGA analysis.

Entry	Generation	Organic Mass (TGA) (%)	Mass Theoretical $M_t(d)$ (%)	Difference (correction factor)[a]	Corrected TGA Mass M(d) (%)	Degree of Growth $M(d)/ M_t(d)$
1	0	7.03	5.22	1.81	5.22	N/A
2	1	18.36	27.4	1.81	16.55	0.604
3	2	19.24	50.58	1.81	17.43	0.345
4	3	23.835	69.8	1.81	22.03	0.316
5	4	26.05	83.04	1.81	24.24	0.303

a) Excess carbon due to methyl capping of the silanol groups on the surface of the support.

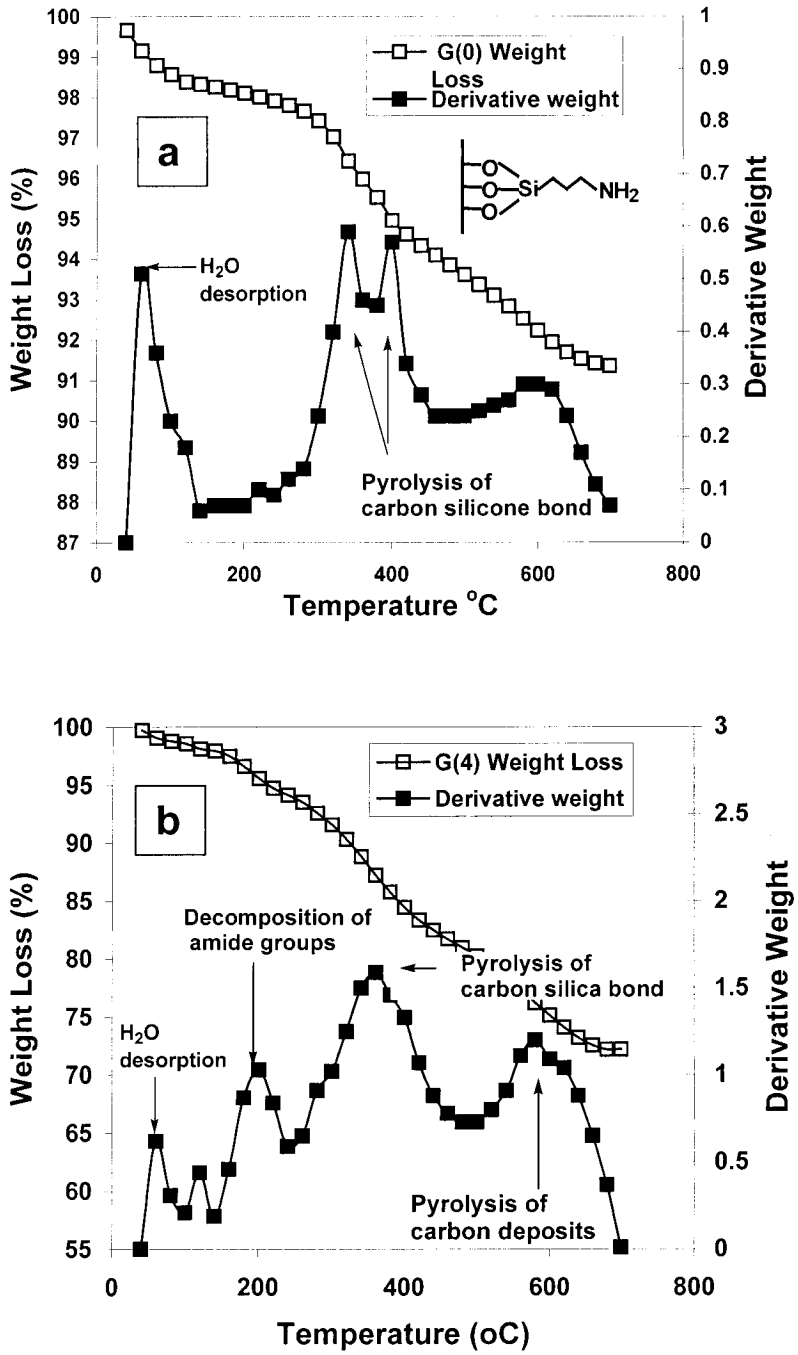

Figure 2-5. TGA with derivative mass for (a) G(0) and (b) G(4) showing regions of desorption.

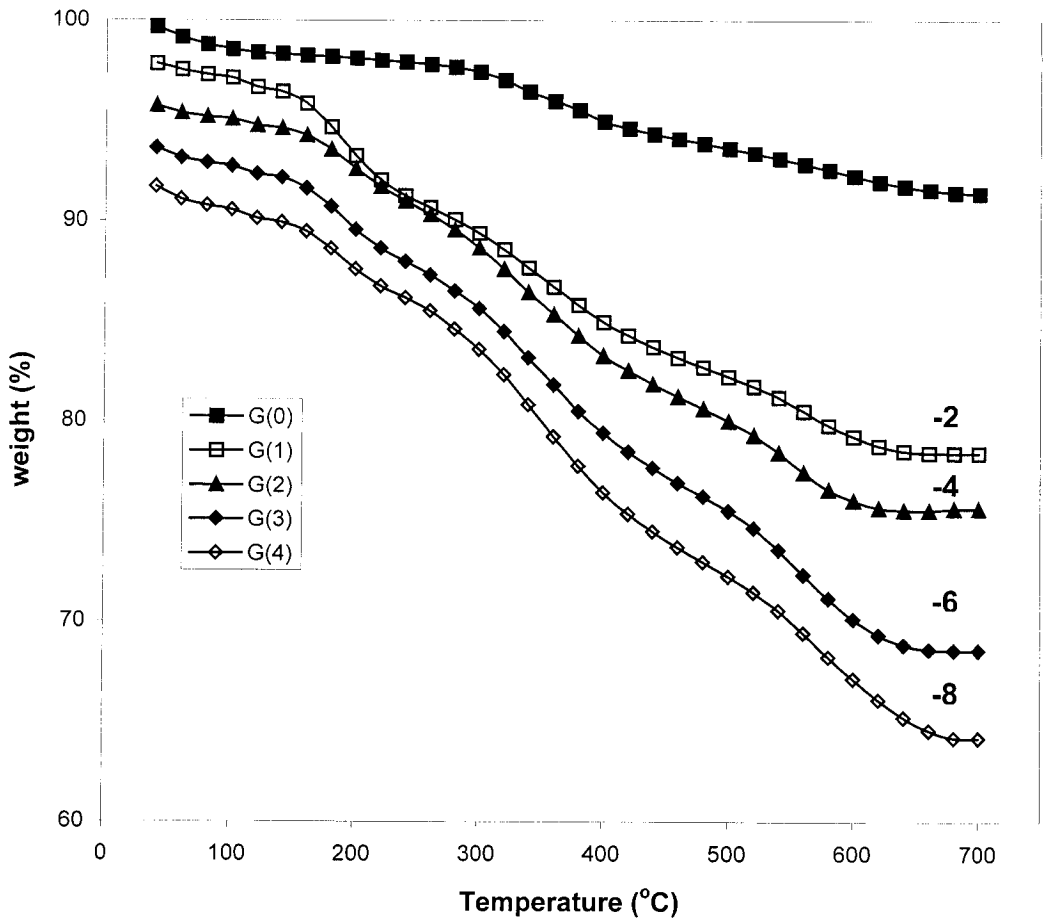

Figure 2-6. TGA of G(0)-G(4) silica supported PAMAM dendrimers

The TGA method is based on the fact that when organic molecules are attached to the surface of an inert solid like silica, they will decompose on heating and even pyrolise in air, leaving the silica support essentially intact. TGA spectra are very useful as they are essentially quantitative in nature. For instance one can determine exactly the percentage of water adsorbed on a surface by this method, as water usually desorbs in a specific temperature range. In this case all the

water desorbs below 150 °C, with most desorbing below 120 °C. The temperature at which desorption occurs, and the amount of substrate desorbed can be used as a measure of the affinity of the substrate for the surface, or the strength of the bond between the surface and the substrate in the case of covalently bonded substrates. All the data in Table 2-3 were calculated by only using the mass loss due to the organic molecules decomposing, and therefore not using the temperature range where water desorbs. The aminopropyl groups of the G(0) complex decompose at 350 °C and the resulting carbonaceous deposits combust at approximately 600 °C. In the TGA spectrum of the G(4) dendrimer an extra peak appears at approximately 200 °C, which is assigned to the amide groups of the dendrimer (Figure 2-5.). The theoretical data were calculated on the basis of the perfect molecule growing on the surface, with the amine loading of the G(0) species as our starting point. The TGA spectra for G(0)-G(4) are presented together in Figure 2-6.

As can be seen in Table 2-3. the degree of growth of the dendrimers is about 0.3-0.6 for the different generations. Therefore about 30 % growth is detected for the higher generations of the dendrimers. This is in accord with the NMR and ICP-MS analyses. It is well documented that the divergent growth approach to the synthesis of dendrimers can lead to flawed dendrimer species. Statistically only a small fraction of the higher generations will be perfect.[10] The following relationship can be used to calculate the yield per reaction: as $OY = (AY)^x$, where x is the number of reactions involved and OY is the overall yield and AY is the

average yield per reaction. Thus, AY = $(OY)^{1/x}$. In the case of the G(4) dendrimer, AY = $(0.303)^{1/60}$ = 0.98. This shows that although the overall yield of the dendrimer at G(4) is only 30.3% the average yield per reaction is in excess of 98%. In this instance a further complication results due to the fact that we are working on a solid support, and therefore separation of imperfect dendrimers is not feasible. Furthermore, some dendrimers might reside inside the pores, and therefore not grow perfectly, also leading to lower D values.

2.4.3 Nitrogen adsorption-desorption analysis.

To test the structural limitations of the support, BET surface areas, pore volumes and pore diameters of the different generations were determined. The results are presented in Table 2-4. It is interesting to note that the surface area of the support decreases with increasing generation of the dendrimer and that the pore volume and pore diameter also decreases with increasing generation. This would support our first assumption that some of the dendrimer growth takes place within the pores of the support. Therefore, steric interference becomes pronounced in the higher generations (especially as we are using the hexamethylenediamine linker instead of a shorter one).

In order to determine if the dendrimers could fit inside a pore, the end-to-end length of the extended dendrimer was determined by using a simple calculation based on the bond lengths of the dendrimer bonds. In the freely rotating model for calculating the end-to-end lengths of polymers, the angle between the bonds

are taken as $\theta = 109.5^{o}$, bond lengths are $\lambda = 1.54$ A, and n, the number of bonds. The bonds are restricted to trans-trans conformation only. Then the end-to-end length for a G(4) (C_6) dendrimer is given by

$$r = n(\lambda \sin(\theta/2))$$

$$= 44(1.54\sin(109.5/2))A$$

$$= 54.61 \text{ A}$$

or

$$r = 5.5 \text{ nm.}$$

As dendrimers grow on the whole inside surface of the pore the pore diameter should at least be twice this value. This would allow for ample space inside the pores. PAMAM dendrimers have significant ability to form hydrogen bonding and thus they will be more compact than this simple calculation suggests. Furthermore, larger dendrimers are prone to back-folding, making the space occupied by the molecule even less. Notwithstanding this, the dendrimers would experience significant steric congestion if the pore is too small. The nitrogen adsorption isotherms are represented in Figure 2-7.

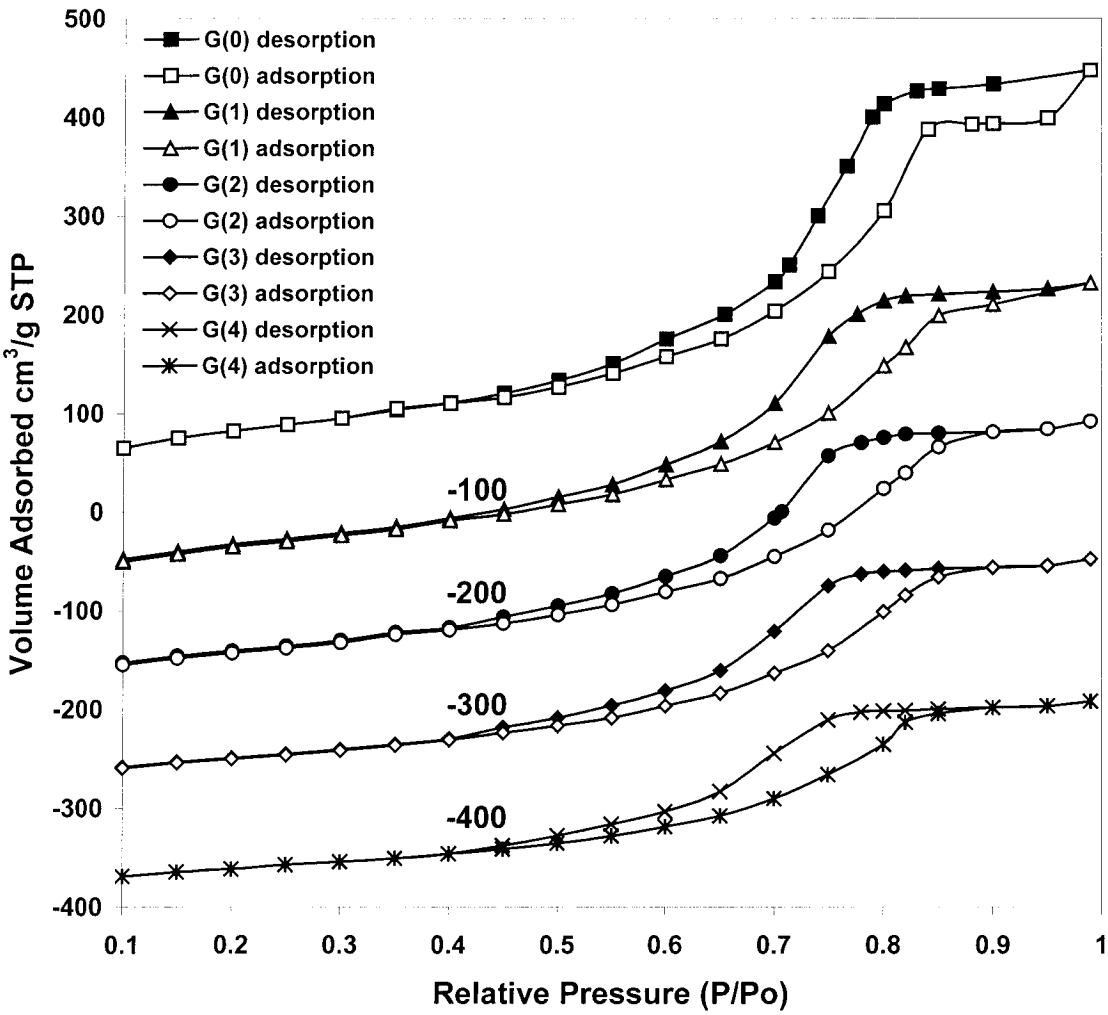

Figure 2-7. Nitrogen adsorption isotherms for silica supported C_6-PAMAM dendrimers.

Table 2-4. Surface area and Pore Volume Data for different generations of PAMAM-silica dendrimers.

Entry	Generation	Surface area (m^2/g)	Total Pore Volume (cm^3/g)	Average Pore Diameter (nm)
1	0 [a]	305.59	0.70	7.68
2	1	248.06	0.51	7.04
3	2	225.16	0.46	7.05
4	3	190.32	0.39	6.90
5	4	147.92	0.33	6.98

a) Determined for commercial aminopropyl silica gel.

From the data in Table 2-4 it is clear that the surface area decreases significantly from 305 m^2/g at G(0) to about 150 m^2/g at G(4) which would suggest a significant portion of the growth takes place inside the pores as most of the surface area resides inside the pores of the silica. This is supported by the decrease in the pore volume from 0.70 cm^3/g for G(0) to 0.33 cm^3/g for G(4). The pore diameter however decreases very slightly with increasing generation, which would suggest that we are measuring an average pore diameter due to the porosity of the dendrimers, which makes it impossible to verify the exact size of the dendrimers species on the surface. This is probably due to the fact that the Kelvin equation used for the determination of pore diameter is derived from first

principles, based on capillary condensation in a cylindrical pore and not a porous organic surface like we have in this case.

Although the characterization results would suggest a highly branched polymeric species as opposed to a perfect dendrimer on the surface, the different generations could still influence the catalytic activity and selectivity, with the higher generations having a more pronounced influence. An evaluation of the catalytic activity was undertaken. This catalytic evaluation will be discussed in chapter 3.

2.5 Preparation of catalyst precursors.

Generation zero complexes (Figure 2-8.) were first synthesized (Scheme 2-2) and tested to find appropriate pre-catalysts and to optimize the reaction conditions, both for catalytic activity and recyclability.

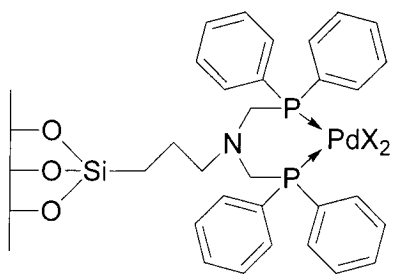

X
34 : Cl
35 : OAc
36 : $(dba)_{0.5}$
29 : PPh_3

Figure 2-8. Generation zero palladium catalysts.

These complexes were characterized using ^{13}C, ^{31}P CP-MAS NMR and ICP-MS analysis

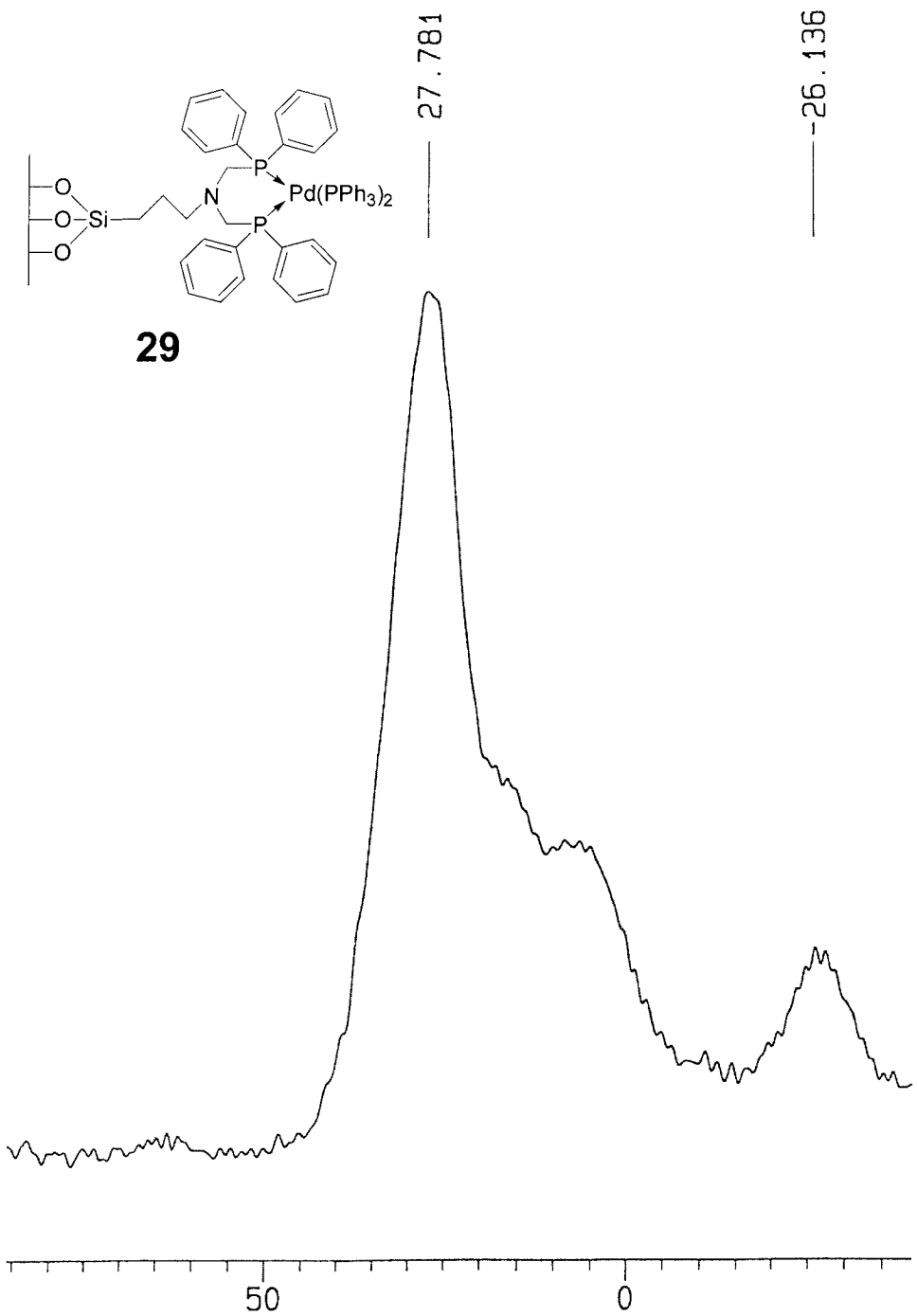

29

Figure 2-9. ^{31}P CP/MAS NMR spectrum of the G(0) $Pd(PPh_3)_2$ complex (29).

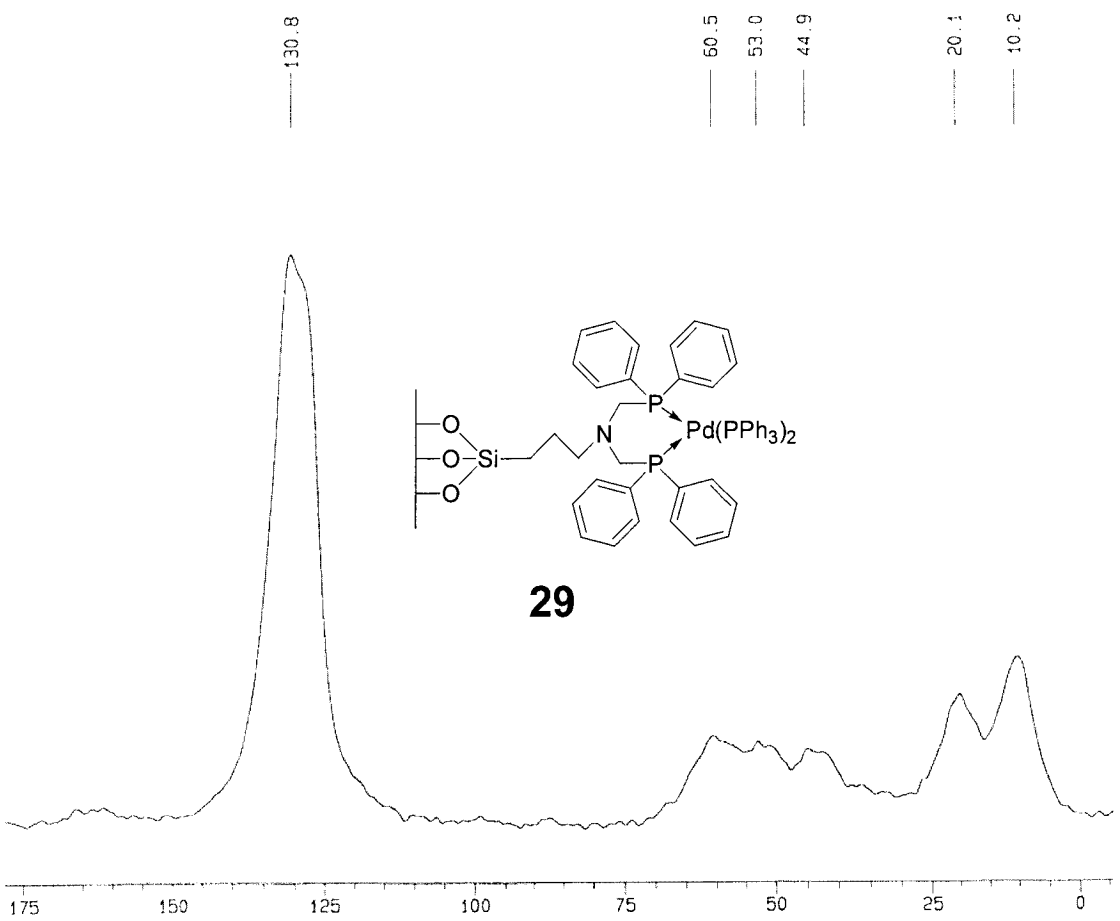

29

Figure 2-10. ^{13}C CP/MAS NMR spectrum of the G(0) $Pd(PPh_3)_2$ complex (29).

Table 2-5. ^{13}C and ^{31}P NMR characterization of palladium-containing PAMAM-silica catalysts.

Entry	Complex	Catalyst	^{13}C (ppm)	^{31}P (ppm)	Ratio P:Pd
1	**34**	G(0) $PdCl_2$	-	28, 13.0*	2
2	**35**	G(0) $Pd(OAc)_2$	-	28.0, 15.8*,-27.6	2
3	**36**	G(0) Pd(dba)	131.1	28.0*	2
4	**29**	G(0) $Pd(PPh_3)_2$	130	27.7*, 7.5, -26.1	3
5	**29a**	G(1) $Pd(PPh_3)_2$	130.5	26.2*, 10.3, -26.2	3
6	**29b**	G(2) $Pd(PPh_3)_2$	129.6	25.9*, 8.7, -27.4	3
7	**29c**	G(3) $Pd(PPh_3)_2$	128.33	27.7*, 13.6, -25.3	3
8	**29d**	G(4) $Pd(PPh_3)_2$	127.8	28.51*, 11.3, -29.0	3

*denotes main peak

The Pd(II) complexes (Entries 1 and 2, Table 2-5.) give a main signal in the ^{31}P NMR, in the 12-16 ppm range, which corresponds to phosphorus attached to Pd(II), but these complexes also exhibit a signal near 28 ppm. Originally we thought that this was due to phosphine oxide bound to Pd(II). To test this a sample was purposefully oxidized to form phosphine oxide groups, which gave a resonance at around 33 ppm. On preparation of the Pd(0) species we found that the signal at 28 ppm became the main signal and these correspond to Pd(0) attached to the phosphines (Figure 2-9). This is an interesting observation as it means that some of the Pd(II) centers are reduced to Pd(0) during the complexation. It is thought that especially $Pd(OAc)_2$ is vulnerable to auto-reduction under the complexation conditions. The ^{13}C NMR of the G(0) $Pd(PPh_3)_2$

exhibits signal at 130.8 ppm corresponding to the large proportion of aryl carbons in the complex. The other signals at 10.2 ppm, 20.1ppm and 44.9 ppm correspond to the three signals of the APS group on the silica surface while the signal at 60.5 ppm represents the bridging carbon atom between the nitrogen atom and the phosphine group in the complex. The presence of the signal at 53.0 ppm is not directly evident from the structure, but could be due to the carbon bridge in uncomplexed phosphine groups (Figure 2-10.). As complexes prepared from $Pd(PPh_3)_4$ were chosen as the best precursors (Chapter 3), we synthesized the higher generations of these. Their characterization data can be seen in Table 2-5.

2.6 Conclusions.

Various methods (^{13}C MAS-NMR, ^{31}P MAS-NMR, ICP-MS, TGA and nitrogen adsorption methods) were used to characterize the silica supported PAMAM dendrimers and the metal complexes attached to the periphery of the dendrimers. All the quantitative methods showed an overall yield at G(4) to be around 30 %. And this translates to an average yield per reaction of around 98%.

The nitrogen adsorption study revealed that the BET surface area of the support significantly decreases with increase in generation from around 300 m^2/g for G(0) to around 150 m^2/g for G(4). The pore volume also decreases from 0.70 cm^3/g at G(0) to 0.33 cm^3/g at G(4). This is taken as evidence that significant dendrimer growth takes place inside the pores of the support.

Although the analytical methods used and developed are useful, there still are some questions that stay unanswered. For instance, how do we distinguish between amide- and ester groups without definitive ^{13}C spectra. We also had to clearly assign the decomposition areas in the TGA. Probably the most interesting question that arose was how to develop supports where the dendrimers only reside inside the pores and to compare these with supports where the dendrimers only reside on the outside surface. These questions are addressed in Chapter 4 and 5.

2.7 References for Chapter 2

1. Alper, H., Bourque, S. C., Maltais, F., Xiao, W., Tardif, O., Arya, P., Manzer. L.E., *J. Am. Chem. Soc.*, **1999**, *121*, 3035-3038.

2. Bourque, S. C., Alper, H., Manzer. L.E., Arya, P., *J. Am. Chem. Soc.*, **2000**, *122,* 956-957.

3. Thomas, J.M., Thomas W.J., *Principles and practice of heterogeneous catalysis,* VCH, Weinheim, **1997**.

4. Kiss, G., *Chem. Rev.*, **2001**, *101*, 3435-3456.

5. Kawana, M., Nakamura, S., Watanabe, E., Urata, H., *J. Organomet. Chem.*, **1997**, *542*, 185-189.

6. Scivanti, A., Beghetto, V., Campagna, E., Zanato, M., Mateoli, U., *Organometallics*, **1998**, *17*,630-635.

7. Reetz, M. T., Lohmer, G., Schwickardi, R., *Angew. Chem. Int. Ed. Engl.*, **1997**, *36*, 1526-1529.

8. Tsubokawa, N., Ichioka, H., Satoh, T., Hayashi, S., Fujiki, K., *Reactive and Functional Polymers*, **1998**, *37*, 75-82.

9. (a) Nayler, A. M., Goddard III, W. A., Kiefer, G. E., Tomalia, D. A., *J. Am. Chem. Soc.*, **1989**, *111*, 2339-2342. (b) Jansen, J. F. G. A., de Brabander-van den Berg, E. M. M., Meijer, E. W., *Science*, **1994**, *266*, 1226-1229.

10. Newkome, G. R., Moorefield, C. N., Vogtle, F., *Dendrimers and Dendrons, Wiley-VCH, Weinheim*, **2001**.

Chapter 3. *Hydroesterification Reactions with Palladium-Complexed C_6-PAMAM Dendrimers Immobilized on Silica*

3.1 Introduction

From the outset, the aim of this research was to find an effective recyclable catalyst for the hydroesterification of olefins. Metal complexed dendrimers immobilized on silica have been used previously as catalysts for the hydroformylation of olefins[1], the Heck reaction[2] and for the carbonylation of aryl iodides[3]. It was thought that the modification of these systems could lead to effective recyclable catalysts for the hydroesterification reaction.

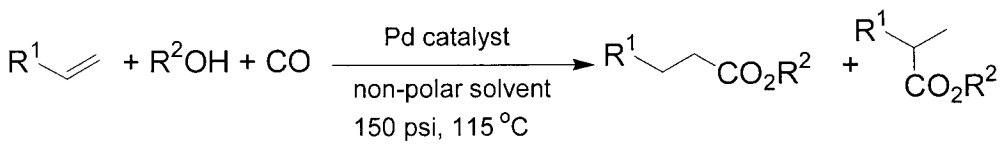

R^1 = a) Ph-R
b) alkyl

20a
20b

21a
21b

Scheme 3-1. The hydroesterification reaction

The hydroesterification reaction (Scheme 3-1.) is a valuable transformation as it is atom efficient and the ester products (**20**, **21**, Scheme 3-1.) are attractive for numerous industrial and pharmaceutical applications. Palladium based catalysts are preferred but these have not found widespread application industrially due to

the challenges involved with catalyst and product separation and the high cost associated with palladium based systems.[4] An effective recyclable catalyst for this reaction is therefore highly desirable.

Only two examples of palladium based recyclable catalysts for hydroesterification reactions have been reported previously. One example was based on a polymer support[5] and the other, based on modified montmorillonite clay[6], was prepared in this laboratory. Both these catalysts could be recycled a few times, but lost activity rapidly in subsequent cycles.

This chapter describes the identification, optimization and evaluation of effective recyclable palladium-complexed dendrimer based catalysts immobilized on silica.

3.2 Proposed mechanism:

To understand the different parameters involved, it is important to look at a proposed mechanism for this reaction Figure 3-1. This mechanism is based on literature data and different observations. A variety of parameters were used to optimize the catalytic activity.

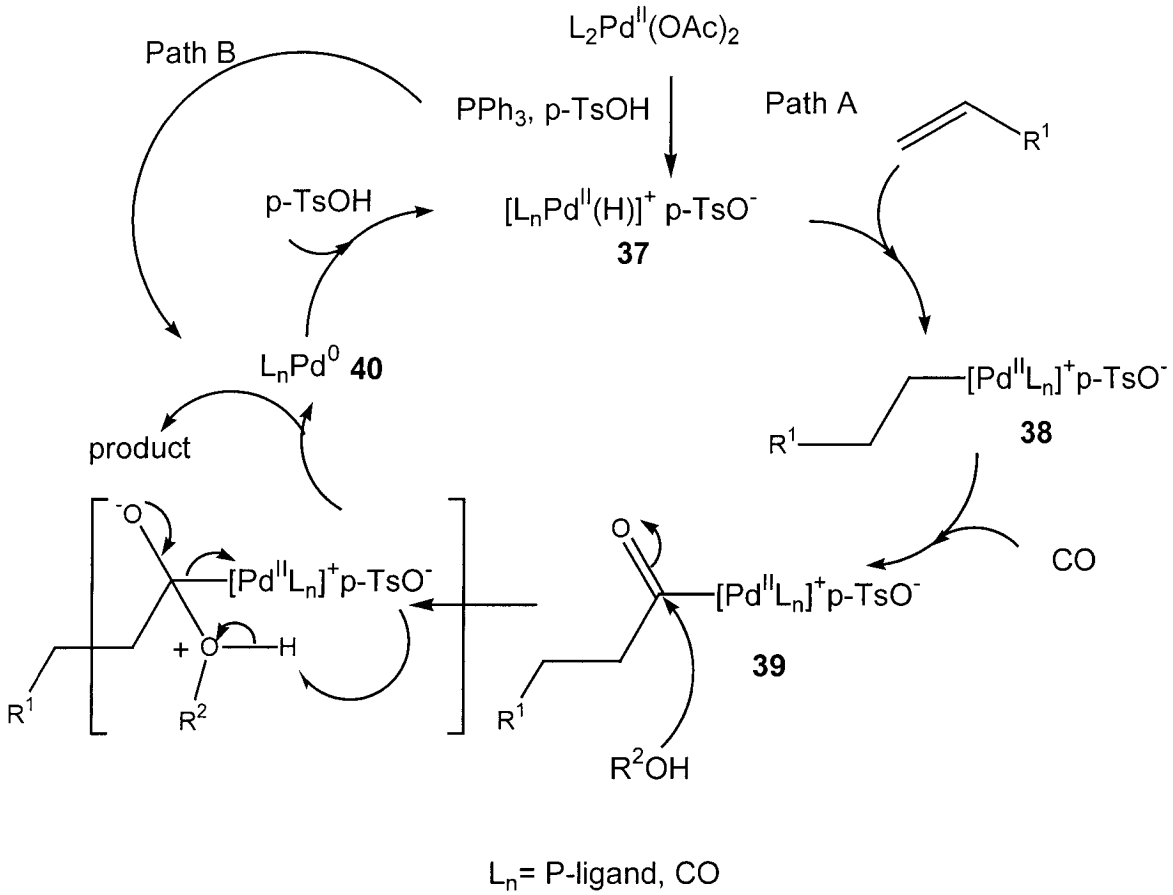

Figure 3-1. Proposed mechanism for the hydroesterification reaction.

Two different pathways (A+B) have been proposed for the reaction. Neither route has been confirmed experimentally. [4, 6, 7, 8, 13] For clarity, the ligands L refer to either phosphine or CO ligands, but at least one phosphine is assumed to be present during the entire catalytic cycle.

After the initial reaction, following Path A, the cationic-palladium hydride complex **37** is formed. It can also be formed by a two-step sequence following Path B. This is followed by an attack by an olefin, perhaps forming a five coordinate square pyramidal intermediate that rearranges to complex **38**. This attack is believed to proceed by an associative mechanism, as the concentration of the olefin affects the rate of this step. Complex **39** is generated from **38** in much the same fashion, but by attack of CO. After CO binds to palladium it inserts into the palladium-carbon bond. The next step is the attack by the alcohol (in this case methanol). Then reductive elimination occurs to generate the Pd(0) species **40**. The cycle is completed by oxidative addition (simple protonation) of the acid to complex **40** regenerating species **37**.

It is clear that the overall reaction rate will depend on the olefin concentration, the acid concentration and the methanol concentration. The rate will also depend on the electrophilic nature of the metal center, and the nucleophillic nature of the alcohol. Based on the assumption that a cationic palladium species is the key intermediate, it follows that the solvent polarity would also have a significant effect on the overall rate. The CO pressure will also affect the rate of the

reaction. The CO pressure was optimized, and as predicted by the proposed mechanism, the reaction rate increases with pressure until a threshold pressure is reached, at which point the CO starts to block the vacant sites, and consequently reduces the reaction rate. The same relationship, although more pronounced, is observed for the acid concentration. At higher acid ratios, side-reactions like isomerization and ether formation are favored. The phosphine ligand concentration, although not directly evident from the mechanism, is also pivotal to the effectiveness of the catalyst. This is due to the electronic interaction of the phosphine and the metal center. At low concentrations the phosphine does not effectively stabilize the intermediates like the palladium (0) species **40**. At higher concentrations the phosphines block the activity by stabilizing the intermediates too much and thereby slowing down the cycle.

3.3 Evaluation of catalyst precursors.

The generation zero complexes were first synthesized and tested to find appropriate pre-catalysts and to optimize the reaction conditions, both for catalytic activity and recyclability.

G(0)$PdCl_2$ (**34**, Figure 2-8.) was synthesized and tested with an acidic solution. The complex showed no activity without added phosphine. Although this is unusual, the motmorillonite catalyst prepared before also showed this behaviour.[7] It could be that a "release and capture" mechanism is at work. This observation is consistent with all the other catalysts tested. Initial test reactions

showed strong temperature, pressure and acid concentration dependence, but a full optimization was postponed until recyclability could be demonstrated. The $G(0)PdCl_2$ (**34**, Figure 2-8.) and $G(4)PdCl_2$ systems were evaluated for recyclability, but the catalysts showed little or no activity in subsequent cycles with some leaching observed for the $G(0)PdCl_2$ (**34**, Figure 2-8.) systems. Initial trials with the $G(0)Pd(OAc)_2$ analog (**35**, Figure 2-8.) gave comparable activity to the $G(0)PdCl_2$ catalysts (**34**, Figure 2-8.), and these could be recycled only after pre-treatment with CO (reduction) (Table 3-1.).

Table 3-1. Recycle study of the $G(0)Pd(OAc)_2$ catalyst with CO pre-treatment .

Entry	Run no.	Conversion (%)	TON	TOF /h	L:B
1	1	25	26.5	1.1	2.1
2	2	50	52.5	2.38	2
3	3	46	55.2	2.9	2
4	4	50	60	3	2
5	5	42	64	3.37	2
6	6	17	-	-	2.8

Conditions: 30 mg catalyst (4.4 μmol Pd (**35**)), PPh_3 (25 eq.), *p*-TsOH (35 eq.), 0.150 ml 1-decene (0.8 mmol), THF:MeOH (1:1 mixture, 5 ml), P_{CO}= 150 psi.

The G(0)Pd(dba) (**36**, Figure 2-8.) [10] analog was also very active, but it did not recycle very successfully even with CO pretreatment (Table 3-2. and 3-3.)

Complex **36** however demonstrated that a Pd(II) species as pre-catalyst is not essential for the reaction.

Table 3-2. Recycle study of the G(0)Pd(dba)$_x$ catalyst without CO pre-treatment.

Entry	Run no	Conversion (%)	Time (h)	TON	TOF /h	L:B
1	1	85	17	91.8	5.4	1.5
2	2	41	23	55	2.38	1.2
3	3	Trace	-	-	-	-

Conditions: 30 mg catalyst (4.4 μmol Pd (**36**)), PPh_3 (25 eq.), *p*-TsOH (35 eq.), 0.150 ml 1-decene (0.8 mmol), THF:MeOH (1:1 mixture, 5 ml), P_{CO}= 150 psi.

Table 3-3. Recycle study of the G(0)Pd(dba)$_x$ catalyst with CO pre-treatment.

Entry	Run no	Conversion (%)	Time (h)	TON	TOF /h	L:B
1	1	50	24	112.5	4.7	1.8
2	2	Trace	24	-	-	-

Conditions: 30 mg catalyst (4.4 μmol Pd (**36**)), PPh_3 (25 eq.), *p*-TsOH (35 eq.), 0.150 ml 1-decene (0.8 mmol), THF:MeOH (1:1 mixture, 5 ml), P_{CO}= 150 PSI.

As the G(0)Pd$(OAc)_2$ complex (**35**, Figure 2-8.) showed the most promise in initial trials, this catalyst was chosen as the test catalyst of choice for the optimization reactions. To understand the reaction parameters better a full optimization of the reaction conditions were undertaken

3.4 Optimization of the reaction conditions.

Several parameters (see following sections) were identified in the initial runs, which affect the activity of the catalyst and these were optimized separately. 30 mg of the catalyst (**35,** Figure 2-8., 4.0 μmol Pd) was used at 115 °C, with 160 equivalents of 1-decene for the optimization reactions.

3.4.1 Pressure optimization.

Optimization reactions were conducted at pressures from 100 to 1000 psi of CO and the results are graphically represented in Figure 3-2.

It is important to note that although the highest conversion was obtained at 250 psi, the catalyst gives more than 90% of the optimum conversion between 150 and 480 psi, thus enabling a window of operation of more than 300 psi over the preferred pressure (150 psi). The optimum pressure was accordingly chosen as 150 psi.

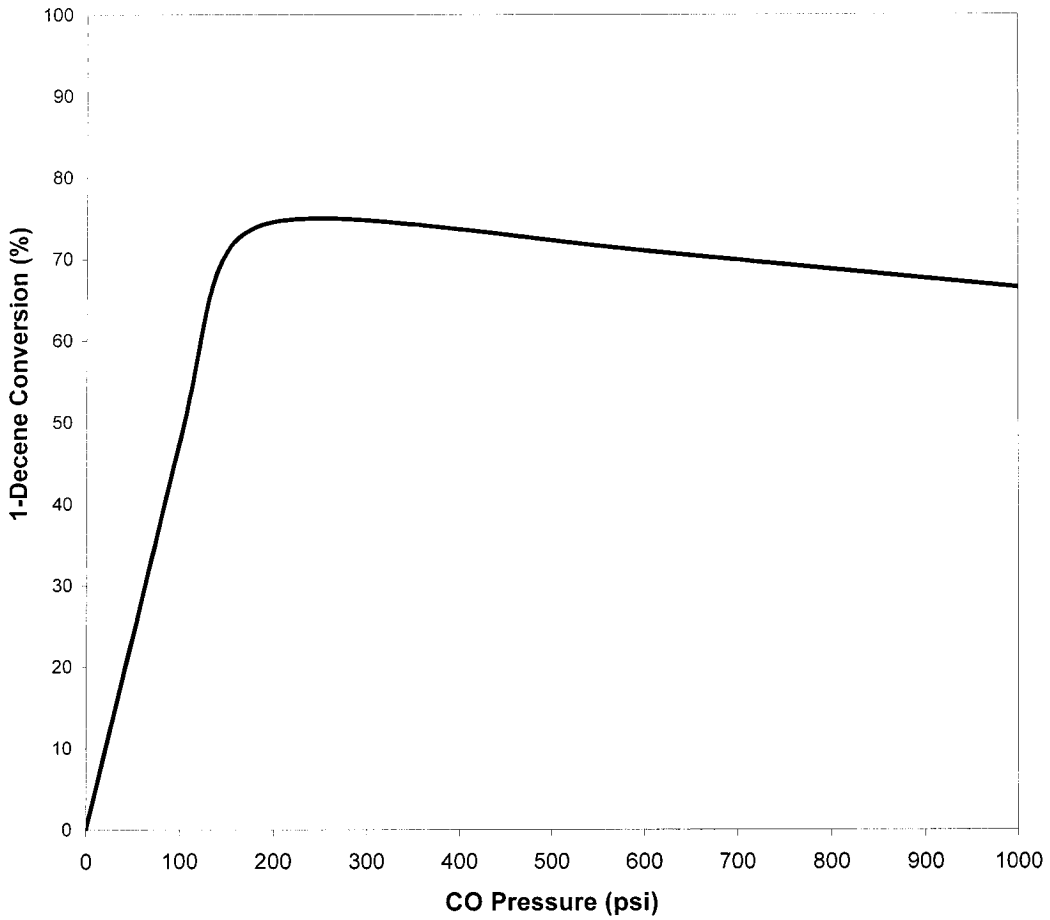

Figure 3-2. Pressure optimization.

Conditions: 30 mg catalyst (4 μmol Pd (**35**)), PPh_3 ligand (25 eq.), *p*-Toluenesulphonic acid (35 eq.), 0.150 ml 1-decene (0.8 mmol), THF:MeOH (1:1 mixture, 5 ml).

3.4.2 Optimization of acid additive.

Various acid additives were tested in an effort to improve the selectivity and conversion. It is clear from the results in Table 4 that methanesulphonic and *p*-toluenesulphonic acid gives the highest conversions, but that hydrochloric acid

gives the best selectivity. Also, strongly coordinating anions like iodide (from HI) form very stable Pd-complexes and all catalytic activity is lost immediately (Entry 4, Table 3-4). For the G(0)Pd(OAc)$_2$ catalyst (**35**, Figure 2-8.), formic acid and trifluoroacetic acid do not activate the catalyst, although these acids will activate the $PdCl_2$ systems but give lower activity than the Pd(OAc)$_2$/$MeSO_2H$/p-TsOH systems.

Table 3-4. Effect of various acids on the hydroesterification of 1-decene.

Entry	Acid	Conversion (%)	L:B
1	p-TsOH	77	1.36
2	HCO_2H	0	-
3	F_3CCO_2H	0	-
4	HI	0	-
5	HCl	73	3.6
6	$MeSO_3H$	82	1.3

Conditions: 30 mg catalyst (4 μmol Pd (**35**)), PPh_3 (25 eq.), acid (35 eq.), 0.150 ml 1-decene (0.8 mmol), THF:MeOH (1:1 mixture, 5 ml), P_{CO}= 150 psi, 22 h.

The molar ratio of *p*-toluenesulphonic acid to palladium is of great importance and an effort was made to optimize this ratio. The acid optimization shows that no catalyst activity can be detected at ratios of acid:palladium of less than 5. Above ratios of 5 there exists a linear relationship between acid concentration

and conversion up to about a ratio of 35, after which the acid concentration is high enough to lead to detrimental side-reactions like isomerization. A ratio of acid to palladium of 35 was selected as the optimum. (Table 3-5.)

Table 3-5. Effect of *p*-toluenesulphonic acid:Pd ratio on the conversion of 1-decene.

Entry	Acid:Pd	Conversion (%)
1	3	0
2	4	0
3	10	17
4	14	23
5	26	39
6	37	71
7	51	36

Conditions: 30 mg catalyst (4 μmol Pd (**35**)), PPh_3 (25 eq.), 0.150 ml 1-decene (0.8 mmol), THF:MeOH (1:1 mixture, 5 ml), P_{CO}= 150 psi, 22 h.

3.4.3 Optimization of added triphenylphosphine.

The amount of added triphenylphosphine was also optimized by varying the ratio of P to Pd between 2 and 100 and the results are graphically represented in Figure 3-3. The catalyst shows no activity up to a P:Pd ratio of 10 and then the optimum is reached at a ratio of 25. At ratios of more than 25 the activity decreases, suggesting that stable Pd complexes are formed, inhibiting catalytic activity. It is common for the activity of hydroesterification catalysts to be highly sensitive to acid and phosphine concentrations. In a related patent, Reman *et al* reported that for the homogeneous $Pd(OAc)_2$ $(PPh_3)_2$ -acid system, the catalyst requires high acid and phosphine ratios for optimum activity.[11]

Up to this point only PPh_3 was tested as an added phosphine ligand, and so other phosphine ligands were tested to assess the effect of the added phosphine on the catalyst. Of the ligands tested only PPh_3 gave any activity.

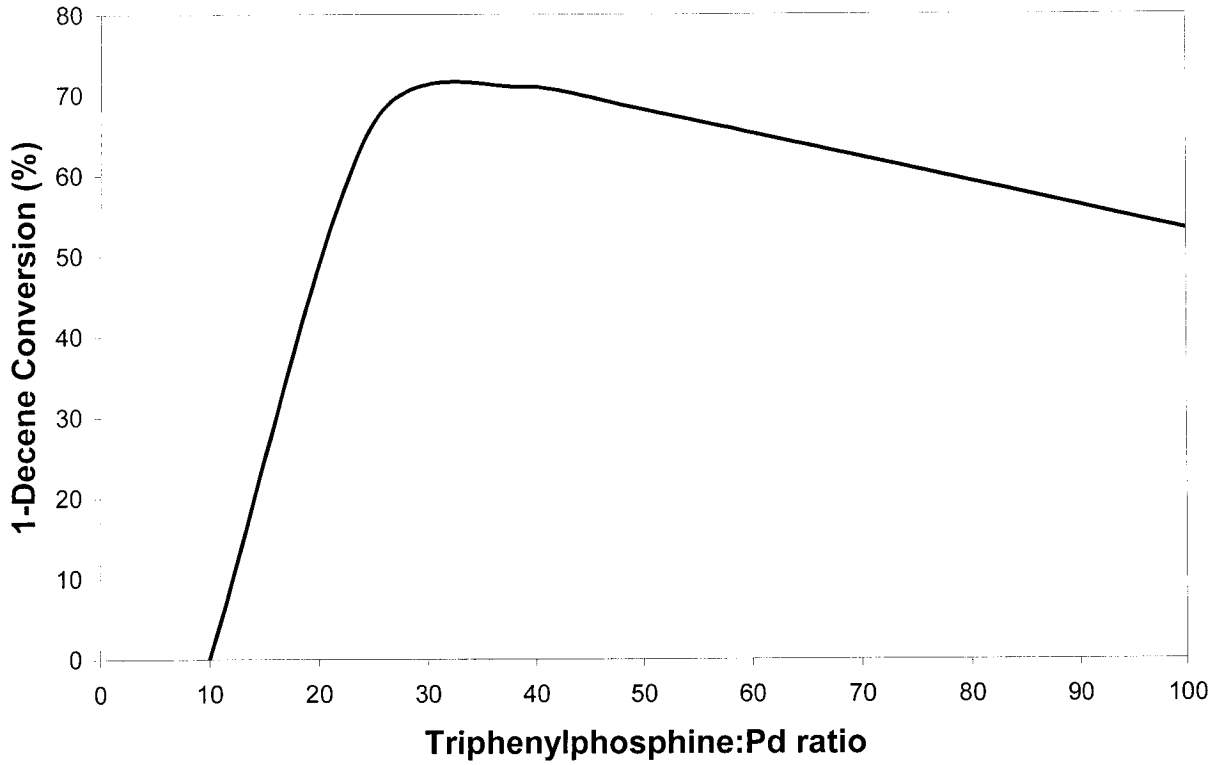

Conditions: 30 mg catalyst (4 μmol Pd (**35**)), *p*-Toluenesulphonic acid (35 eq.), 0.150 ml 1-decene (0.8 mmol), THF:MeOH (1:1 mixture, 5 ml), P_{CO}= 150 psi.

Figure 3-3. Effect of the ratio of added triphenylphosphine.

3.4.4 Solvent optimization.

Solvents with different polarities were employed, and the catalyst performed best in solvents with low polarity (Entry 1, 2 and 3, Table 3-6.). although intermediate polarity solvents (Entry 4 and 5, Table 3-6.) also gave acceptable results. Almost no activity is observed with very polar solvents like NMP (Entry 6, Table 3-6.). It became apparent that lower polarity solvents are superior in recycle reactions. (Table 3-7, 3-8 and 3-9)

3.4.5 Temperature optimization.

The catalyst shows activity between 60 °C and 150 °C, and from Figure 3-4 the optimum temperature lies between 100-120 °C. For the rest of the reactions 115 °C was chosen as the optimum temperature.

Table 3-6. Solvent optimization for the hydroesterification of 1-decene.

Entry	Solvent	Dielectric constant	Conversion (%)
1	Hexane	1.9	90
2	Toluene	2.38	89
3	Dimethyl ether	4.34	86
4	THF	7.6	78
5	CH_2Cl_2	9.08	81
6	NMP	32	0

Conditions: 30 mg catalyst (4 μmol Pd (**35**)), PPh_3 (25 eq.), p-TsOH (35 eq.), 0.150 ml1-decene (0.8 mmol), solvent:MeOH (1:1 mixture, 5 ml), P_{CO}= 150 psi, 22 h

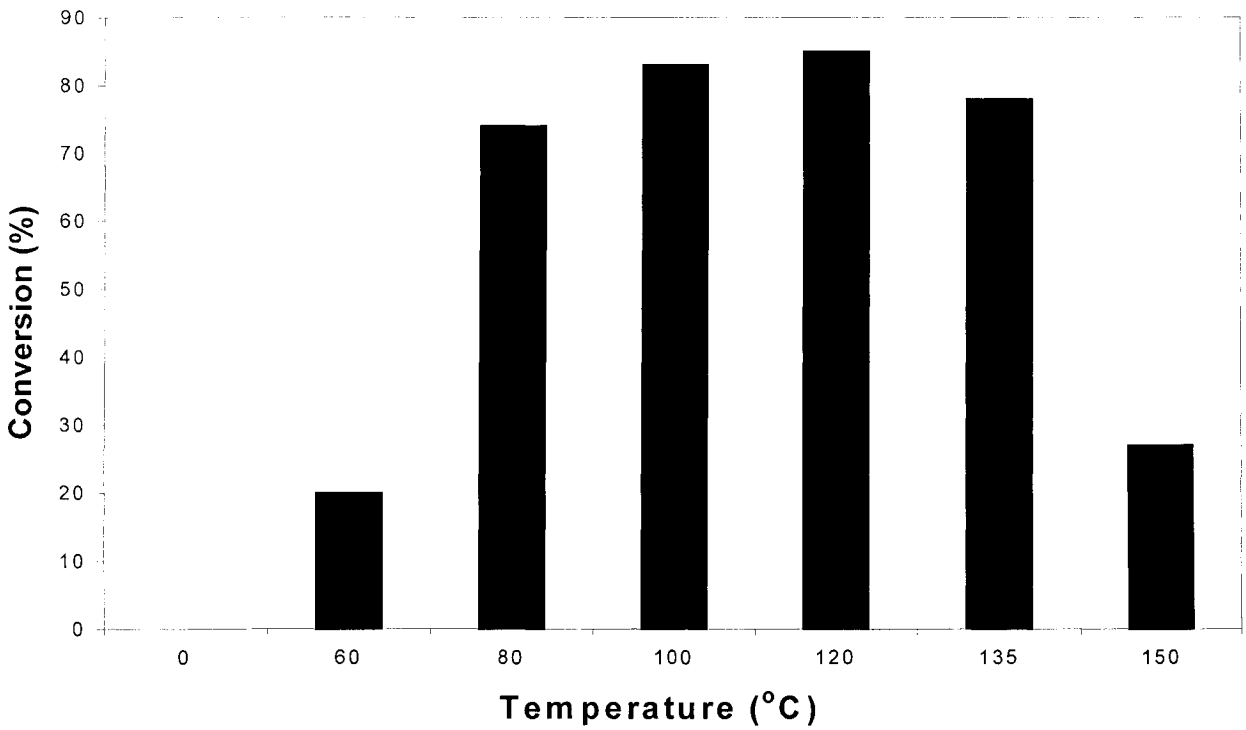

Figure 3-4. 1-Decene conversion as a function of temperature.

Conditions: 30 mg catalyst (4 μmol Pd (**35**)), PPh_3 (25 eq.), *p*-TsOH (35 eq.), 0.150 ml 1-decene (0.8 mmol), THF:MeOH (1:1 mixture, 5 ml), P_{CO}= 150 psi.

3.5 Recycle reactions:

From the first attempts at recycling with the $PdCl_2$ functionalized dendrimers it was apparent that these could not be recycled without pre-treatment with carbon monoxide and PPh_3. Therefore the $Pd(OAc)_2$ functionalized dendrimers were tested. As with the $PdCl_2$ functionalized catalysts, the optimum recyclability was achieved after the catalyst was pre-treated. After pre-treatment, the catalyst could be used for six consecutive reactions. Because the palladium is effectively reduced during the pretreatment step, it was thought that starting off with a

palladium (0) precursor could eliminate the necessity of a pre-treatment step, and a $Pd(dba)_{0.5}$ functionalized catalyst (**36**, Figure 2-8.) was prepared and tested. Although this catalyst was highly active, it could not be satisfactorily recycled.

We purposefully exposed a large quantity of the catalyst to the reducing environment of the reaction, without the addition of substrate. In this manner we were able to generate a sample (200mg) for solid-state NMR analyses. A broad signal at 3.6-5.0 ppm in the ^{31}P NMR was attributed to PPh_3 bound to a palladium zero species attached to the dendrimer.

3.5.1 $Pd(PPh_3)_4$ as the complexation agent.

It is clear from previous results that PPh_3 stabilizes the catalyst, and is crucial for catalytic activity. It's therefore likely that the resting state of the catalyst would be a complex where two coordination sites are occupied by the phosphines of the bidentate moiety on the dendrimer and two by PPh_3. The $G(0)Pd(PPh_3)_2$ catalyst (**29**, Figure 2-8.) was then synthesized and characterized. The first test showed comparable activity to the $Pd(OAc)_2$ complexed catalyst and for the first time the complex could be recycled effectively without pre-treatment with CO. The catalyst could be recycled for three runs at 135 °C in THF (low yields observed during 2^{nd} and 3^{rd} cycles). By changing the solvent to toluene and effecting the reactions at 115 °C, the catalyst showed good activity for up to 5 cycles and 11% conversion in the sixth (Table 3-7.). The ratio of linear to branched products improved during the recycle runs. This could be due to a different reactivity of the

complexes grafted on the inside surface as opposed to the outside surface. One would expect from the crowding inside the pores that the catalysts residing there would favor the linear products. It is also conceivable that the outside complexes would be more susceptible to leaching when compared to the complexes residing inside the pores. The catalyst therefore evolves by the leaching of outside grafted palladium molecules to a more selective system where the catalyst sites are protected inside the pores. Johnson *et al* prepared grafted homogeneous catalysts in MCM-41 and carbosil to study the effect of the pore walls on the selectivity of the catalyst. They found that the catalyst supported inside the pores of MCM-41 showed completely different selectivity than both the carbosil-supported catalyst and the homogeneous catalyst.[12] The catalyst was also tested for activity without added phosphine or acid. In both cases the catalyst showed no activity, but the catalyst could be activated by adding acid (*p*-TsOH) and phosphine (PPh_3) to the reactor after the preliminary tests were done.

Table 3-7. Recycle test of G(0)Pd(PPh_3)$_2$ catalyzed hydroesterification of 1-decene.

Entry	Run No.	Conversion (%)	L:B
1	1	78	1.35
2	2	52	2.60
3	3	62	2.36
4	4	71	3.20
5	5	36	4.50
6	6	11	-

Conditions: 50 mg catalyst (4.5 μmol Pd (**29**)), PPh_3 (25 eq.), pTsOH (35 eq.), 1-decene (160 eq.), Toluene:MeOH (1:1 mixture, 5 ml), P_{CO}= 150 psi, T= 115 °C, 22 h.

The ability of the catalyst to be recycled was very promising and the next step was to synthesize the generation one through four analogs of this complex. The G(1) to G(4) analogs of complex **29** were tested for activity without added phosphine, but like the G(0) catalyst no activity was detected. The catalysts were then used for recycle tests under the same conditions as the G(0) catalyst but leaching was observed, and the catalysts showed little or no activity in subsequent runs (Table 3-8.). However by changing the solvent system to a mixture of hexane and methanol, activity could be afforded up to at least the third cycle and in most of the cases up to five cycles (Table 3-9.). The improved recyclability is probably due to the lower polarity of hexane as opposed to THF,

lowering the solubility of the catalyst and therefore decreasing the extent of leaching. Lower initial activity was observed here, possibly due to the low solubility of methanol in hexane. The G(1) to G(4) catalysts were also evaluated with the addition of a small amount of toluene to afford mixing of the two main solvents. This improved the initial activity without changing the recycling significantly (Entries 3, 4, 5, 8, Table 3-9.).

An interesting observation is that the higher generations, although having higher activity initially, do not recycle as well as the G(0) catalysts (Table 3-9.). This could be due to better solvation of the dendrimer molecules in the solvent system, leading to increased leaching and lower activity in subsequent cycles

Various generations of the $Pd(PPh_3)_2$ complexed dendrimers were selected for representative tests to determine the scope of the reaction and the ratio of substrate to palladium was increased to at least 1000 to gauge the activity of the catalysts. The results can be seen in Table 3-10.

Table 3-8. Recycle test of G(1)Pd(PPh_3)$_2$ and G(2)Pd(PPh_3)$_2$ in Toluene:MeOH.

Entry	Generation	Run No.	Conversion (%)	L:B
1	1	1	76	3.41
2	1	2	30	-
3	2	1	86	2.23
4	2	2	Trace	-

Conditions: 50 mg catalyst (4.5 μmol Pd), PPh_3 (25 eq.), *p*-TsOH (35 eq.), 1-decene (160 eq.), Toluene:MeOH (1:1 mixture, 5 ml), P_{CO}= 150 psi, T= 115 °C, 22 h.

Table 3-9. Recycle test of G(1)-G(4) $Pd(PPh_3)_2$ catalysts in Hexane:MeOH.

Entry	Generation	Conversion (%)				
		Run 1	Run 2	Run 3	Run 4	Run 5
1	1	87	73	61	55	44
2	2	87	78	55	26	-
3[b]	1	>99	53	33	-	-
4[b]	2	>99	83	57	35	-
5[b]	3	>99	86	29	-	-
6	3	83	84	36	-	-
7	4	89	72	53	37	-
8[b]	4	92	75	73	45	-

Conditions: 50 mg catalyst (4.5 μmol Pd), PPh_3 (25 eq.), *p*-TsOH (35 eq.), 1-decene (160 eq.), Hexane:MeOH (1:1 mixture, 5 ml), P_{CO} = 150 psi, T= 115 °C, 22 h. b) Hexane:MeOH (1:1 mixture, 5 ml) 1drop Toluene.

Table 3-10. Other substrates tested with G(1)-G(4)Pd(PPh_3)$_2$.

Entry	Generation	Substrate	Conversion (%)	TON	TOF (h^{-1})	L:B
1	1	styrene	>99	1100	50	2.4
2	2	*o*-methylstyrene	>99	1200	53	12.5:1
3a	4	*p*-chlorostyrene	>99 (73[a])	829	38	2.2
3b[a]	2		20	232	10	-
4	1	*p* –^{t}butylstyrene	>99(56%esters)	1478	67	2
5	2	*p*-vinylbenzoic acid	polymerized	-	-	-
6	2	*p*-methoxystyrene	oligomerized	-	-	-
7	4	1-decene	>99	1243	56	1.9
8	1	1-octene	75	1108	50	3.2
9[b]	1	1-hexene	63	931	42	2.47
10	4	2-decene	No reaction	-	-	-
11	1	vinyl acetate	No reaction	-	-	-
12	2	vinyl benzoate	No reaction	-	-	-
13	2	cyclohexene	No reaction	-	-	-

Conditions: 20 mg catalyst (1.8 μ mol Pd), PPh_3 (25 eq.), *p*-TsOH (35 eq.), olefin (2 mmol, 1000 eq.), Toluene:MeOH (1:1 mixture, 5 ml), P_{CO}= 150 psi, T= 115 °C, 22 h. a) 85 °C. b) 300 psi. (a) Isolated yield.

The catalyst shows no activity for internal olefins. (Entries 10 and 13, Table 3-10.). To determine if the internal olefins deactivate the catalyst, or if the catalyst is just inactive towards internal olefins, pre-mixed 1-decene and 2-decene were exposed to the catalyst. The catalyst was able to react with the 1-decene selectively without any discernable reaction with 2-decene. Also styrene containing an electron withdrawing-group shows completely different activity, favoring oligomerization and polymerization at the reaction temperature. (Entries 3, 5 Table 3-10.) The reaction with *p*-chlorostyrene was repeated at 85 °C, in an effort to eliminate polymerization, but the conversion was substantially lower (Entry 3b, Table 3-10.). The most surprising observation however was that even for styrene the linear product is favored. This is a unique observation as the branched product is usually formed in a highly regioselective manner. For *o*-methylstyrene (Entry 2, Table 3-10.) remarkable selectivity was observed for the linear product with the ratio of linear to branched isomers being 12.5:1. This large difference between the selectivity of styrene and *o*-methylstyrene is due only to the presence of a methyl group in the 2-position on the ring. This shows sensitivity of the catalyst system to steric factors. *p*-^{t}Butylstyrene (Entry 4, Table 3-10.) also afforded full conversion, with 56 % selectivity for the ester products (L:B ratio of 2). The other 44% was converted to ether-type products formed by the direct addition of methanol to the double bond. (A side reaction that was also observed due to the acid). 1-Octene and 1-hexene (Entries 8 and 9, Table 3-10.) showed lower activity than 1-decene. Carbonyl containing substrates like vinyl

benzoate and vinyl acetate (Entries 11 and 12, Table 3-10.) proved to be completely unreactive under the reaction conditions. The catalysts do however show high activity (TON of up to 1200) especially as 1-2 mole % of palladium (TON of 50 to 100) is usually employed for homogeneous reactions of higher olefins.

3.6 Conclusions:

We have developed a new recyclable catalyst for the hydroesterification of olefins, based on palladium complexed dendrimers immobilized on silica. The catalysts show high activity for styrene derivatives and linear long chain olefins (TON of up to 1200) and favor the linear product of the reaction even for styrene. The catalysts can be recycled up to 6 times by simple filtration in air.

References for Chapter 3:

1. Alper, H., Bourque, S. C., Maltais, F., Xiao, W., Tardif, O., Arya, P., Manzer. L.E., *J. Am. Chem. Soc.*, **1999**, *121*, 3035-3038.

2. Alper, H., Bourque, S. C., Jefferson, G.R., Arya, P., Manzer. L.E., *Can. J. Chem.*, **2000**, *78*, 920-924.

3. Alper, H., Antebi, S., Arya, P., Manzer. L.E., *J. Org Chem.*, **2002**, *67*, 6623-6631.

4. Kiss, G., *Chem. Rev.*, **2001**, *101*, 3435-3456.

5. Pittman, Jr., C. U., Ng, Q.Y., *United States patent,* no. 4258206, **1981**.

6. Alper, H., Lee, C. W., *J. Org. Chem.*, **1995**, *60*, 250-252.

7. Kawana, M., Nakamura, S., Watanabe, E., Urata, H., *J. Organomet. Chem.*, **1997**, *542*, 185-189.

8. Scivanti, A., Beghetto, V., Campagna, E., Zanato, M., Mateoli, U., *Organometallics*, **1998**, *17*,630-635.

9. Lee, C. W., Alper, H., *J. Org. Chem.*, **1995**, 60, 250-252.

10. Amatore, C., Jutand, A., *Coord. Chem Rev.*, **1998**, 178-180, 511-528.

11. Reman, W. G., De Boer, G. B. J., Van Langen, S. A. J., Nahuijsen, A., *European patent*, no. EU 0411721A2, **1990**.

12. Johnson, B. F. G., Raynor, S. A., Shephard, D. S., Mashmeyer, T., Thomas, J. M., Sankar, G., Bromley, S., Oldroyd, R., Gladden, L., Mantle, M. D., *Chem. Commun.*,**1999**,1167-1168.

13. Cavinato, G., Vavasori, A., Tonolio, L., Benetollo F., *inorg. Chim. Acta.*, **2003**, *343*, 183-188.

Section B:

Hydroformylation of olefins catalyzed by Rhodium-Complexed C_2-PAMAM dendrimers Supported on Mesoporous and periodic Mesoporous silica

Chapter 4. *Preparation of Rhodium-Complexed C_2-PAMAM Dendrimers Immobilized on Mesoporous and Periodic Mesoporous Silica as Catalysts for the Hydroformylation of Olefins*

4.1 Introduction:

From our previous work, discussed in chapter two, it became apparent that the structural characteristics of the support cannot be ignored, nor is it trivial to the success of the synthesis of anchored dendrimers. We also came to the conclusion that although the C_6 linkers give favorable recyclability, their size causes the dendrimers to be too large for the pores of the support. This causes the dendrimers molecules inside the pores of the support to be subject to significant steric crowding and inhibits functionalization at the periphery and therefore also the effectiveness of catalysts based on these systems. We wanted to clarify our observations by using specifically designed experiments. These would involve independently synthesizing dendrimers on the outside surface and on the inside (inside pores) surface of a support and comparing the two systems with reference to the success of the synthesis and the activity and selectivity of the resulting catalysts. It is unfortunately impossible to construct dendrimers selectively on the outside surface (or on the surface inside the pores) of the amorphous silica we used previously. By selecting designer supports for

the construction of dendrimers we will show in this chapter that it is possible to build dendrimers on the inside surface (or on the outside surface) of these supports. This was achieved by using two classes of supports: Periodic mesoporous supports, where the whole surface (95%) resides inside the pores and large pore low surface area supports where the pores are essentially open and approach a flat surface (davisil). By using the characterization methods developed in Chapter 2 and others we are able to confidently deduce the effect of the support on the effectiveness of the synthetic regime and the catalytic activity of the dendrimers. To limit complications from the catalytic reaction we selected the hydroformylation of olefins as our test reaction. This reaction is very valuable to industry and although it is quite complicated, there are fewer variables involved than with the hydroesterification reaction. For instance no acid or extra phosphine have to be added to make the catalysts active, something that could influence our results due to mass transfer phenomena in highly porous media like mesoporous silicas. We also selected dendrimers based on the C_2 linker as these pose the lowest steric encumbrance of the available linkers. This is important especially when using mesoporous silica, as there is limited space available inside the pores of these materials, and we want to synthesize the largest dendrimers possible.

4.2 Mesoporous and periodic mesoporous silica supports.

The supports used for this investigation were selected on the basis of their porosity, surface area and pore volume. First SBA-15 was selected because of

its large pores (8.5 nm, 0.81 cm^3/g) coupled with its large surface area 767 m^2/g. SBA-15 however has significant microporisity in the walls of the mesopores. It was not anticipated that these would limit its usefulness, but it became apparent that MCM-41 would be a better support. MCM-41 generally has a large surface area (about 1000 m^2/g) but it has small pores (around 3nm) when compared to SBA-15. It is however possible to expand the pores of MCM-41 using either a direct route or a post-synthesis treatment and we used two pore expanded MCM-41 supports. The first was LPMCM-41 (LP = Large Pore, our designation) with a pore size of 6.5 nm and a pore volume of 0.77 cm^3/g and a surface area of 585 m^2/g. The second was PEMCM-41 (PE = Pore Expanded, also our designation) with a pore size of 10.6 nm and a pore volume of 2.23 cm^3/g and a surface area of 1385 m^2/g. These mesoporous supports were used to build dendrimers on the inside surface of the pores. For the outside surface study a non-periodic mesoporous support was selected: Davisil 623 has pores in the 18 nm range but due to their size, the pores resemble large indentations on the surface of the silica. It obviously does not have the large surface area of the periodic mesoporous supports, but it has a respectable surface area of 280 m^2/g and a pore volume of 0.77 cm^3/g.

In this chapter we will discuss the synthesis and characterization of dendrimers on these supports. Because the characterization methods are essentially the same for all the supports we will present the detailed characterization of the LPMCM-41 series, with a short overview of the results of the other supports for

each characterization method. This is done to establish the validity and utility of the method and then to compare the results of the various supports, without unnecessary repetition.

4.3 Results and Discussion.

4.3.1 Synthesis of C_2-PAMAM dendrimers.

4.3.1.1 Synthesis of C_2-PAMAM dendrimers on LPMCM-41.

Polyamidoamine (PAMAM) dendrimers, up to the third generation (G(3)) (Figure 4-1.) were prepared using a modified multistep procedure based on literature methods[1,11] (Scheme 4-1.), on amine modified large pore MCM-41. Samples will be referred to as G(x), where x is the number of the dendrimer generation. The starting LPMCM-41 material will be designated as G(-0.5), and the propylamine modified material as G(0). The synthesis of G(0.5) was as follows. Aminopropyl functionalized LPMCM-41 (6.9 mmol NH_2, 6 g) and methyl acrylate (0.14 mol, 11.82 g) were stirred at 50 °C in dry methanol (300 ml) under a nitrogen atmosphere for 5 days. The mixture was cooled and filtered through a medium pore frit under nitrogen flow and washed with dry methanol (3 X 50 ml). The residual solvent was removed in vacuo, affording methyl propylaminopropionate functionalized LPMCM-41 in 98 % yield.

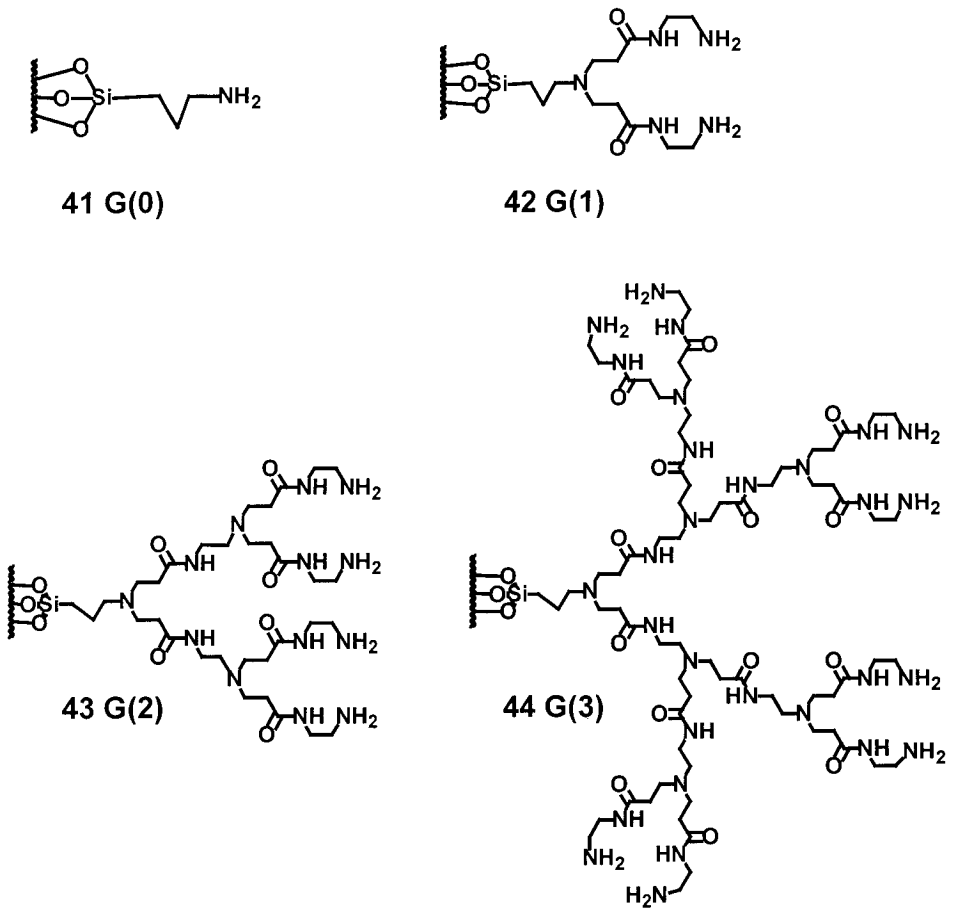

Figure 4-1. Structure of generations 0-3 of silica supported PAMAM dendrimers.

Supported G(1) dendrimer was prepared as follows. Methyl propylaminopropionate functionalized MCM-41 (0.13 mol ester groups, 6 g) was added to ethylenediamine (65 ml) in dry methanol (300 ml) under a nitrogen atmosphere. The reaction was stirred for 5 days and the resulting G(1) dendrimer supported on LPMCM-41 was isolated by filtration through a medium pore frit. The solid was washed with dry methanol (3 X 50 ml), and the residual solvent

was removed in vacuo. The higher generations were prepared by repetition of the two steps described above, the amount of reagents being adjusted as required.

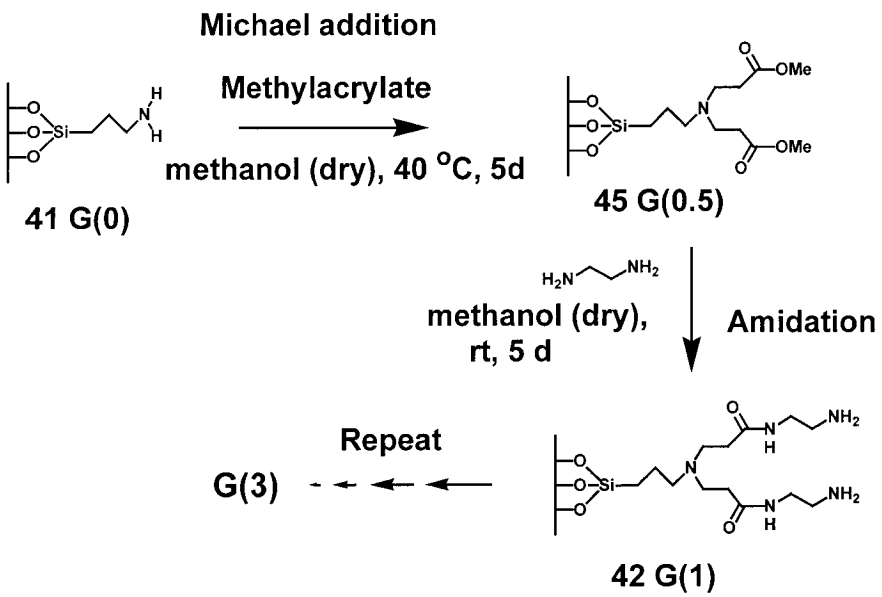

Scheme 4-1. Preparation of LPMCM-41 silica supported dendrimers.

4.3.1.2 Synthesis of C_2-PAMAM dendrimers on SBA-15.

The synthesis of dendrimers was attempted on SBA-15 following the same procedure as for LPMCM-41, but only dendrimers up to G(1.5) was synthesized. The reason for this was that although SBA-15 has large pores, large surface area and large pore volume, the effective inside surface available to us was in this case significantly lower than anticipated. SBA-15 unfortunately has significant microporosity in the walls of the mesopores. It is thought that the ends of the

surfactant template, used for the synthesis of SBA-15, sticks into the pore walls during synthesis and leads to microporosity. This has the effect that a significant portion of the large surface area of SBA-15 resides inside these micropores. This surface area is not available for modification as the micropores are too small and this therefore decreases the effective surface area available for modification.

To explain this, a model can be generated using a perfectly cylindrical pore (Figure 4-2). If the *w*S/Vp ratio is taken for such a pore a value of 4 is obtained. If the experimental *w*S/Vp differs from this value, the pore will not be cylindrical or micropores occur in the pore walls. If the value is larger it means that the inside surface is not smooth, and therefore a larger surface area than would be expected for a perfectly cylindrical pore is observed.

Table 4-1. Surface area, pore size, pore volume and *w*S/V ratio for the SBA-15 and LPMCM-41 series.

Entry	Sample	S_{BET} (m^2/g)	Pore size (nm)	Vp (cc/g)	wS/Vp
1	SBA-15	767	8.5	0.82	7.96
2	SBA-15 G(0)	360	7.7	0.50	5.57
3	LPMCM-41	585	6.5	0.77	4.50
4	LPMCM-41 G(0)	409	5.6	0.51	4.30

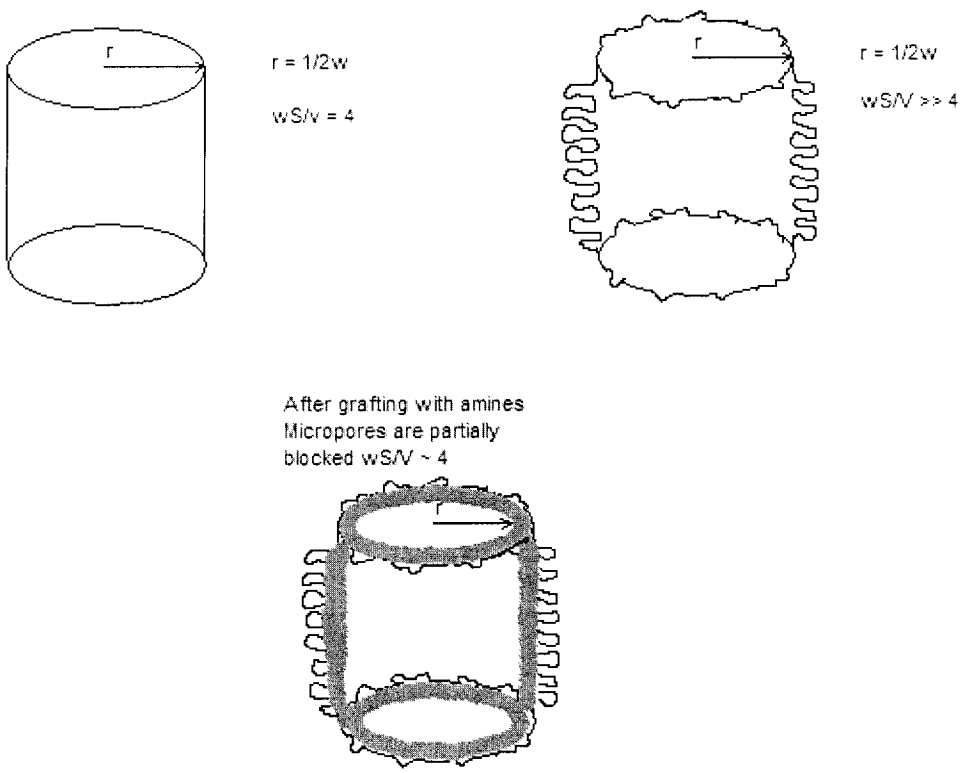

Figure 4-2. Graphical representation of the *w*S/V ratio.

As can be seen from Table 4-1 the surface area decreases significantly for the SBA-15 sample after grafting. The *w*S/V ratio for the SBA-15 is also far removed from the ideal value of 4, whereas the LPMCM-41 is much closer to the ideal value of 4. This means that the SBA-15 has significant micropores in the walls of the mesopores. The LPMCM-41 however does not exhibit this and the internal surface can therefore be seen as smooth. It is also instructive to note that for the SBA-15 series the *w*S/V ratio decreases significantly after grafting and

approaches the ideal value of 4. This in conjunction with the decrease in the surface area indicates that the surface associated with the micropores are not accessible for grafting, and that one should determine the effective smooth surface that is available for functionalization. To this end we used the α_s plot method (Figure 4-3., Figure 4-4.) to determine the pore volume associated with the micropores and subtracted this from the total pore volume and back calculated the smooth or effective surface area for the SBA-15 sample. It can be seen from the data in Table 2 that the effective smooth surface area of the SBA-15 sample is much lower than the measured BET surface area (647 m^2/g as opposed to 767 m^2/g). The effective surface area for LPMCM-41 on the other hand is only slightly different than the measured surface (Table 2).

The micropore volume, V_m, was calculated using the α_s-plot method in the range of 0.7-1.1 α_s-values. The α_s-values were calculated by curve fitting of the standard α_s values for LiChrospher Si-1000 silica provided in the literature.[12] Using the α_s plots the following data was generated. The lower horizontal part of the α_s plots were subjected to linear regression to generate the micropore volume. The total pore volume was determined before and the difference was used to back calculate the effective smooth inside surface.

Table 4-2. Pore volume calculations for mesopores and micropores for the SBA-15 and LPMCM-41 series.

Entry	Sample	S_{BET} (m^2/g)	S_{smooth} (m^2/g)	V_m (cc/g)	Vp (cc/g)
1	SBA-15	767	663	0.1104	0.82
2	SBA-15 G(0)	360	359	0.0014	0.50
3	LPMCM-41	585	582	0.0046	0.77
4	LPMCM-41 G(0)	409	409	-	0.51

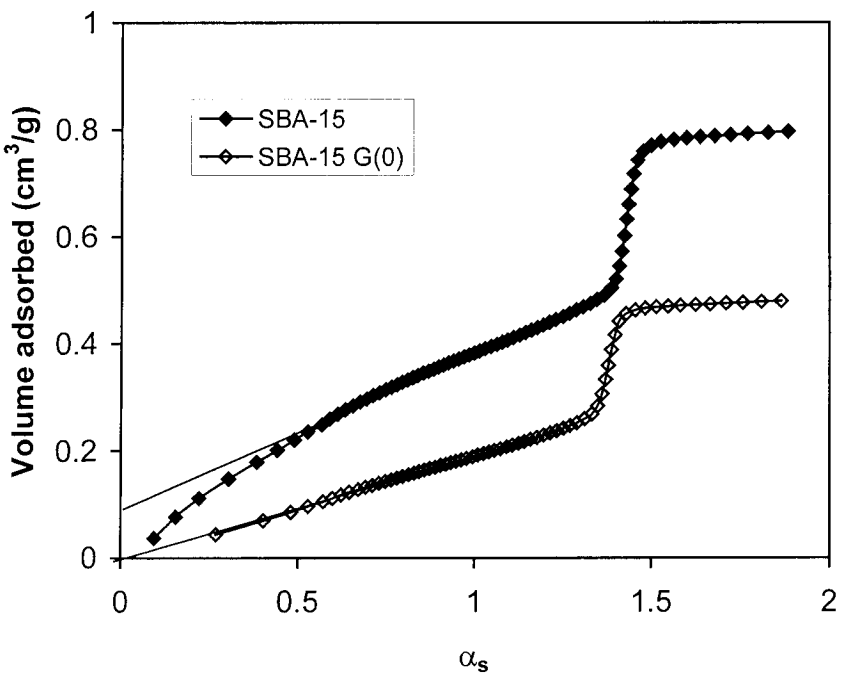

Figure 4-3. The α_s plot for SBA-15 series.

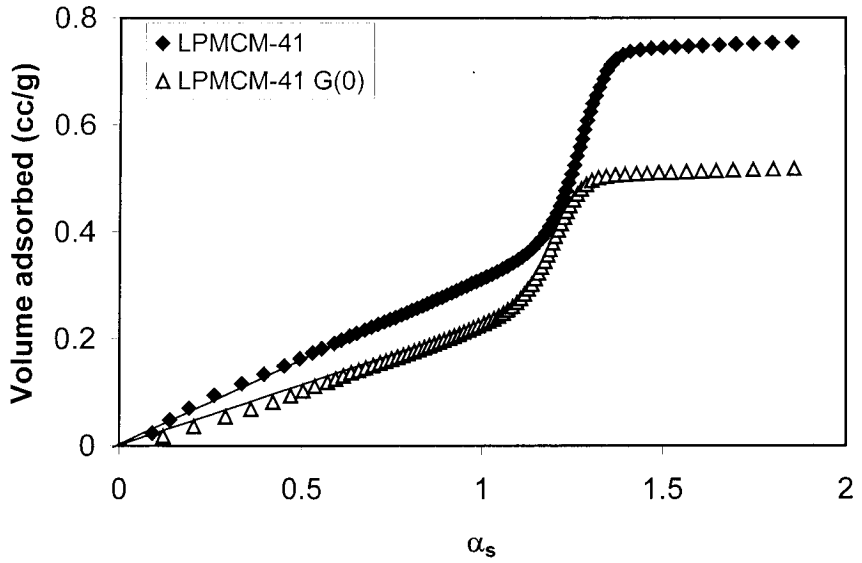

Figure 4-4. The α_s plot for the LPMCM-41 series.

As can be seen from Table 4-2. around 14% of the total pore volume of the SBA-15 support resides inside the micropores, which leads to the significant drop in the total surface area upon grafting (from 767 m^2/g to 360 m^2/g). SBA-15 was therefore not a suitable support for the synthesis of dendrimers. And the LPMCM-41 series was pursued.

4.3.1.3 Synthesis of C_2-PAMAM dendrimers on Davisil.

Polyamidoamine (PAMAM) dendrimers, up to the third generation (G(3)) (Figure 4-1) were prepared on amine modified Davisil using the same modified multistep

procedure used for the preparation of the dendrimers on large pore MCM-41. (Scheme 4-1)

4.3.1.4 Synthesis of C_2-PAMAM dendrimers on PEMCM-41.

Polyamidoamine (PAMAM) dendrimers, up to the fourth generation (G(4)) (Figure 4-5.) were prepared on amine modified PEMCM-41 using the same modified multistep procedure used previously for the preparation of the dendrimers on LPMCM-41 and Davisil, but with the steps repeated one more time. (Scheme 4-1.)

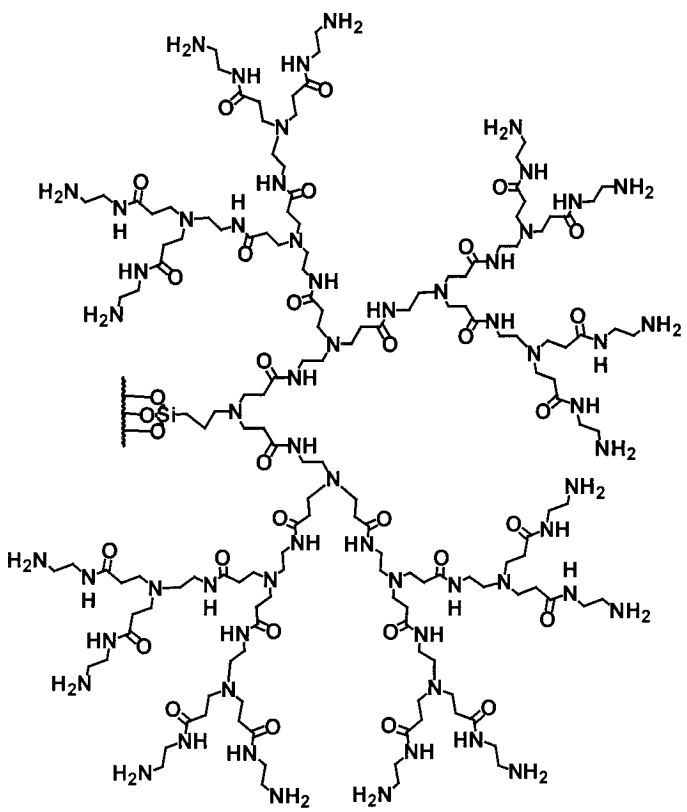

Figure 4-5. The G(4) C_2-PAMAM dendrimer supported on PEMCM-41 .

4.4 Characterization results.

4.4.1 X-ray diffraction.

X-ray diffraction was used to determine the structure of the silica mesophase for the periodic mesopourus silica, before and after the surface modification reactions that are involved in preparing the dendrimer-supported materials.

4.4.1.1 X-ray diffraction of LPMCM-41.

The XRD patterns shown in Figure 4-6 indicate that the materials exhibit two-dimensional hexagonal symmetry characteristic of a MCM-41 silica mesophase.[2] The dominant peak at 2θ = ca. 1.3°, attributable to the (100) diffraction peak hardly changed during the various surface modifications steps, indicating that the overall structure of the mesophase has been preserved. The unit cell dimension *a* was found to be 7.8 ± 0.1 nm for the starting material and for all surface modified materials. It was calculated using $a = d_{100}(2/\sqrt{3})$, where the interplanar spacing d_{100} was determined using the Bragg equation.

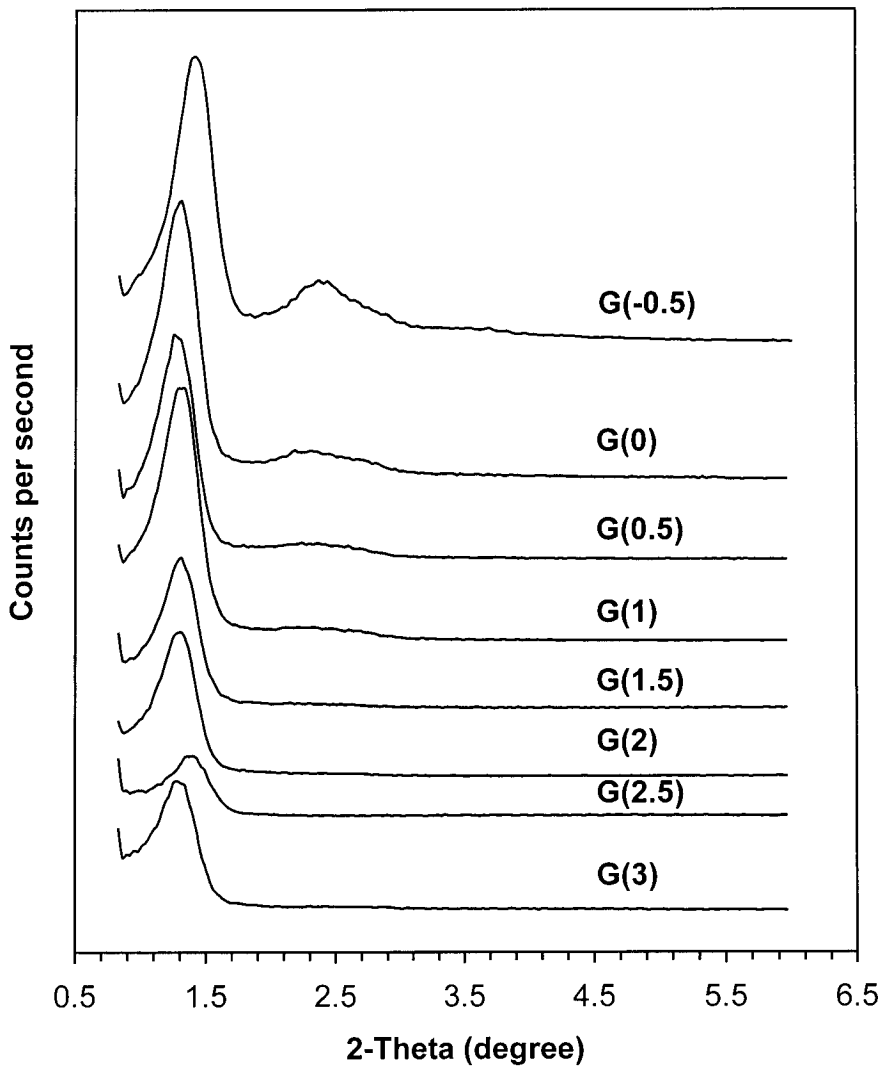

Figure 4-6. Powder X-ray diffraction patterns of LPMCM-41 supported dendrimers.

4.4.1.2 X-ray diffraction of the other materials.

As X-ray diffraction can only be used for periodic mesoporous materials no XRD patterns was recorded for davisil. The SBA-15 series and PEMCM-41 series are also periodic mesoporous materials, but as the XRD was only used to determine if the pores retain their integrity during the dendrimers synthesis no XRD experiments were performed for these supports. This is due to the observation that during the synthesis of the dendrimers for the LPMCM-41 series no change was observed in the pore integrity.

4.4.2 Nitrogen adsorption-desorption analysis.

4.4.2.1 Nitrogen adsorption-desorption analysis of dendrimers supported on LPMCM-41.

Figures 4-7a and 4-7b depict the nitrogen adsorption-desorption isotherms and the pore size distributions (PSD) for LPMCM-41 and the supported dendrimers. They are all of type IV isotherms, and exhibit the condensation and evaporation steps, characteristic of periodic mesoporous materials.[2,3,4]

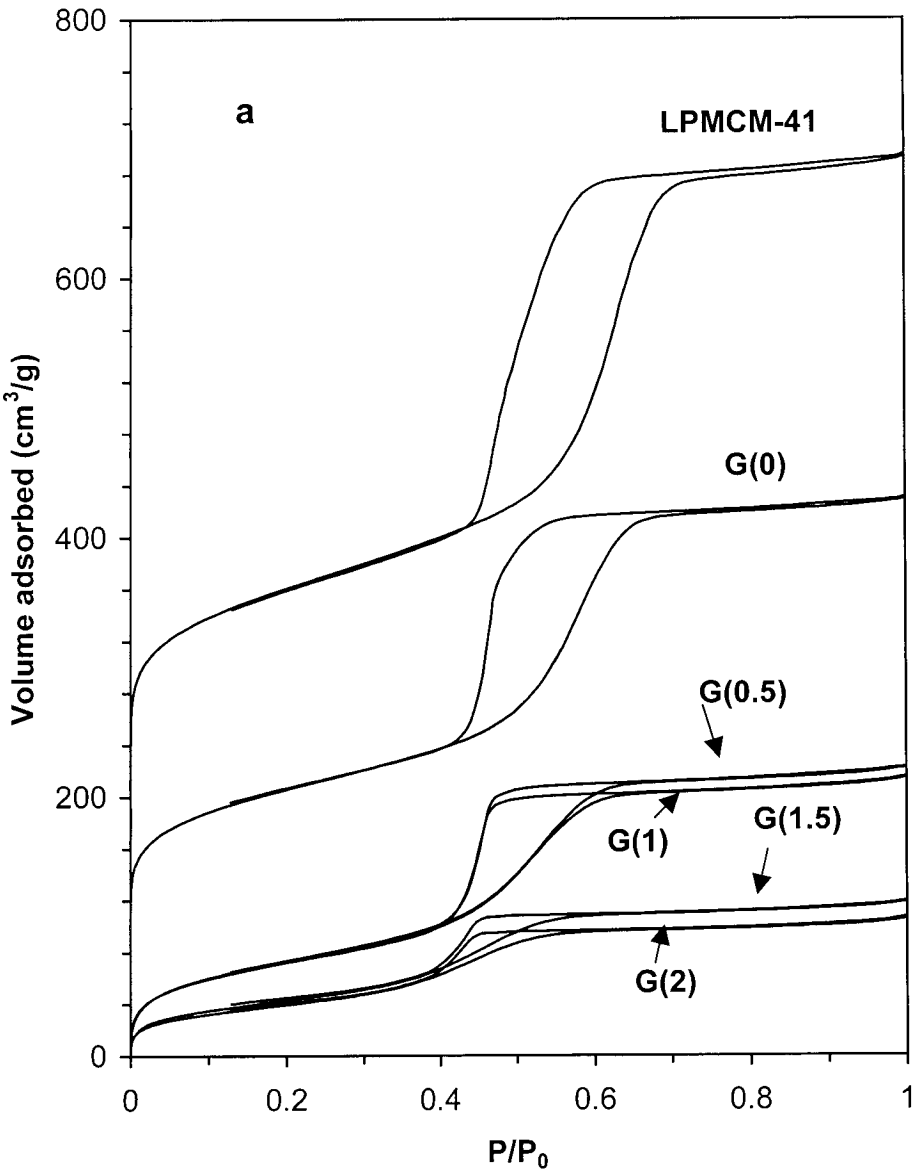
a
LPMCM-41
G(0)
G(0.5)
G(1)
G(1.5)
G(2)
Volume adsorbed (cm3/g)
P/P0
800
600
400
200
0
0
0.2
0.4
0.6
0.8
1

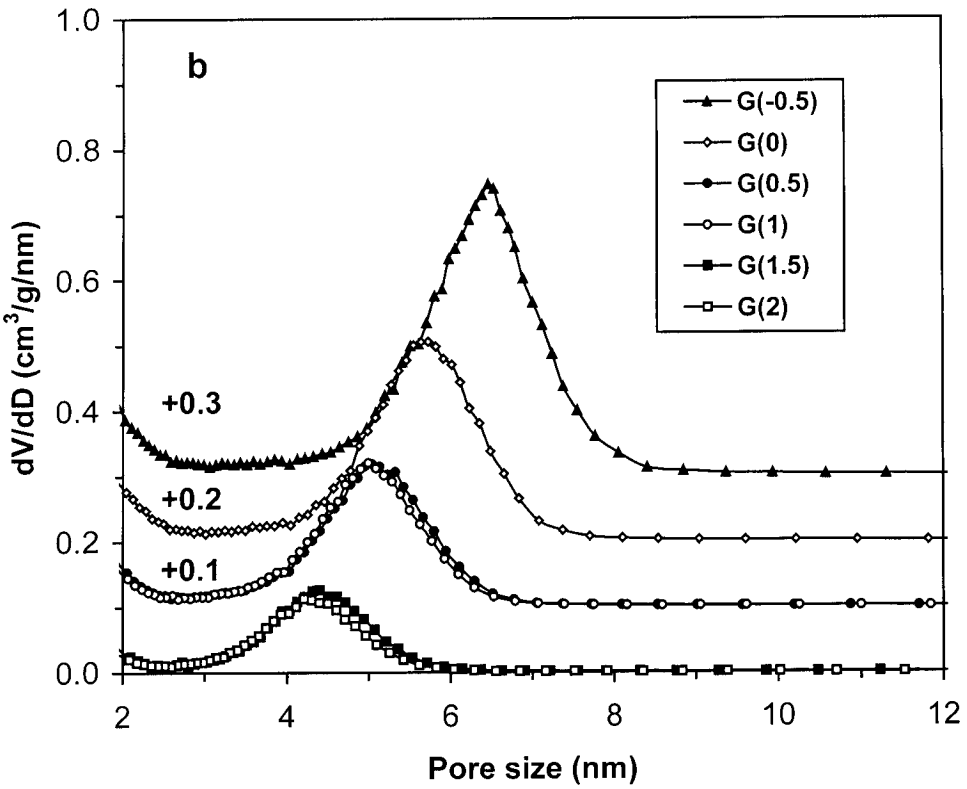

Figure 4-7. Nitrogen adsorption isotherms (a) and pore size distributions (b) for LPMCM-41 supported dendrimers. As indicated, several curves were shifted upward for clarity.

All the structural properties calculated based on nitrogen adsorption data are shown in Table 4-3. It is instructive to note that the surface area, the pore volume and pore size decrease significantly, but not linearly with increasing dendrimer generations. Compared to G(-0.5) material, i.e., pure LPMCM-41, the G(0), i.e., APTES-grafted LPMCM-41, exhibited significantly lower BET surface area (390 vs. 585 m^2/g), pore volume (0.51 vs. 0.78 cm^3/g) and pore size (5.6 vs. 6.5 nm). This is consistent with similar observations reported in the literature.[5-7] Further

decrease of the specific surface area, and the pore volume and size took place upon reaction of methyl acrylate with G(0) material to obtain G(0.5). Compared to the starting material, the surface area and pore volume decreased by about 50 %, whereas the pore size decreased by ca. 22 %. However, as shown in Table 4-3, upon reaction of methyl propylaminopropionate functionalized LPMCM-41 (G(0.5)) with ethylenediamine to obtain G(1) material, the structural properties hardly changed. This is most likely due to the fact that there is only a small difference in size between the half generations and the next full generations, whereas the radius of the dendrimers changes significantly between full generations and the following half generations. Thus substantial decrease of S_{BET}, V and w_{KJS} takes place only during the branching steps. Consistent with this observation, the surface area, pore volume, and size of G(1.5) were much lower than those of G(1), but almost identical to those of G(2). As shown in Table 4-3, the thickness of the pore walls also increased stepwise, while remaining almost constant for materials containing grafted dendrimers corresponding to half and the next full generation.

The values of the structural properties for G(2.5) and G(3) were not included in Table 4-3 as these samples did not adsorb any nitrogen indicating that the pore system was completely blocked. Interestingly, the size of the grafted third generation dendrimer, calculated based on bond lengths, was found to be around 2.7-3.0 nm, which is approximately half of the pore size of the starting materials,

i.e., 5.6 nm. This lends strong support to the fact that the pore systems for G(2.5) and G(3) materials are essentially blocked.

Table 4-3. Structural Properties of LPMCM-41 Supported Dendrimers.

Generation[a]	S_{BET} (m^2/g)	w_{KJS} (nm)	b (nm)[b]	V^c (cm^3/g)	Experimental[d] V/Vo	Calculated[d] V/Vo
-0.5	585	6.5	0.68	0.77	1	1
0	390	5.6	2.25	0.51	0.71	0.74
0.5	271	5.0	2.97	0.34	0.56	0.59
1	265	5.0	2.79	0.33	0.54	0.59
1.5	157	4.3	3.49	0.18	0.34	0.44
2	145	4.2	3.59	0.16	0.30	0.42
2.5	-	-	-	0	0	-
3	-	-	-	0	0	-

(a) Generation (-0.5) refers to the LPMCM-41 support. (b) *b* is the pore wall thickness. (c) V is the pore volume of the material per g of silica. (d) V_0 is the pore volume of the starting material.

The behavior of the structural properties as a function of dendrimer generation provides clear evidence that the dendrimers grew inside the pore channels. However, based on strictly geometrical considerations, assuming that the organic modifier forms a "smooth" layer, the pore volume and the pore size of any two

materials would be related by the following equation $V_1/V_2 = (w_1/w_2)^2$. Using the starting material as a reference, the relative pore volumes for all samples were calculated using this equation and compared to the experimental data. As seen in Table 4-3, the actual pore volume decreased as a function of dendrimer generation faster than the calculated pore volume. Moreover, the difference between the experimental and calculated pore volume increased with dendrimer generation. Close scrutiny of literature data also indicate that upon surface modification of periodic mesoporous materials by organic species, the average pore size is often higher than $w_0(V/V_0)^{1/2}$, where V is the pore volume of the modified material, and V_0 and w_0 are the pore volume and size of the starting material, respectively.[5-7] However, potential reasons for such behavior have not been explored.

4.4.2.2 Nitrogen adsorption-desorption analysis of dendrimers supported on Davisil.

Figure 4-8 depicts the nitrogen adsorption-desorption isotherms for Davisil and the supported dendrimers. They are all of type IV isotherms, but in this case there is no well-defined step in the isotherms as found for the LPMCM-41 series dendrimers. This shows the wide pore size distribution, but the pores are significantly larger than the pores of the LPMCM-41. It is also clear from Table 4-4 that the growth of the dendrimers has a smaller effect on the surface area and the pore size when compared to the LPMCM-41 series. For instance the surface area decreased from 280 m^2/g for the Davisil support to 126 m^2/g for the G(3) dendrimer. The experiments however prove that a larger pore and the pore shape are important in determining the success of the dendrimer growth. This effectively represents dendrimer growth on the outside surface of the supports, as the size of the pores is much larger than the dendrimer molecules. In This case the G(3) dendrimers are easily synthesized and there is no pore blocking observed. These results show that the pore geometry is very important to the success of the dendrimer synthesis.

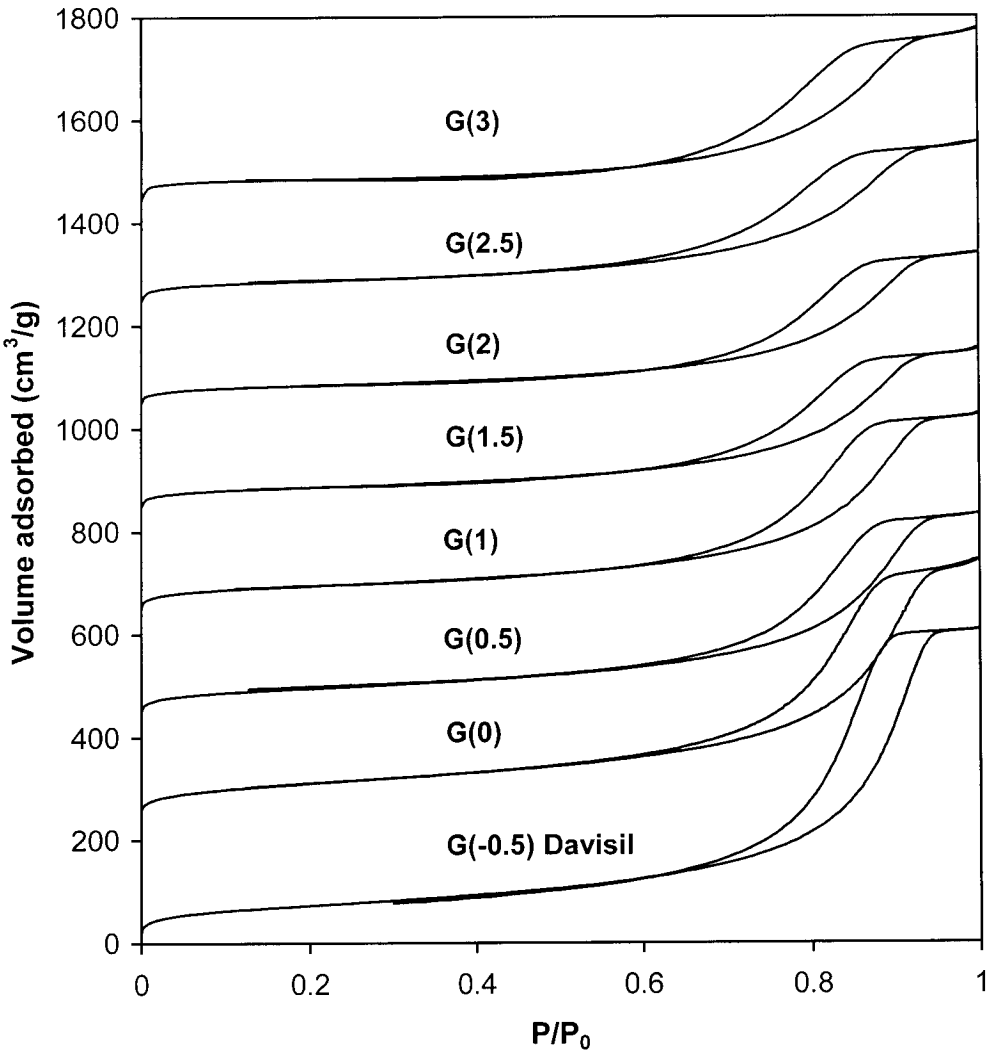

Figure 4-8. Nitrogen adsorption isotherms for the davisil series dendrimers. (Isotherms were shifted upward for clarity)

Table 4-4. Surface area, pore size and pore volume for Davisil series dendrimers.

Generation	S_{BET} (m^2/g)	Pore size (nm)	Pore Volume (cm^3/g)
G(-0.5) Davisil	280	18.0	0.95
G(0)	230	17.5	0.77
G(0.5)	169	15.5	0.60
G(1)	163	14.4	0.59
G(1.5)	133	13.4	0.52
G(2)	132	13.5	0.50
G(2.5)	130	11.1	0.48
G(3)	126	11.9	0.50

4.4.2.3 Nitrogen adsorption-desorption analysis of dendrimers supported on PEMCM-41.

Figures 4-9a and 4-9b depict the nitrogen adsorption-desorption isotherms and the pore size distributions (PSD) for PEMCM-41 and the supported dendrimers. They are all also of type IV isotherms, and exhibit the condensation and evaporation steps, characteristic of periodic mesoporous materials around for the LPMCM-41 series.[2,3,4]

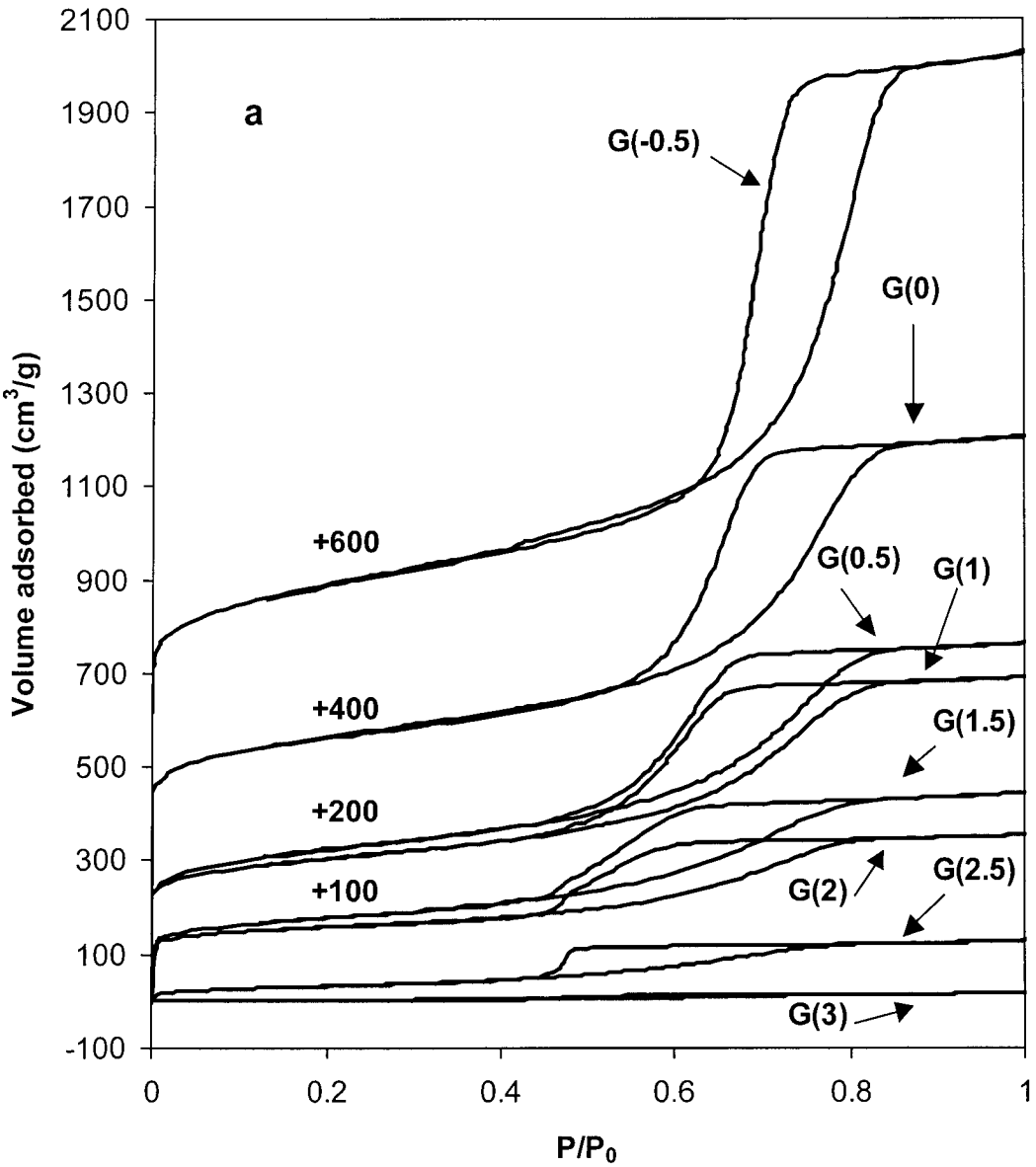
a
G(-0.5)
G(0)
G(0.5)
G(1)
G(1.5)
G(2)
G(2.5)
G(3)
+600
+400
+200
+100
Volume adsorbed (cm3/g)
P/P0
2100
1900
1700
1500
1300
1100
900
700
500
300
100
-100
0
0.2
0.4
0.6
0.8
1

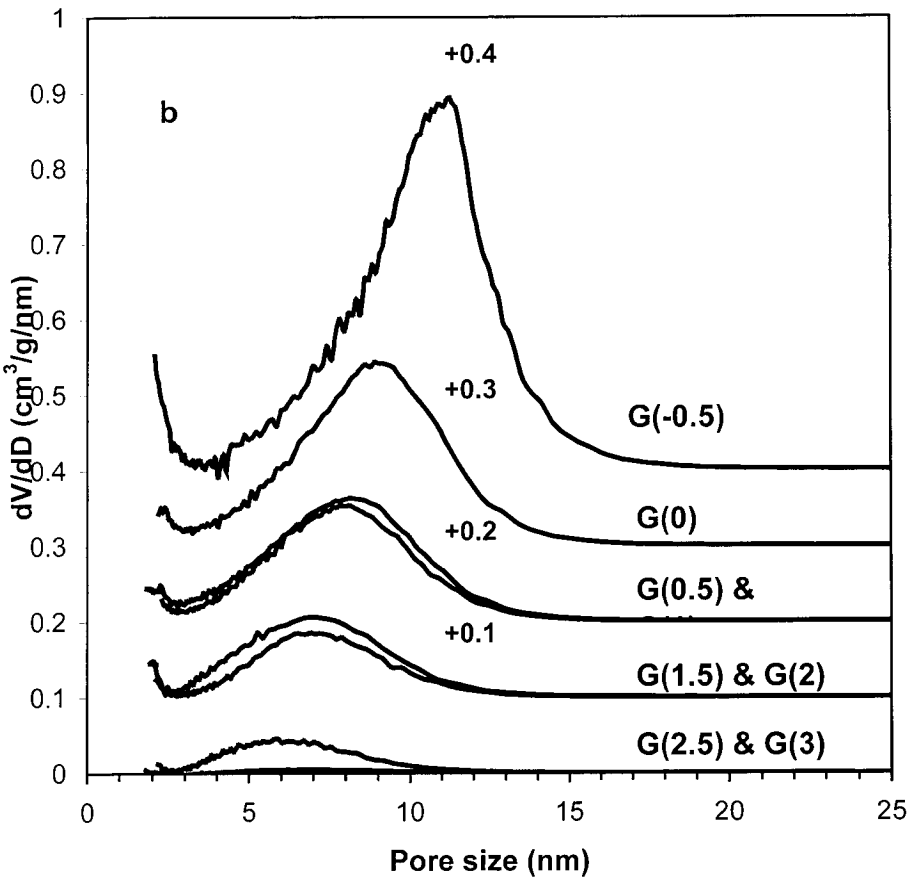

Figure 4-9. Nitrogen adsorption isotherms (a) and pore size distributions (b) for PEMCM-41 supported dendrimers. As indicated, several curves were shifted upward for clarity.

The PEMCM-41 results are very similar to the LPMCM-41 as expected. The half generations are again similar to the next full generation, but in this case the effect is less pronounced. This could be due to the very large pores.

Table 4-5. BET surface data for PEMCM-41 series dendrimers.

Entry	Generation	S_{bet} (m^2/g)	Pore size	Pore volume (cm^3/g)
1	-0.5	1385	10.6	2.23
2	0	612	8.9	1.26
3	0.5	457	8.1	0.88
4	1	385	7.7	0.77
5	1.5	286	7	0.54
6	2	215	6.8	0.40
7	2.5	119	5.8	0.20
8	3	13	5.6	0.03
9	3.5	0	0	0.00
10	4	0	0	0.00

It is clear from these results that G(3) (Entry 8, Table 4-5.) is in this case the point where pore blocking takes place. We cannot explain this at this moment as the IR spectra clearly shows that the G(4) species form, although not completely.

Figure 4-10 shows the surface area of the grafted dendrimers as a function of the generation for the PEMCM-41 series. In this case the surface area data does not exhibit the same step with the branching as in the LPMCM-41 series. The surface area does however drop significantly from the support to G(3).

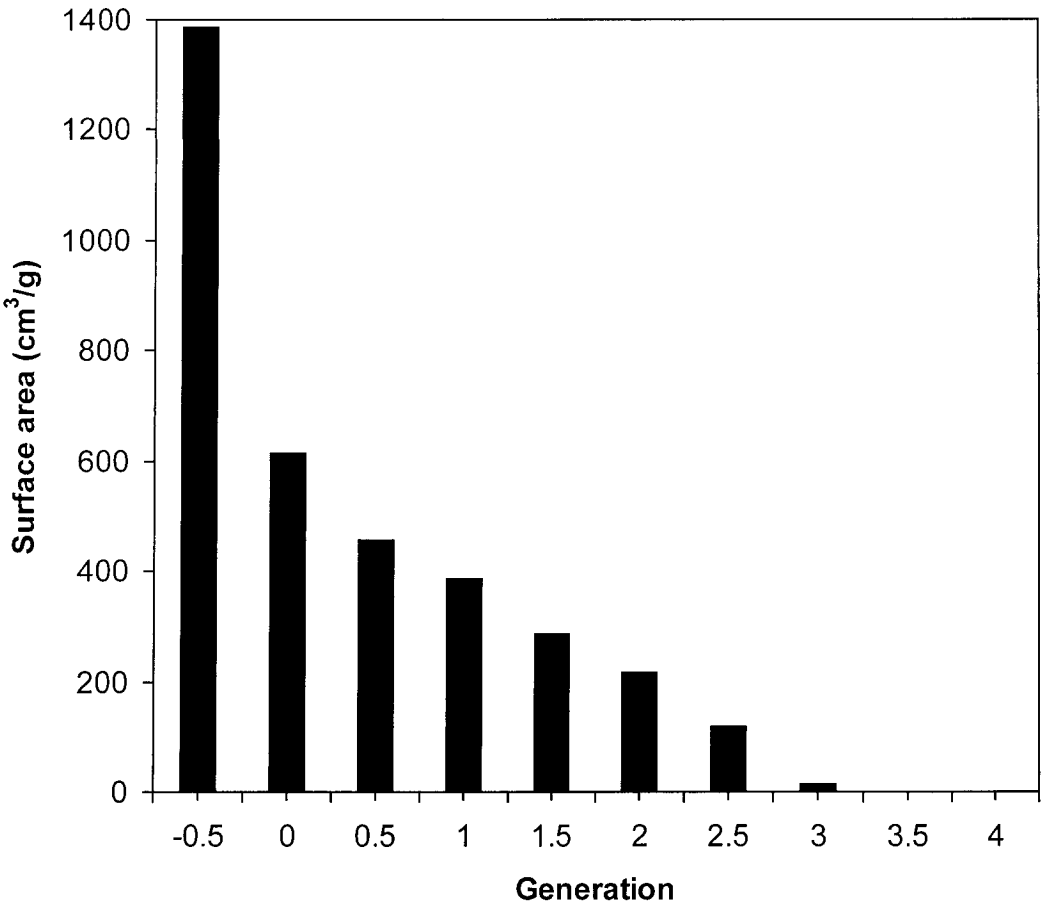

Figure 4-10. Surface area as a function of generation for the PEMCM-41 series C_2 PAMAM dendrimers.

4.4.3 NMR analysis.

4.4.3.1 NMR analysis of LPMCM-41 series dendrimers.

4.4.3.1.1 Cross polarization magic angle spinning ^{13}C NMR analysis of LPMCM-41 series dendrimers.

Cross-polarized magic angle spinning (CP/MAS) ^{13}C NMR was used in this study for the identification of functional groups. Representative ^{13}C NMR spectra are shown in Figure 4-11. Figure 4-11a is the ^{13}C NMR for the aminopropylsilane grafted LPMCM-41 (G(0)). In this case, three signals were observed at 8.76 ppm, 25.34 ppm and 43.35 ppm. They were attributed to the three carbons between the Si atom and the nitrogen, with increasing distance from the Si atom leading to a higher ppm value. There were also small signals at 58.89 ppm and 15.88 ppm, which can be attributed to small amounts of unhydrolyzed ethoxy groups attached to the Si atom. Figure 4-11b is the ^{13}C NMR of the G(1.5) species attached to the LPMCM-41. In this spectrum, 5 types of carbons can be identified. The signals at 10.20, 22.23 and 32.88 ppm are again the three carbons of the original aminopropylsilane species that are slightly shifted due to the reactions that took place. The signal at 32.88 ppm also includes some of the carbons from the methacrylate moiety attached to the nitrogen at the branching points. This would explain the stronger intensity of this signal when compared to the other two peaks at 10.20 and 22.23 ppm. The signal at 50.61 ppm corresponds to the sum of two signals attributable to the carbon atoms in two functional groups, namely the methoxy carbons of the ester functionalities as well as the carbons attached directly to nitrogen in the ethylenediamine species. The

signal at 172.79 is due to the ester carbonyl carbons in the molecule. Figure 4-11c is the ^{13}C NMR spectrum of the G(3) dendrimer species attached to the surface of LPMCM-41. This spectrum shows the same general features with the signals at 51.74 and 39.45 ppm now similar in size. The two remaining carbons from the aminopropylsilane are barely visible at 10.58 and 21.98 ppm. This spectrum serves to show that the amide signals at 173.51 ppm, although clearly visible and large, is subject to considerable line broadening and therefore does not allow for clear distinction between amide and ester groups (172.79 ppm) in the molecule. This is a limitation of the ^{13}C NMR technique because the full generations were prepared by changing ester groups into amide groups and should therefore only contain amides. It is thus impossible to ascertain from ^{13}C NMR if full conversion between half generations and full generations was accomplished. As discussed in Section 4.4.1., FTIR spectroscopy was used to address this shortcoming.

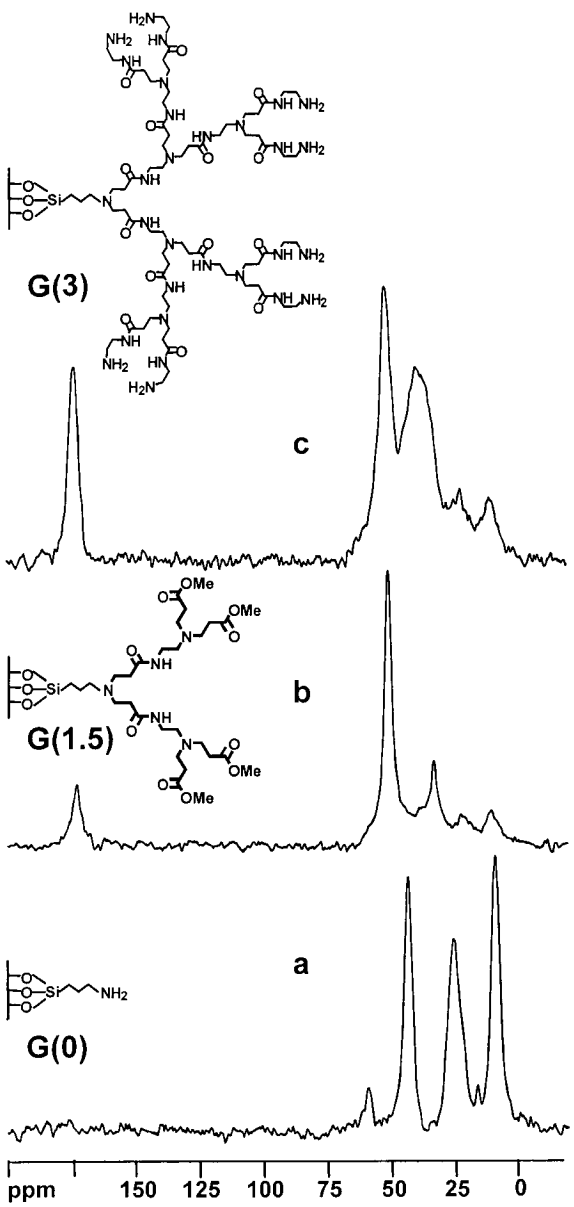

Figure 4-11. Selected ^{13}C CP/MAS NMR spectra of the C_2 PAMAM dendrimers supported on LPMCM-41.

4.4.3.1.2 Cross polarization magic angle spinning ^{29}Si NMR analysis of LPMCM-41 series dendrimers.

^{29}Si CP/MAS NMR analysis was also used to characterize the supports. These spectra can be very useful in determining the mode of attachment of the grafted species to the support as well as to confirm the stability of the grafted material. The ^{29}Si CP/MAS NMR spectrum of the ungrafted LPMCM-41 is represented in Figure 4-12. This spectrum exhibits a large signal at –100.6 ppm and a broad shoulder at –110 ppm. The signal at –110 is assigned as the Q_4 Si-atoms i.e. those Si atoms attached to 4 other Si atoms through oxygen bridges (=Si=). The signal at –100.6 is assigned to the Q_3-Si atoms i.e. those Si-atoms attached to 3 other Si atoms through oxygen bridges and one OH group (≡Si-OH). The Q_4 Si-atoms therefore represent the walls of the support and the Q_3 Si-atoms represent the surface atoms that can be functionalized. It is clear from Figure 4-12 that the Q_3 Si-atoms seem to outnumber the Q_4 Si-atoms, but this is due the cross polarization that is non equivalent for the two species. The Q_3 Si-atoms are attached directly to the hydrogen containing hydroxyl group. This causes the magnetization transfer in the ^{1}H-^{29}Si system to take place at a faster rate than for the Q_4 Si-atoms, leading to a spectrum where Q_3 Si-atoms are positively distorted. To circumvent this observation a ^{29}Si NMR spectrum of this species was recorded without ^{1}H-^{29}Si cross polarization leading to a more quantitative spectrum. This experiment however is impractical as the acquisition period is

very long and therefore the CP/MAS method was chosen for the evaluation of the higher dendrimers.

After grafting of the aminopropylsilane group the ^{29}Si NMR spectrum (Figure 4-13.) exhibits signals for both Q_3 and Q_4 at –101.0 ppm and –109.6 respectively. In addition to the Q_3 and Q_4 signals the spectrum also exhibit signals at –64.6 and –58.5 ppm. These signals are designated T_3 and T_2 respectively. (T_n = [C-$Si(OSi)_n(OH)_{3-n}$).[6]

In an effort to rule out Si-O-Si bond hydrolysis ^{29}Si CP/MAS NMR spectra were also recorded for all the higher generation dendrimers on LPMCM-41. A representative spectrum is Figure 4-14. Figure 4-14 is the ^{29}Si CP/MAS NMR spectrum for the G(2) C_2-PAMAM dendrimer supported on LPMCM-41. This spectrum exhibits the same signals as the APES grafted G(0) species. This shows that the attachment of the dendrimers is quite stable to the reaction conditions and no hydrolysis or pore degradation takes place. It is however instructive to note that the T_2 and T_3 signals seem lower in intensity for the G(2) species when compared to the G(0) species. This is however due to the increased magnetization transfer that takes place to the surface silanols and the pore wall Si-atoms due to the increased concentration of protons in close proximity to these atoms. We are confident that very little or no hydrolysis takes place during the reactions.

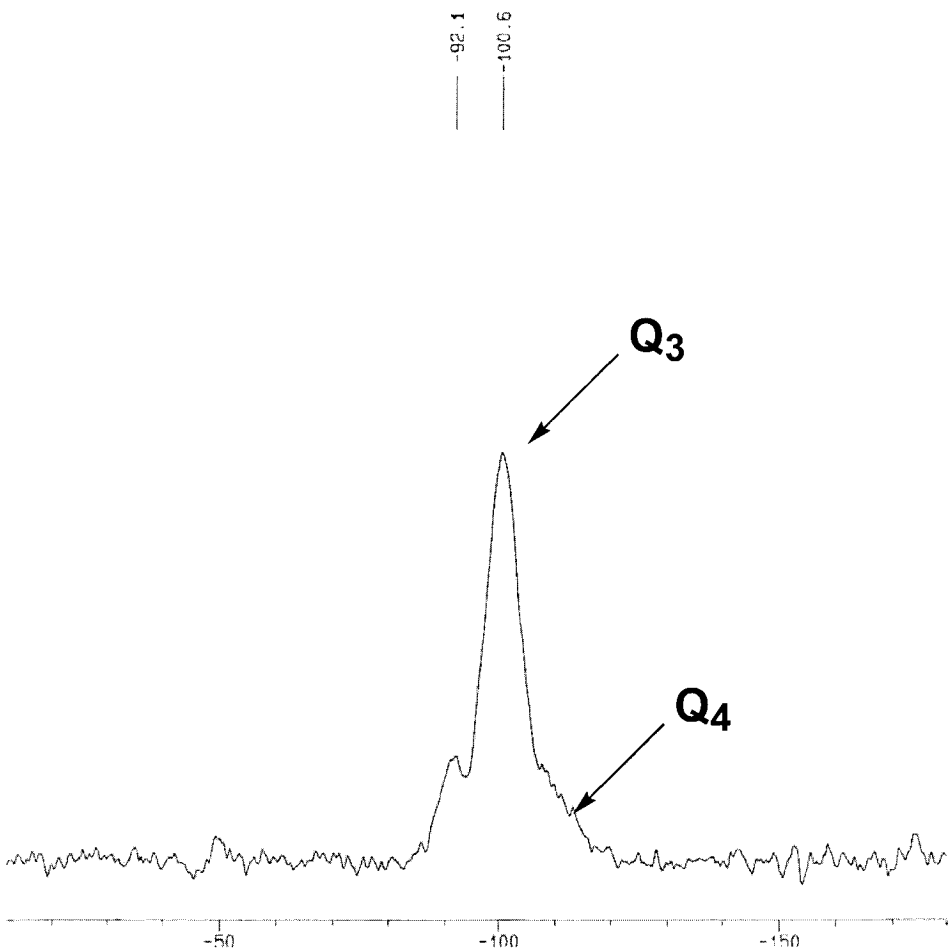

Figure 4-12. ^{29}Si NMR of LPMCM-41 Support.

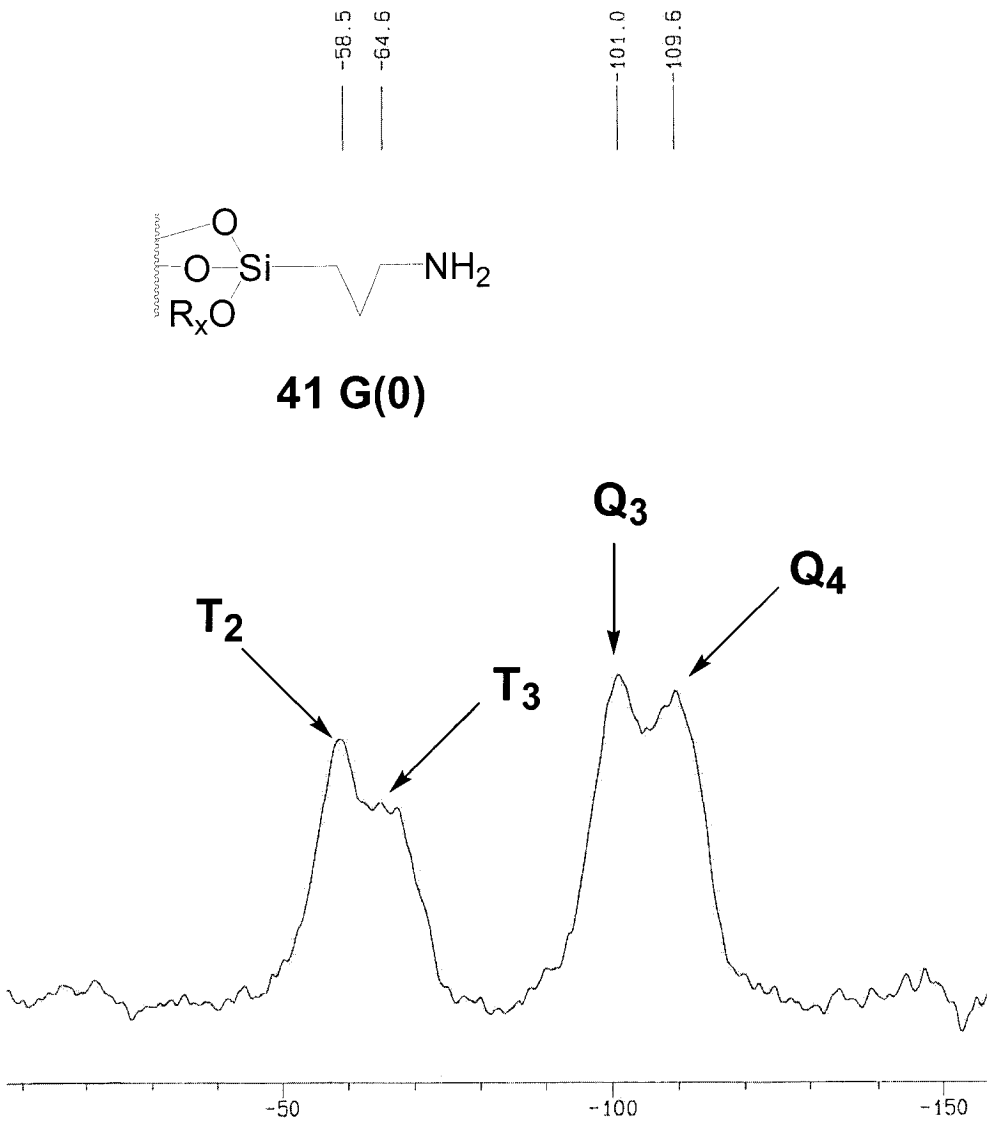

Figure 4-13. ^{29}Si NMR of LPMCM-41 Support after grafting of aminopropylsilane (G(0)).

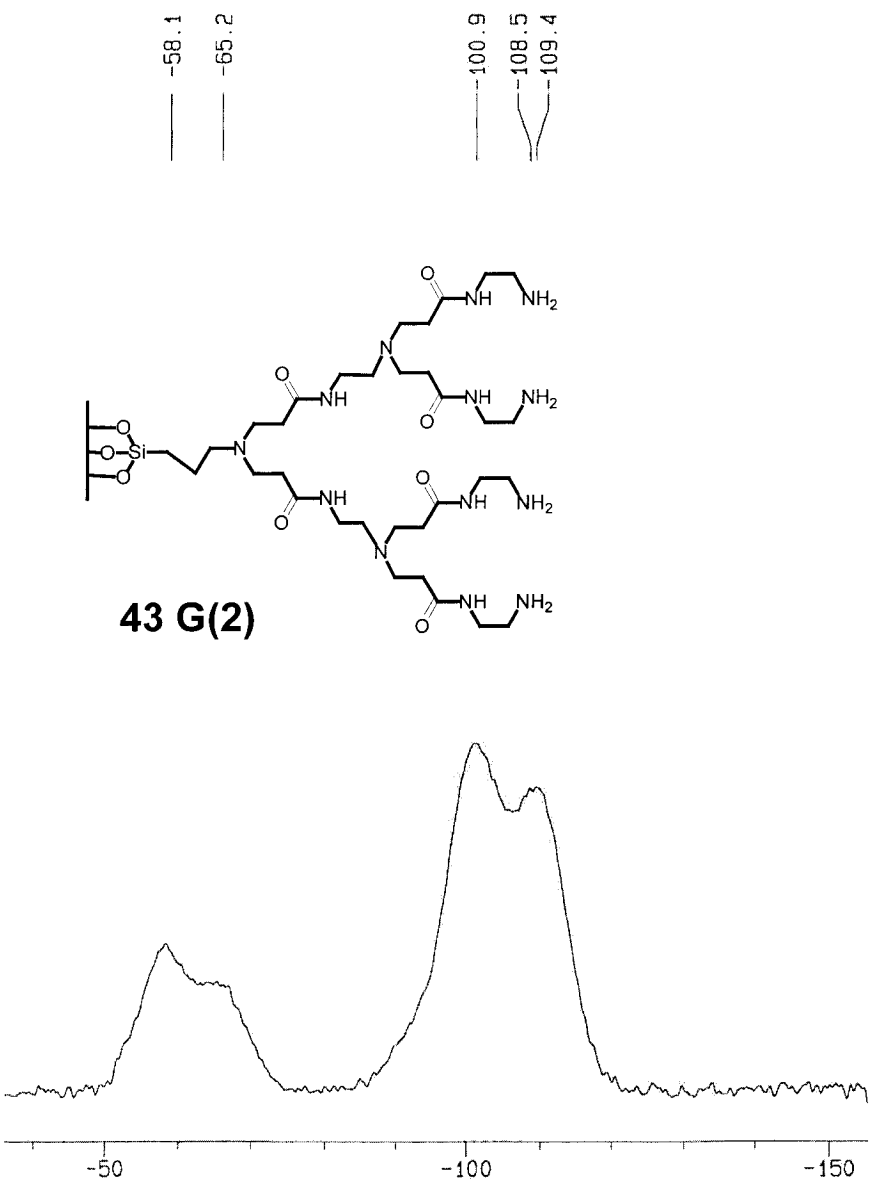

Figure 4-14. ^{29}Si NMR of LPMCM-41 Support after various reactions to prove that the structure of the support stays intact (G(2)).

4.4.3.2 NMR analysis of Davisil series dendrimers.

4.4.3.2.1 Cross polarization magic angle spinning ^{13}C NMR analysis of Davisil series dendrimers.

^{13}C CP/MAS NMR spectra were also recorded for the Davisil series dendrimers and the PEMCM-41 series dendrimers. A representative spectrum of the davisil G(3) C_2 dendrimer is shown in Figure 4-15. It is clear that the spectrum is virtually identical with that of the G(3) LPMCM-41 dendrimer. The spectrum again exhibits large signals at 51.74 and 38.04 ppm and the remnants of the APS group on the silica are represented by the signals at 10.09 and 23.02 ppm. The rather large amide signal at 173.91 ppm again shows the extensive line-broadening characteristic of the solid-state ^{13}C NMR method.

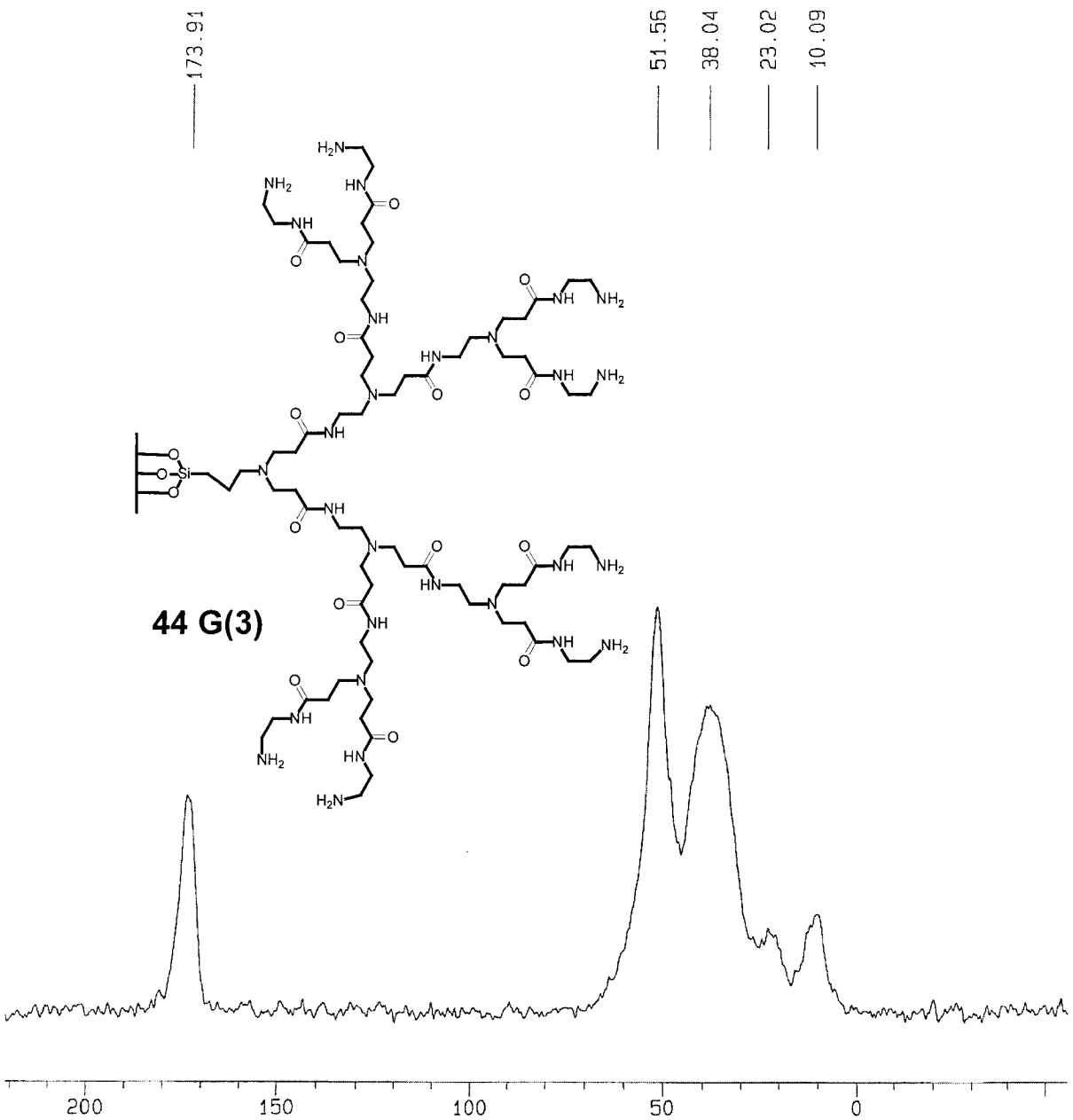

Figure 4-15. The ^{13}C CP/MAS NMR spectrum of the G(3) C_2 PAMAM dendrimer supported on Davisil.

4.4.3.3 NMR analysis of PEMCM-41 series dendrimers.

4.4.3.2.1 Cross polarization magic angle spinning ^{13}C NMR analysis of PEMCM-41 series dendrimers.

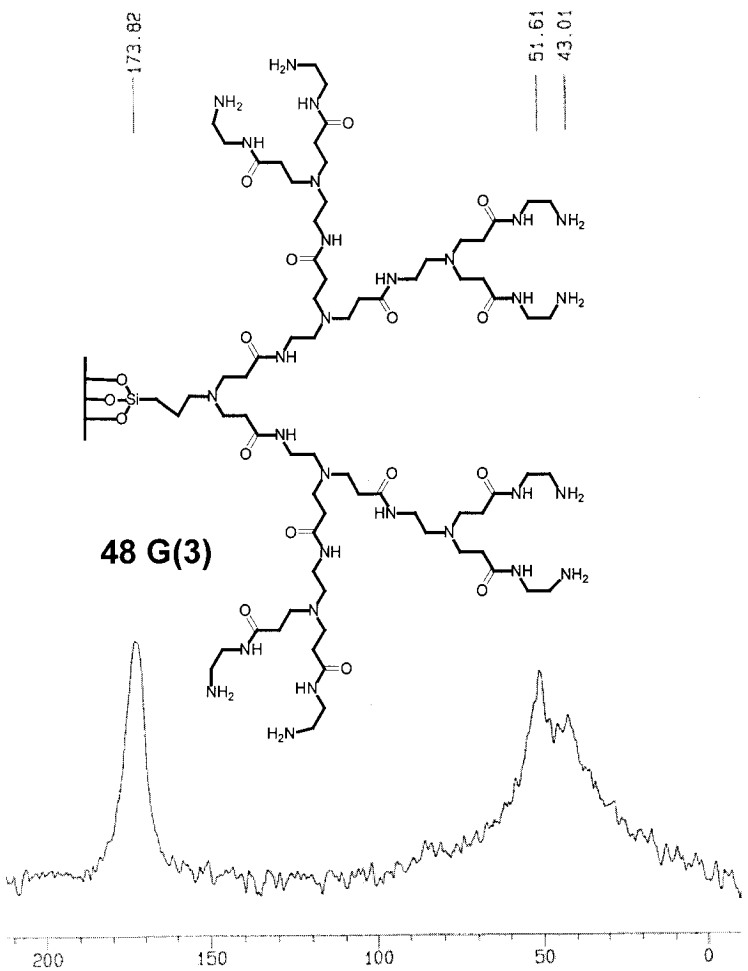

Figure 4-16. ^{13}C CP/MAS NMR spectrum of the G(3) C_2-PAMAM dendrimer supported on PEMCM-41.

The ^{13}C CP/MAS NMR spectra of the PEMCM-41 are also similar to the spectra of the LPMCM-41 and the Davisil series dendrimers. The G(3) C_2 ^{13}C CP/MAS NMR spectrum is represented in Figure 4-16.

In this spectrum the amide signal at 173.82 ppm is very large and for the first time has a higher intensity than the aliphatic carbons. It is therefore clear that the grafting on the PEMCM-41 was very successful when compared directly to the LPMCM-41 and Davisil series.

4.4.3.4 Cross polarization magic angle spinning ^{29}Si NMR analysis of Davisil and PEMCM-41 series dendrimers.

^{29}Si CP/MAS NMR analysis was also used to characterize the Davisil and PEMCM-41 series dendrimers. The spectra are similar to the LPMCM-41 series, and were used to determine if Si-O-Si bond hydrolysis takes place. As with the LPMCM-41 series, no Si-O-Si bond hydrolysis was observed, and the supports retain their integrity through the dendrimer synthesis steps.

4.4.4 Infrared spectroscopy.

4.4.4.1 Infrared spectroscopy for LPMCM-41series dendrimers.

Infrared spectroscopy proved to be a very useful technique to complement ^{13}C NMR data. The IR spectra for the support (G(-0.5)), grafted molecule (G(0)) and dendrimers (G(0.5)-G(3)) are shown in Figure 4-17. The absorption band at 1740 cm^{-1}, clearly visible in all the half generations, was attributed to the CO stretching of the ester groups. The adsorptions at 1643 cm^{-1} and 1547 cm^{-1} were due to the CO stretching and the N-H bending/CN stretching of the secondary amide groups, respectively. It is therefore possible to distinguish between the amide function in the full generation dendrimers and the ester function in the half generations. Thus FTIR spectroscopy offers a simple tool to determine if the amidation reactions proceed to full conversion. However, FTIR does not provide much quantitative evidence as to whether the Michael additions proceed to completion or not. The FTIR spectrum of the G(0.5) species clearly shows the ester incorporation but at G(1), some ester functional groups can still be detected even though the amides now represent the largest part of the functional groups. Then from G(1) to G(1.5), the incorporation of the ester groups is again clearly demonstrated. Likewise, at G(2), FTIR offered evidence of unreacted ester groups and even up to G(3) a small amount of ester groups remained. It is instructive to note that the spectra were recorded using an ATR system that allows direct comparison between the samples due to the uniform contact of the sample with the ATR crystal. Therefore the increasing intensity of the adsorptions

can be directly related to the amount of amides and esters in the samples. It is however difficult to quantify this increase exactly due to the increasing organic mass added to the LPMCM-41 and it is impossible to correct these spectra without using other information like silica content from TGA data. The TGA experiments will be discussed in the next section, but first there were other minor peaks in the IR spectra that deserve some mention. The adsorption at 3277 cm^{-1} was assigned to the amide N-H stretching. The adsorptions at 2951 cm^{-1} and 2824 cm^{-1} were due to C-H stretching in the molecule.

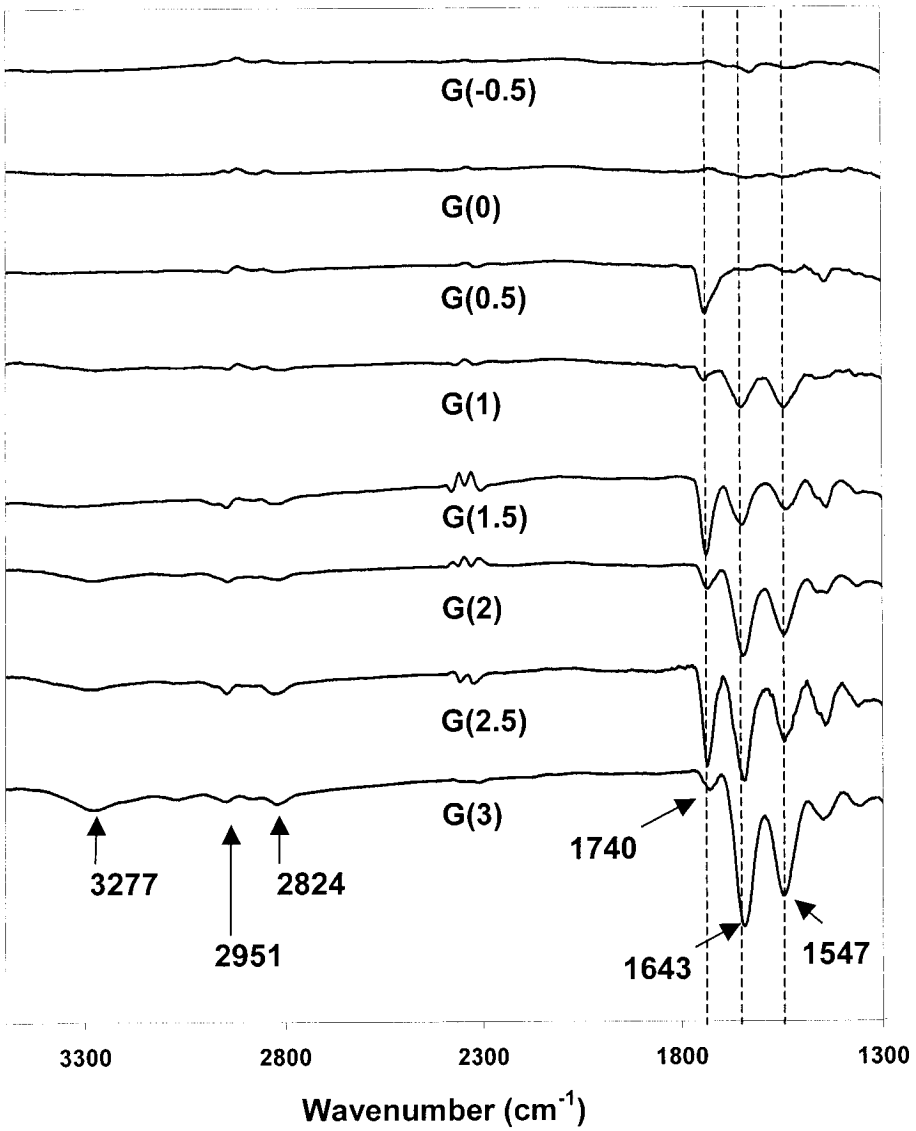

Figure 4-17. FTIR spectra for LPMCM-41 supported dendrimers.

4.4.4.2 Infrared spectroscopy for the Davisil and PEMCM-41 series dendrimers.

The infrared spectra were recorded for both the Davisil (support –G(3) Figure 4-18.) and PEMCM-41 (support –G(4) Figure 4-19) series dendrimers. It is clear from the Infrared spectra that the half generations have both ester (1742 cm^{-1}) and amide (1640 cm^{-1} and 1540 cm^{-1}) adsorptions and that the full generation have only amide adsorptions. It is interesting to note that in this series there are almost no remnants of the ester adsorption in the full generations (except for G(4) in the PEMCM-41 series. (Figure 4-19.), where these were quite visible in the LPMCM-41 series (Figure 4-17.). Unfortunately the S_{BET} shows that pore saturation again takes place at G(3) for the PEMCM-41 .

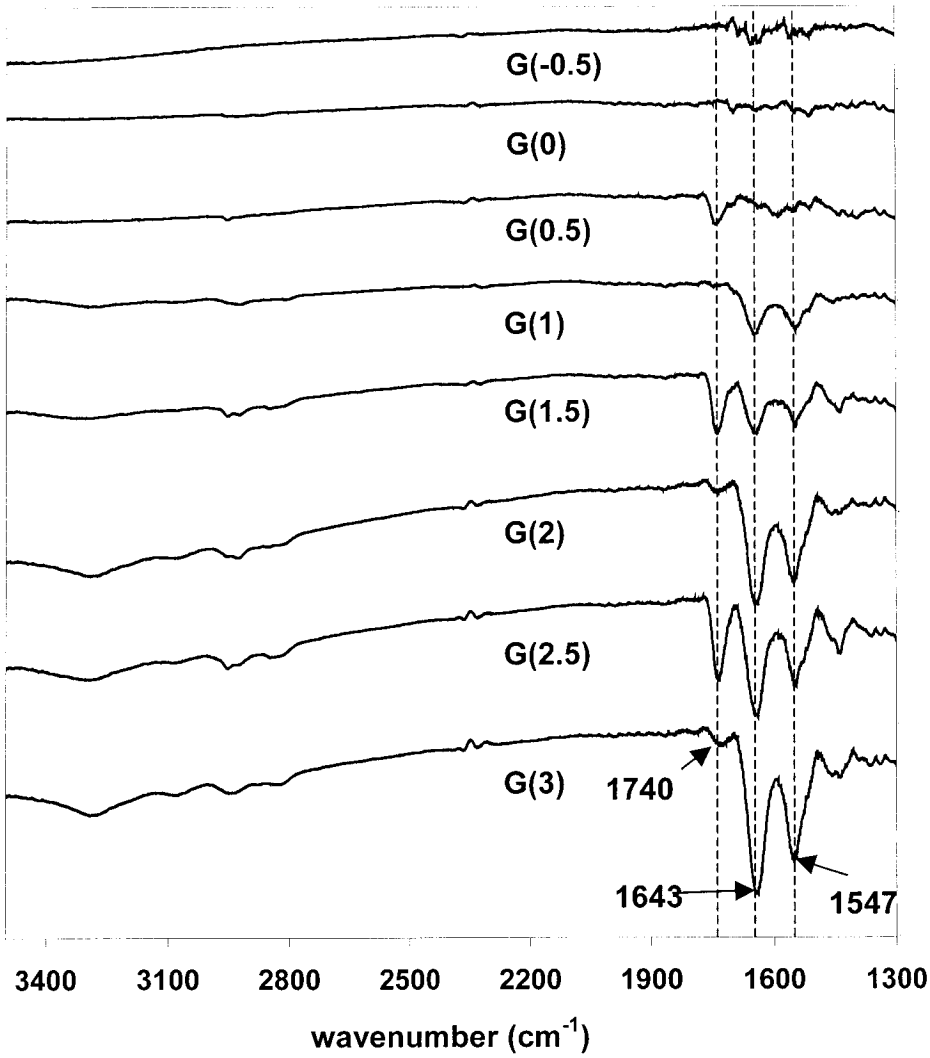

Figure 4-18. FTIR spectra for Davisil supported dendrimers.

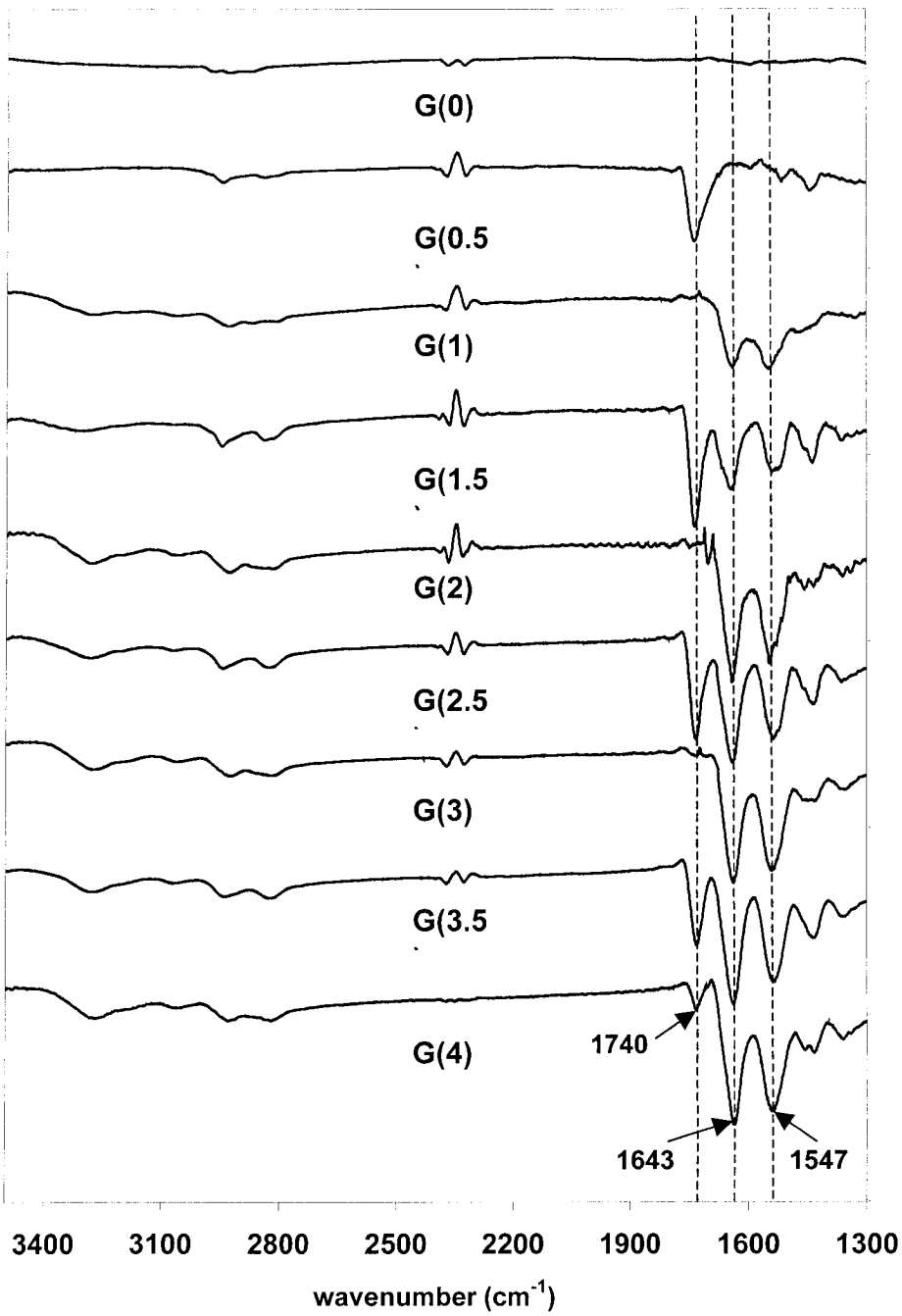

Figure 4-19. FTIR spectra for PEMCM-41 supported dendrimers.

4.4.5 Thermal analysis and Elemental analysis.

4.4.5.1 Thermal analysis of LPMCM-41 series dendrimers.

Thermal analysis curves for representative samples are shown in Figure 4-20. From Figure 4-20A, it is clear that pristine LPMCM-41 lost weight between 25 and 121 °C. This event was associated with the desorption of water.[5] The rest of the curve (121 – 1000 °C) showed very slow, but continuous weight loss. The weight loss between 121 and 800 °C was used as a baseline amount for the dendrimer-containing samples to correct for the weight loss of the silica in these samples. In Figure 5B, the DSC-TGA curve for the G(0) material was slightly different as two large peaks were observed. There was still some water that desorbed completely by 121 °C. The second peak at about 325 °C was attributed to the pyrolysis of the aminopropyl group. This weight loss was accompanied by the release of a large amount of energy due to the strength of the carbon silicon bond. This conclusion was inferred from the DSC curve (Figure 4-20Bc) that shows a large exothermic peak at this point. In direct contrast to this, the DSC peak corresponding to the desorption of water shows that this event is slightly endothermic. In addition, the TGA peak at 325 °C had a large shoulder that extended to around 700 °C. This broad peak was attributed to further combustion of carbonaceous species (coke) that formed during the pyrolysis of the aminopropyl species at 325 °C. This shoulder was observed in all the samples containing higher generation dendrimers. Thermogravimetric analysis data for the product of the double Michael addition to the G(0) LPMCM-41 species are shown in Figure 4-20C. In this case, a new peak was observed at about 210 °C

in addition to the previous peaks associated with the water desorption and the pyrolysis of the aminopropyl group. The peak at 210 °C was attributed to the decomposition of the ester branches. Like the H_2O desorption, this event was also endothermic suggesting that decomposition, rather than pyrolysis, took place. A separate TGA experiment coupled with mass spectrometry (Pfeiffer ThermoStar instrument) lent further support to this contention. Indeed, the TGA peak at 210 °C was accompanied by the release of fragments with 55-60 and 85-86 amu corresponding to the decomposition of the methyl acrylate species. At higher temperature, the formation of CO_2 was prevalent indicative of the combustion of the remaining organic species. Figure 4-20D shows the thermogravimetric analysis data for the G(1) material, which differs from the G(0.5) material (Figure 4-20C), only by the end group. As seen, the curves were very similar to those of the G(0.5) species with the amide decomposition giving a peak at 210 °C like the ester group in Figure 4-20C. This peak however had a shoulder at about 250 °C, which could be due to some ester groups remaining, as supported by FTIR data. In this case, a large shoulder at 600 °C was again observed and the high intensity of this peak could be due to the larger organic content of this material in comparison to the G(0) material.

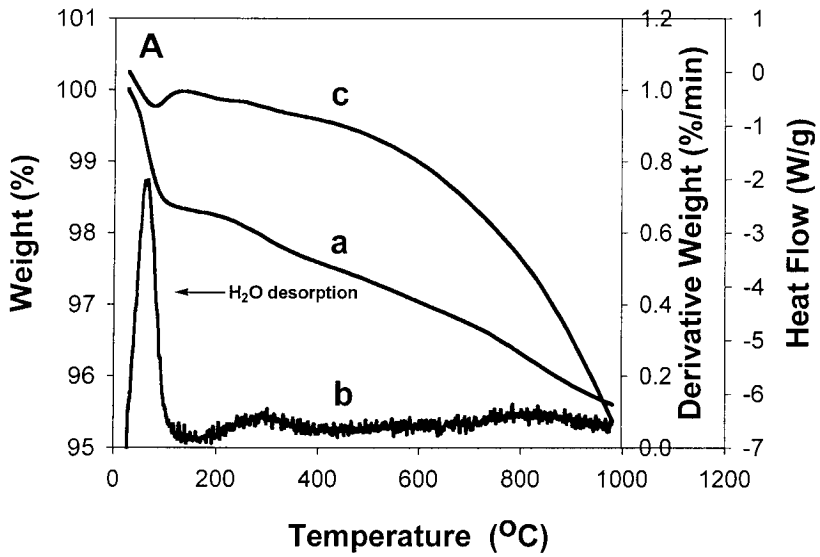
A
c
a
b
H_2O desorption
Weight (%)
Derivative Weight (%/min)
Heat Flow (W/g)
Temperature (^oC)

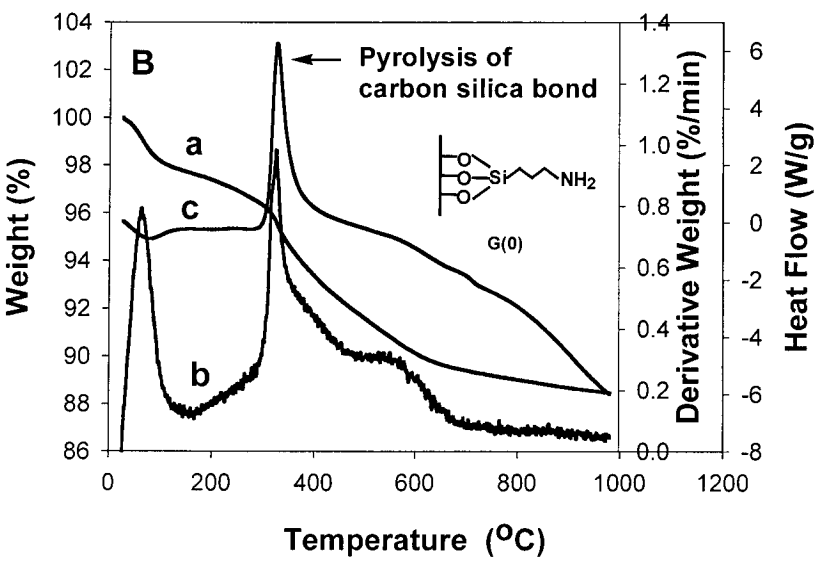
B
Pyrolysis of carbon silica bond
a
c
b
Si
NH_2
G(0)
Weight (%)
Derivative Weight (%/min)
Heat Flow (W/g)
Temperature (^oC)

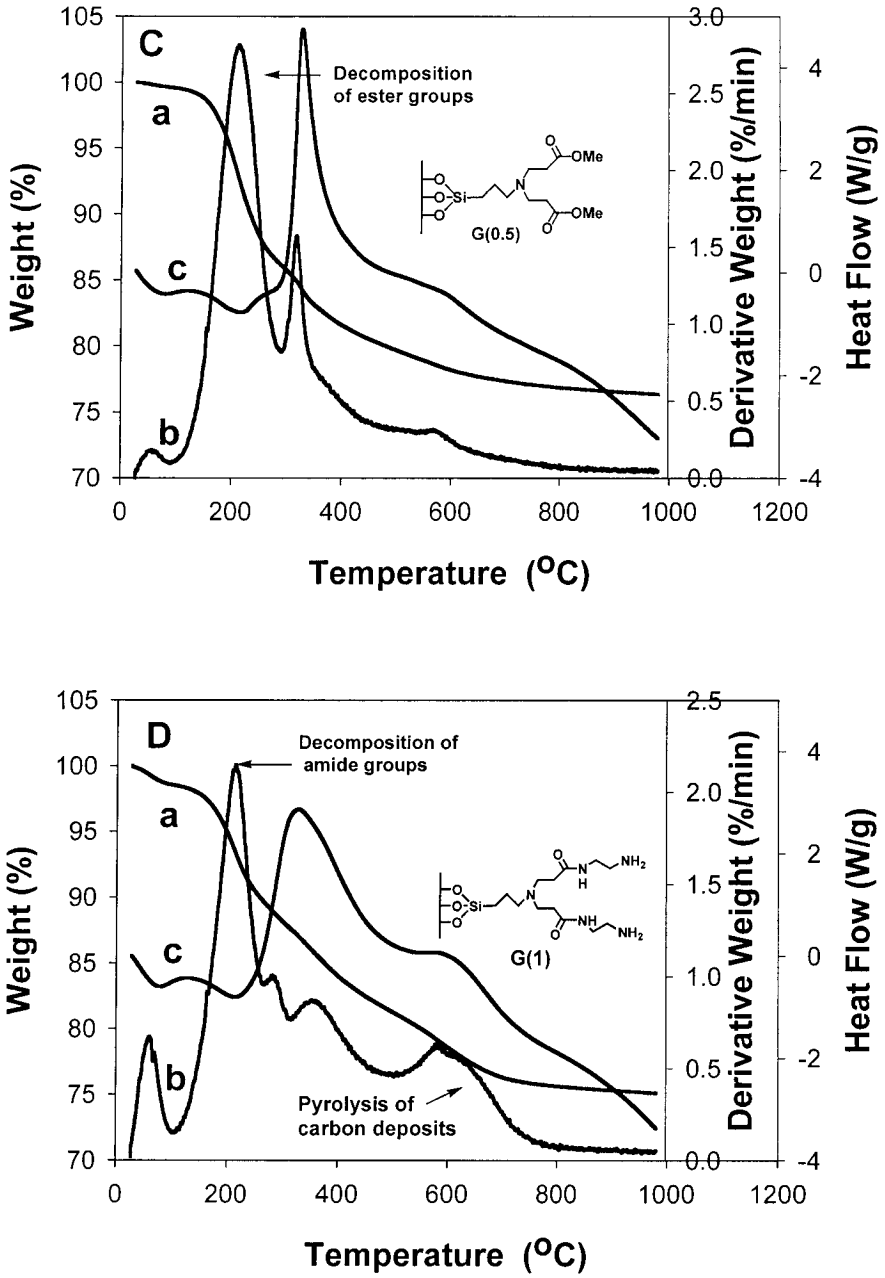

Figure 4-20. DSC-TGA data for LPMCM-41 supported dendrimers of different generations (a) TGA curve, (b) derivative weight curve, (c) heat flow curve; (A) G(-0.5), LPMCM-41 support; (B) G(0); (C) G(0.5), (D) G(1).

The TGA spectra of the all the half and full generations are represented together in Figure 4-21.

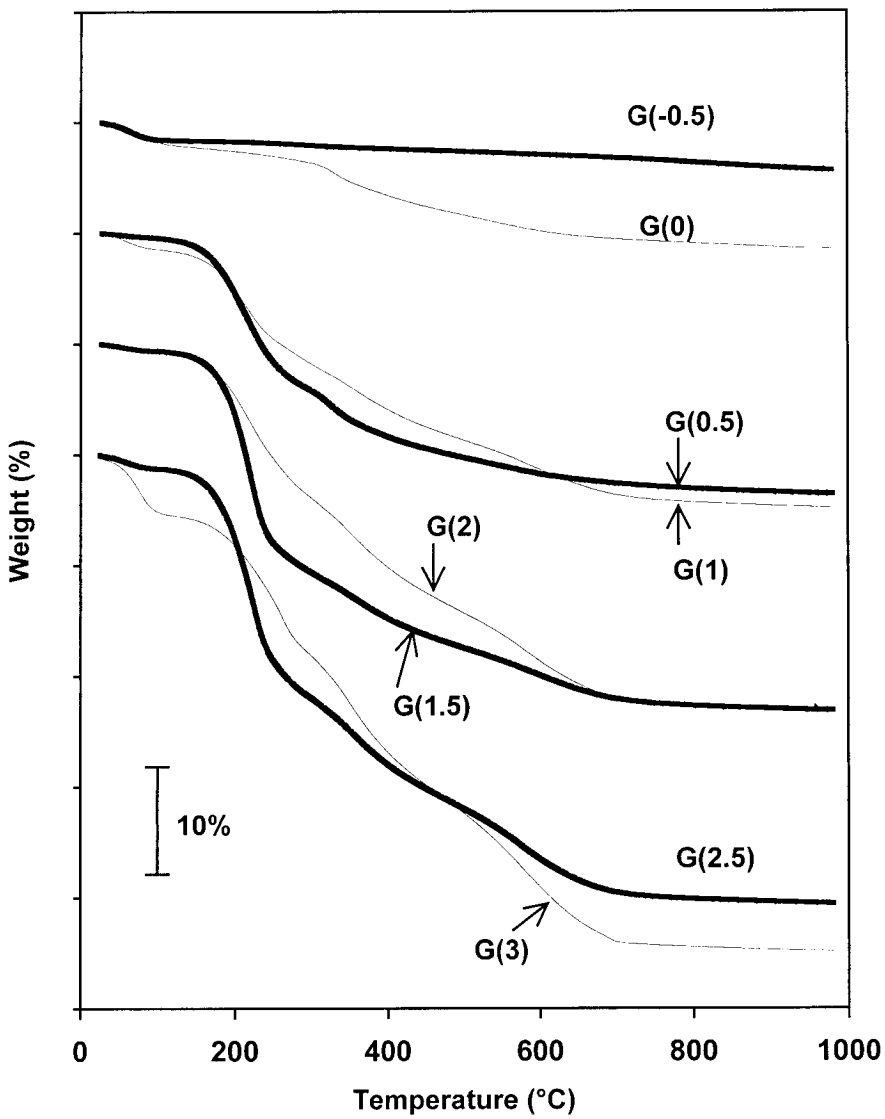

Figure 4-21. Weight loss as measured by TGA for LPMCM-41 supported dendrimers.

It is clear that the half generations and the next full generations exhibit similar behavior indicating that the dendrimers are of similar molecular weights, and by inference similar sizes. This is consistent with behavior of pore size and volume as determined by nitrogen adsorption (Figure 4-7., Table 4-3) and by the theoretical weight losses as shown in Table 4-6. The spectra for the half generations in every group (G(x.5) and G(x+1)) shows that the ester moieties start to decompose at lower temperatures, which is consistent with the greater stability of amides when compared to ester groups.

Table 4-6. Comparison between Experimental (TGA and Elemental Analysis) and Theoretical Weight Losses for LPMCM-41 series dendrimers.

Generation	%N	%C	%H	Experimental weight loss (%) (corrected)	E A weight loss (%)	Theoretical weight loss (%)	Overall yield (%)
-0.5[a]	0	0.15	0.73	0.00	0.00	0.00	-
0	1.72	4.59	1.67	7.00	7.34	7.13	98.16
0.5	1.45	11.49	2.18	20.94	21.75	23.33	89.74
1	4.03	11.73	2.6	21.22	20.20	27.45	77.29
1.5	3.31	16.55	2.88	30.81	30.30	45.45	67.79
2	5.7	16.98	3.71	30.63	29.39	49.54	61.83
2.5	5.28	21.1	3.96	37.99	40.53	65.42	58.07
3	7.36	19.59	4.32	37.95	35.33	68.68	55.26

(a) Generation (-0.5) refers to the LPMCM-41 support

To assess the effectiveness of the reactions leading to different dendrimer generations, it is imperative to develop a methodology to accurately calculate the yield of such reactions. To this end, the DSC-TGA data was used for the quantification of the growth of the dendrimers on the surface. This method was used earlier in Chapter 2, but for this study, the approach was significantly refined by incorporating elemental analysis (EA) data and baseline correction. The EA was incorporated to determine the amount of amines on the surface of the LPMCM-41 after grafting of APTES, i.e., G(0). This procedure is in our view more accurate, and reproducible than previously used acid base titration.[8] As shown in Table 4-6 (column 7), the EA data for the G(0) material allowed us to calculate the weight loss that would correspond to complete formation of dendrimers at every step of the synthesis. The actual weight loss corresponding to the combustion of supported dendrimers was determined by thermogravimetry as the weight loss between 121 and 800 °C, i.e., excluding the weight loss due to the desorption of water. This value was further corrected for the weight loss due to the amount of silica in the sample by using the weight loss of the unmodified LPMCM-41 silica support (Table 4-6, column 5). The weight losses for all materials were also calculated by adding the experimental amounts of C, N and H obtained by EA and the amount of oxygen calculated based the theoretical oxygen to nitrogen ratio of any given dendrimer (Table 4-6, column: 6). It is interesting to note that the obtained weight losses were consistent within 1-2 % with corrected TGA derived weight losses (Table 4-6, column 6).

Assuming that all synthesis steps proceed with 100 % yield, theoretical weight losses (Table 4-6, column 7) were calculated based on the nitrogen content of material G(0). Comparison between the corrected experimental TGA weight loss and the theoretical weight loss allowed us to calculated the overall yield (OY) for each dendrimer generation (Table 4-6, column 8). It is seen that as the dendrimer generation increases, the OY decreases to reach 55.26 for the G(3) species. Although better than our previous results[9], this may seem at first glance, disappointing. However, a closer inspection of the statistics of dendrimer growth shows otherwise. At issue is the determination of the average yield (AY) per reaction (i.e., synthesis step) based on the overall yield, which represent a cumulative yield of all the steps involved. To address this question, let's consider the synthesis of G(3) material. The G(3) dendrimer was obtained from G(0) via 28 reaction steps. The following relationship holds: $OY = (AY)^x$, where x is the number of reactions involved. Thus, $AY = (OY)^{1/x}$. In the case of the current G(3) dendrimer, $AY = (0.5526)^{1/28} = 0.979$. This shows that although the OY for the dendrimer at G(3) is only 55.26% it is probably as good as is attainable in the divergent dendrimer synthesis approach without purification, and with all the steric interactions involved.

This finding obviously means that some reactions did not go to completion and it is believed that the largest hindering factor is the steric interference involved, especially for reactions with the higher dendrimers. Some evidence for this can

be seen in the IR study where residual ester functionalities were found in all the full-generation dendrimers.

4.4.5.2 Thermal analysis of Davisil series dendrimers.

The Davisil series dendrimers show similar TGA spectra when compared to the LPMCM-41 series dendrimers Figure 4-22. The half generations and the next full generations again group together due to their similar size, and the overall yield (51.30% at G(3) Table 4-7.) and yield per reaction was again calculated as in the case of the LPMCM-41 series. The yield per reaction was 97.6 %.

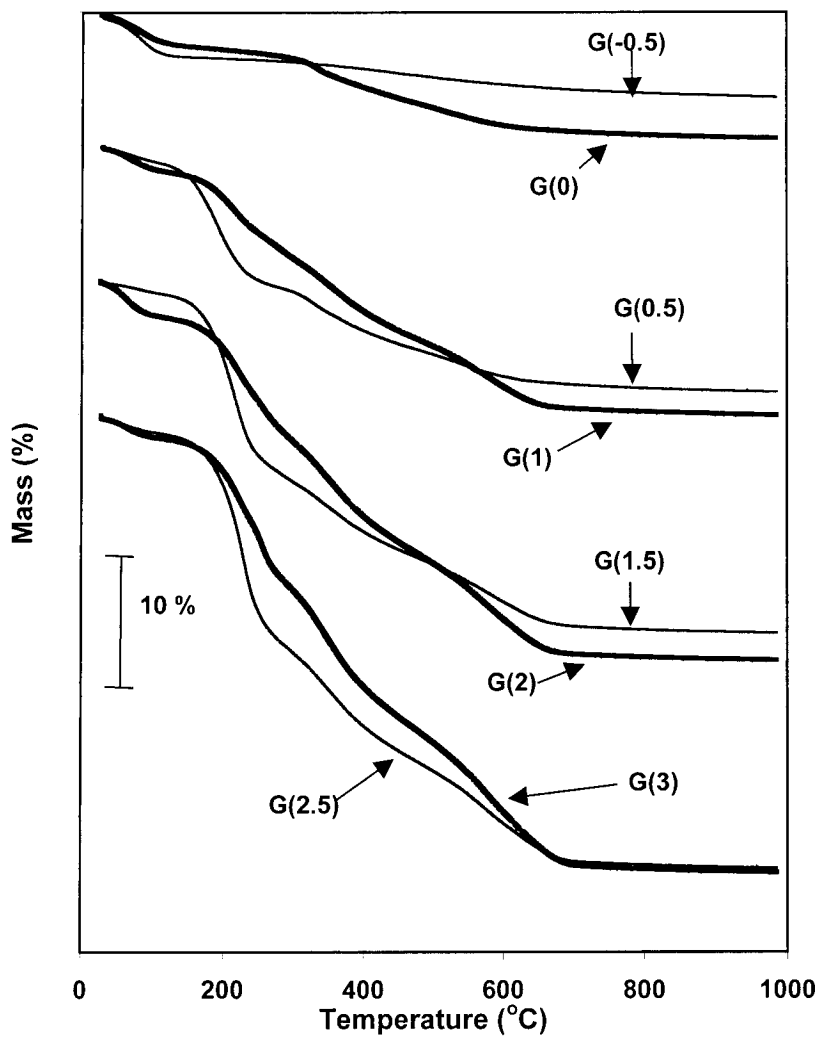

Figure 4-22. Weight loss as measured by TGA for Davisil supported dendrimers

Table 4-7. Comparison between Experimental (TGA and Elemental Analysis) and Theoretical Weight Losses for Davisil series dendrimers

Generation	%N	%C	%H	Experimental weight loss (%) (corrected)	E A weight loss (%)	Theoretical weight loss (%)	Overall yield (%)
-0.5[a]	0	0	0	0.00	0.00	0.00	-
0	1.23	3.12	1.09	3.84	5.44	5.10	75.28
0.5	1.16	8.93	1.94	14.48	17.33	17.55	82.51
1	3.22	9.76	2.15	15.83	16.60	20.93	75.64
1.5	2.90	13.51	2.51	23.35	25.55	36.83	63.39
2	4.67	13.74	2.70	23.77	23.57	40.76	58.33
2.5	4.20	17.08	3.03	30.96	32.42	56.98	54.33
3	5.93	17.00	3.23	31.04	29.43	60.51	51.30

(b) Generation (-0.5) refers to the davisil support

As for the LPMCM-41 the following calculation was used to determine the average yield, AY = $(0.5130)^{1/28}$ = 0.976.

4.4.5.2 Thermal analysis of PEMCM-41 series dendrimers.

TGA analysis was again done on all the samples and the G(4) sample is represented below. As can be seen the weight loss was ca. 62%, which is very large. All TGA data is represented together in Figure 4-23.

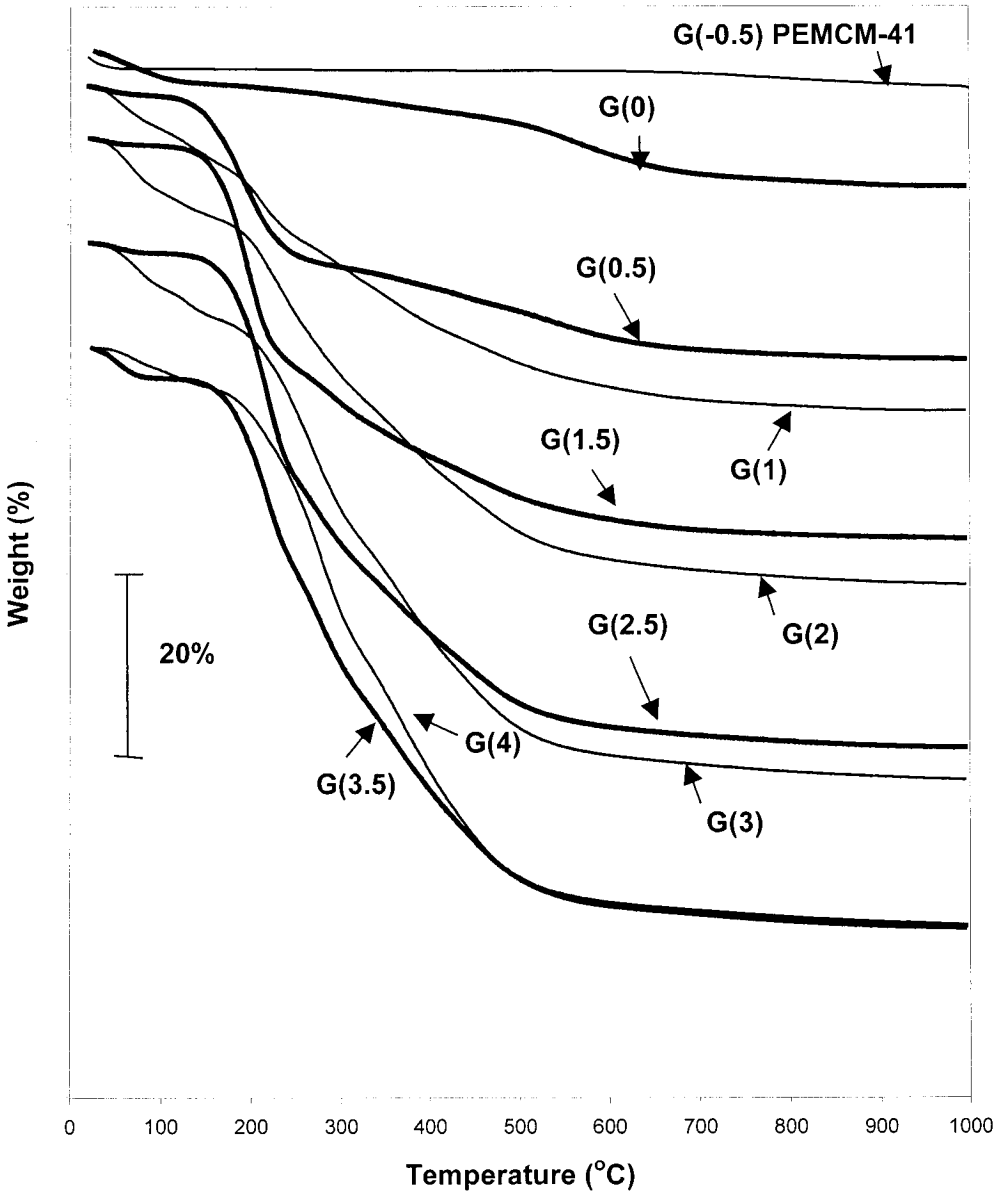

Figure 4-23. Weight loss as measured by TGA for the PEMCM-41 supported dendrimers G(0)-G(4).

Table 4-8. Comparison between Experimental (TGA and Elemental Analysis) and Theoretical Weight Losses for PEMCM-41 series dendrimers

Generation	%N	%C	%H	Experimental weight loss (%) (corrected)	E A weight loss (%)	Theoretical weight loss (%)	Overall yield (%)
-0.5[a]	-	-	-	0.00	0.00	0.00	-
0	2.28	6.33	2.33	9.61	10.93	9.65	99.59
0.5	1.89	15.19	2.86	28.02	28.56	29.30	95.63
1	7.42	16.28	4.11	29.27	31.19	34.00	86.08
1.5	4.91	22.83	4.06	43.31	43.04	53.15	81.48
2	9.90	22.58	5.28	41.63	42.98	57.2	72.79
2.5	7.42	28.15	5.13	54.96	55.03	72.04	76.29
3	11.59	27.11	5.90	53.49	50.99	74.88	71.43
3.5	9.59	31.28	5.83	60.97	63.25	84.52	72.14
4	13.03	32.03	6.50	61.59	58.87	86.24	71.42

(c) Generation (-0.5) refers to the MCM-41 support

As for the LPMCM-41 the following calculation was used to determine the average yield at G(4) is , AY = $(0.7142)^{1/60}$ = 0.994.

A yield of 99.4% per reaction over 60 reactions should be about as good as possible with the divergent approach. This value is significantly better than any other dendrimers synthesized and reported in this thesis and shows that the pore size is very important for the success of the dendrimer growth.

4.4.6 Phosphinomethylation and complexation.

4.4.6.1 Phosphinomethylation and complexation of the different generations of LPMCM-41 series dendrimers.

The different generations were phosphinomethylated as described earlier. The phosphinomethylated dendrimers were characterized by solid-state ^{31}P and ^{13}C CP/MAS NMR. The ^{13}C NMR spectra showed a new signal at 129 ppm corresponding to the aromatic carbons of the phosphine groups. A signal at –28.44 ppm in the ^{31}P NMR spectrum compares well with previously reported systems[4] and the internal standard ($[MeP^{+}Ph_3]Br^{-}$) gave a signal at 20.74 ppm (Figure 4-24). After complexation, the ^{31}P NMR spectrum had 2 signals, one at –27.31 ppm corresponding to the uncomplexed phosphines, and the other at 28.15 ppm corresponding to the rhodium complexed phosphines[1,11].(Figure 4-26). The ^{13}C CP/MAS NMR spectrum of complex 48 can be seen in Figure 4-25.

To carry out further metal complexation, it was imperative to determine the amount of phosphine that was incorporated into the material. To this end the internal standard method, developed earlier (Chapter 2), based on ^{31}P NMR measurements were used. This afforded a close approximation of the phosphine

content. To determine the phosphine levels more precisely we used ICP-MS analysis (Table 4-9).

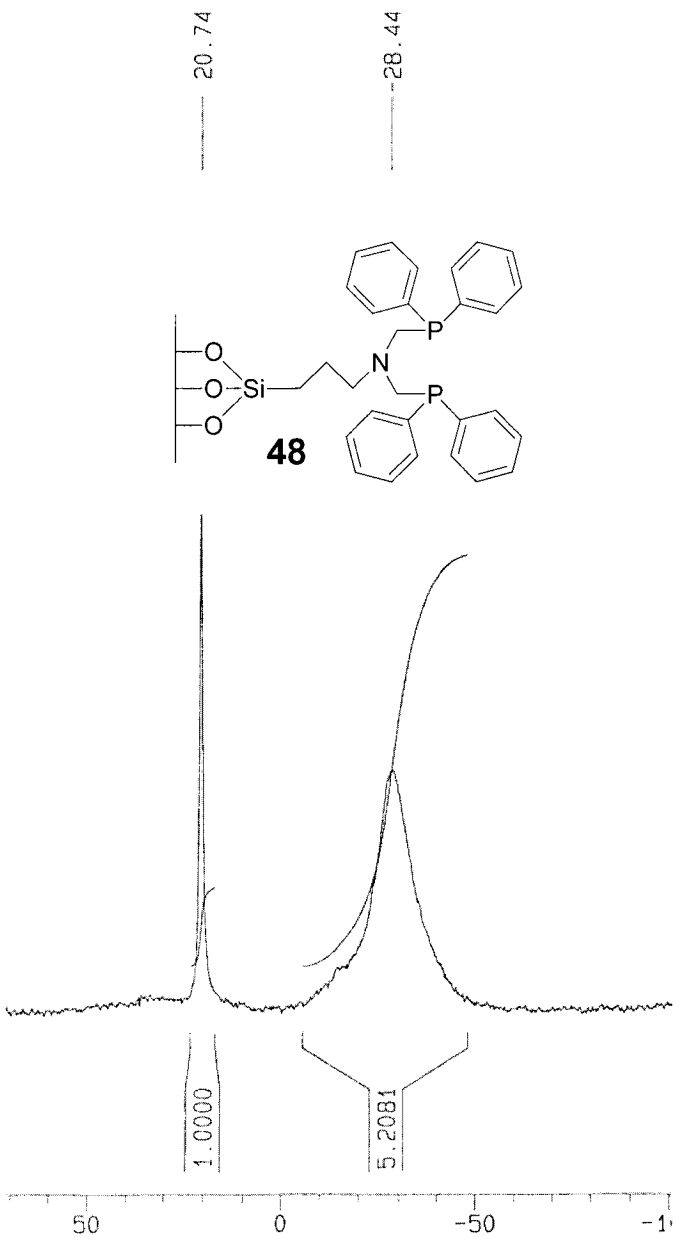

Figure 4-24. ^{31}P CP/MAS NMR spectrum of G(0)Phos LPMCM-41.

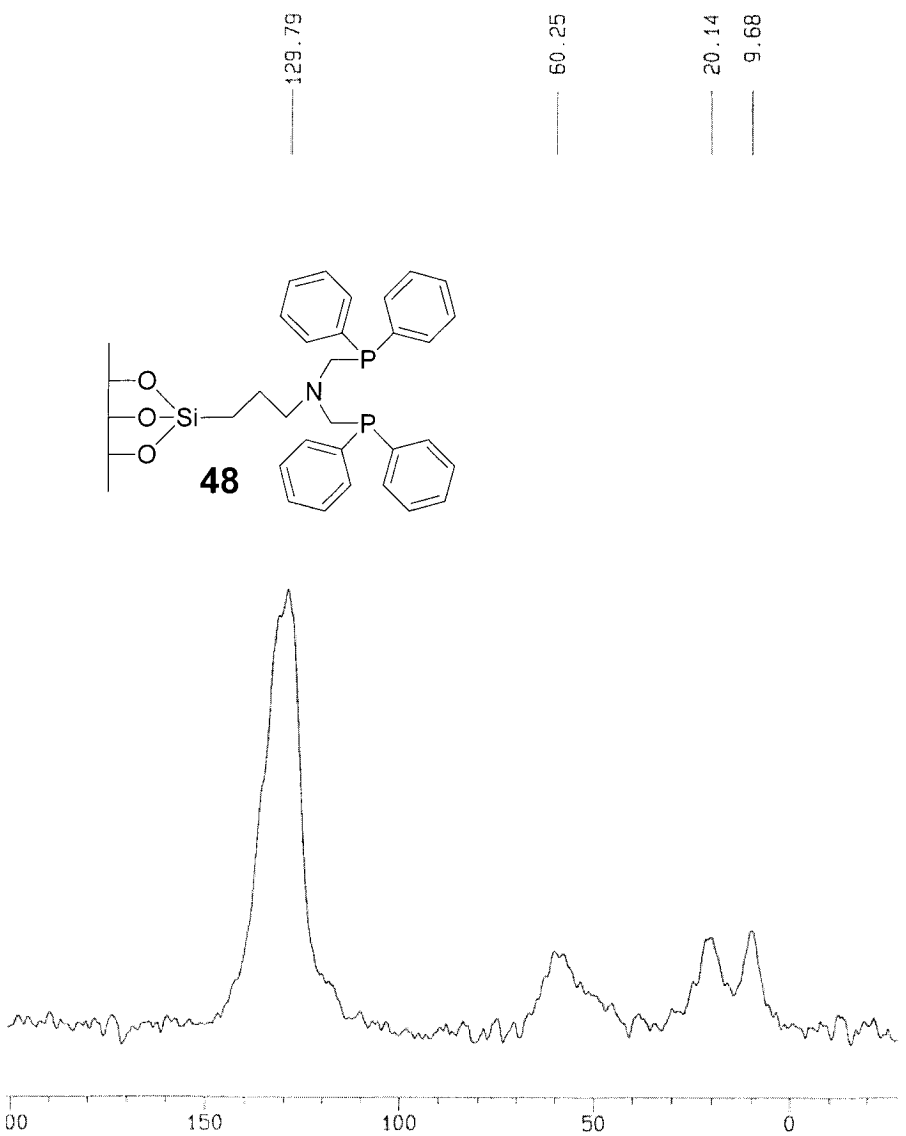

Figure 4-25. ^{13}C CP/MAS NMR spectrum of G(0)Phos LPMCM-41.

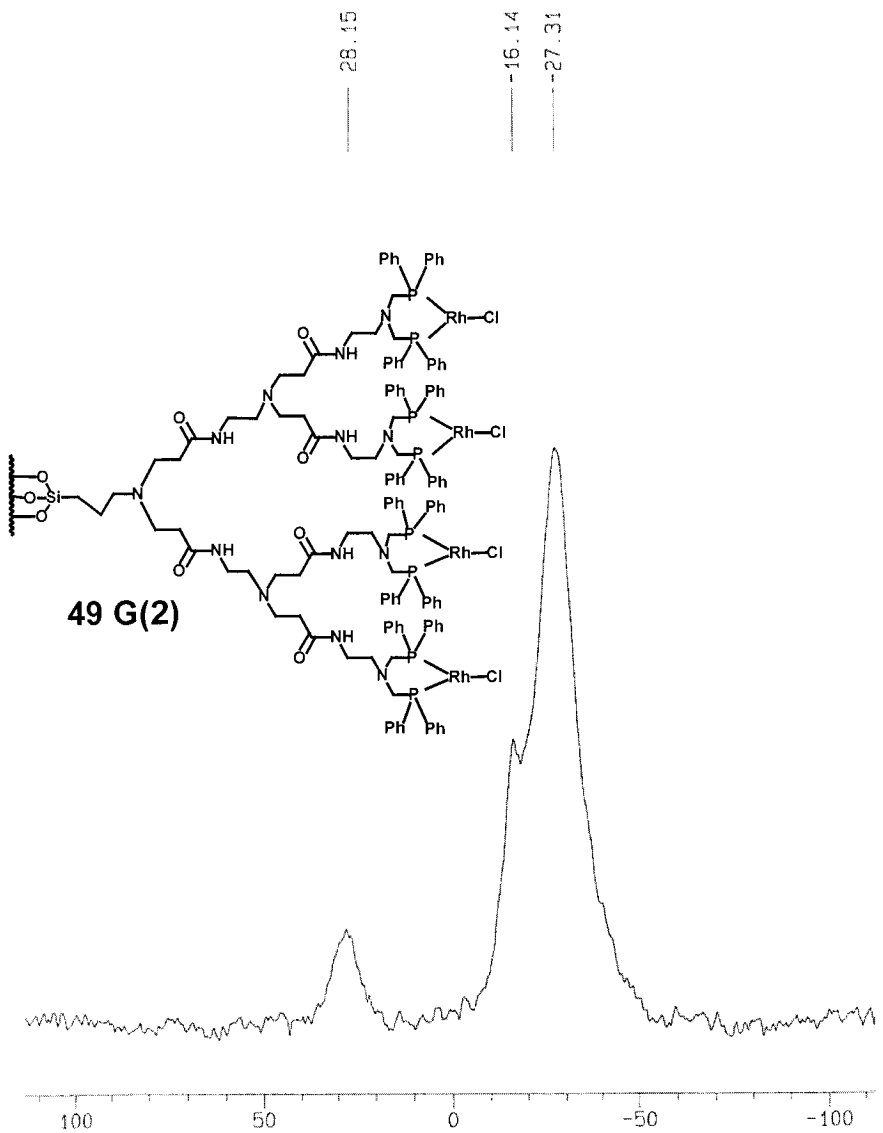

Figure 4-26. ^{31}P CP/MAS NMR spectrum of G(2)Rh-LPMCM-41.

Table 4-9. Rhodium and phosphorus ICP-MS analysis of LPMCM-41 series dendrimers

Generation	P (%)	Rh (%)
P-G(0)	2.41	
R-G(0)	1.65	1.81
P-G(1)	1.90	
Rh-G(1)	2.02	.830
P-G(2)	2.12	
Rh-G(2)	1.81	.619
P-G(3)	.370	

Although useful, the NMR method was less precise than the ICP-MS analysis, but the results nonetheless could be used to determine the amount of rhodium for the complexation. This final synthesis step was achieved by reacting the rhodium containing metal complex with the phosphinomethylated dendrimer (two equivalents of phosphine for each metal) species under argon in toluene. It is interesting to note that at this point our initial observation of the steric interaction of the dendrimer branches became very important. From the data it is clear that the G(0) and G(1) species incorporated much more phosphine and metal than the G(2) and G(3) species. Actually, the G(3) complexation was not even attempted due to the fact that almost no phosphine was present even after 48 h of phosphinomethylation. This clearly supports our previous findings that the steric encumbrance of the higher generations has a detrimental effect on the phosphinomethylation and metal complexation.[1,9] Therefore all reactions of

higher generations of the dendrimers were critically affected by the space available for the reacting species. With the growth of the dendrimers in a support with well-defined pore structure, we are able to determine when the saturation point is reached and can therefore now design supports to accommodate the desired degree of dendrimer growth.

4.4.6.2 Phosphinomethylation and complexation of the different generations of Davisil series dendrimers.

The Davisil dendrimers were phosphomethylated and complexed following the same procedure as for the LPMCM-41 series dendrimers. The phosphine and rhodium content was determined by ICP-MS and the results are presented in Table 4-10.

Table 4-10. Rhodium and phosphorus ICP-MS analysis of Davisil series dendrimers.

Generation	P (%)	Rh (%)
P-G(0)	1.99	
Rh-G(0)	2.43	1.70
P-G(1)	1.86	
Rh-G(1)	1.50	2.87
P-G(2)	1.99	
Rh-G(2)	2.02	3.30
P-G(3)	2.87	
Rh-G(3)	2.10	2.03

The results are very different from the LPMCM-41 series. The phosphine content increases with generation and the highest level of 2.87% is reached at G(3). This along with the nitrogen adsorption analysis shows that the morphology of the support greatly influences the success of the dendrimer catalyst preparation. These catalysts along with the LPMCM-41 series dendrimer catalyst were tested for activity in the hydroformylation reaction of olefins and the results are presented in Chapter 5.

4.5 Conclusions.

Polyamidoamine (PAMAM) dendrimers up to the third generation were grown for the first time inside the channels of LPMCM-41 (6.5 nm) and on the outside surface of Davisil (18 nm) silica. Polyamidoamine (PAMAM) dendrimers up to the fourth generation were grown for the first time inside the channels of PEMCM-41 (10.6 nm) silica. Detailed characterization using nitrogen adsorption, solid state NMR, FTIR, thermogravimetry, and chemical analysis showed that the dendrimers formed inside the channels with an average yield higher than 97 %, all synthesis steps being included. The third generation on the LPMCM-41 (6.5 nm) was found to almost completely fill the pore system, whereas the generation three dendrimers on the Davisil support still adsorb nitrogen and are less affected by steric interactions than the dendrimers on LPMCM-41. The dendrimers on the PEMCM-41 reach pore saturation at one generation higher (G(4)) than LPMCM-41, but the overall yield for these dendrimers are significantly higher than anticipated (71% at G(4)). This translates to a yield per reaction of over 99%.

Dendrimers of generations 0, 1 and 2 on LPMCM-41 were phosphinomethylated and complexed with rhodium and dendrimers of generations 0, 1, 2 and 3 on Davisil were phosphinomethylated and complexed with rhodium.

It is clear that the pore geometry is very important in determining the size of the dendrimer that can be constructed on the support. The MCM-41 supports, where the dendrimers are grown on the inside surface are subject to significant steric encumbrance. The dendrimers grown on the Davisil support are less prone to steric encumbrance, and dendrimers up to generation three can be easily synthesized, phosphinomethylated and complexed. Although the PEMCM-41 has significantly larger pores, the threshold in the growth of the dendrimers is reached at G(4) instead of G(3) for the LPMCM-41. This was disappointing and the PEMCM-41 was not phosphinomethylated or complexed.

4.6 References for Chapter 4:

1. Bourque, S. C., Alper, H., Manzer, L. E., Arya, P. *J. Am. Chem. Soc.* **2000**, *122*, 956.
2. Kresge, C. T., Leonowicz, M. E., Roth, W. J., Vartuli, J. C., Beck, J. S., *Nature* **1992**, *359*, 710.
3. Sayari, A., Liu, P., Kruk, M., Jaroniec, M., *Chem. Mater.* **1997**, *9*, 2499.
4. Kruk, M., Jaroniec, M., Sayari, A., *Langmuir* **1997**, *13*, 6267.
5. Jaroniec, C. P., Kruk, M., Jaroniec, M., Sayari, A., *J. Phys. Chem. B.* **1998**, 102, 5503.
6. Sayari, A., Hamoudi, S., *Chem. Mater.* **2001**, *13*, 3151.
7. Huang, H. Y., Yang, R. T., Chinn, D., Munson, C. L., *Ind. Eng. Chem. Res.* **2003**, 42, 2427.
8. Tsubokawa, N., Ichioka, H., Satoh, T., Hayashi, S., Fujiki, K., *React. Funct. Polym.* **1998**, *37*, 75.
9. Reynhardt, J. P. K., Alper, H., *J. Org. Chem.* **2003**, *68*, 8353.
10. Bourque, S. C. Maltais, F., Xiao, W.-J., Tardif, O., Alper, H., Arya, P., Manzer, L. E., *J. Am. Chem. Soc.* **1999**, *121*, 3035.
11. Reetz, M. T., Lohmer, G., Schwickardi, R., *Angew. Chem. Int. Ed. Engl.* **1997**, *36*, 1526.
12. Jaroniec, M., Kruk, M. Olivier, J. P., *Langmuir,* **1999**, *15*, 5410.

Chapter 5. *Hydroformylation Reactions with Rhodium-Complexed C_2-PAMAM Dendrimers Immobilized on Mesoporous and Periodic Mesoporous Silica supports.*

5.1 Introduction:

The hydroformylation reaction of olefins (Scheme 5-1) is a very important industrial reaction.[1] As discussed in Chapter 1 the reaction can be used to produce high value aldehydes or alcohols for numerous applications. One of the largest challenges remaining in this field is the effective commercialization of processes involving long chain linear olefins.[2] To this end the catalysts synthesized in Chapter 4 was mainly tested with 1-octene as substrate. Although 1-octene is not strictly defined as a long chain olefin (usually R=C_{10} or higher is defined as a long chain olefin), it lies at the lower end of the chainlengths where boiling point separations become problematic.

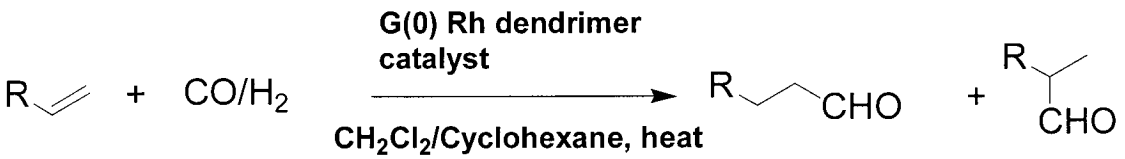

Scheme 5-1. The hydroformylation reaction

The catalysts derived form the LPMCM-41 series dendrimers and the Davisil series dendrimers were tested for activity, selectivity and recyclability. It would be a great advance in the art if supported catalysts could be used in fixed bed

reactors as opposed to homogeneous catalysts in stirred tank reactors. This would introduce a significant cost advantage, as separation of catalysts and feed from the products is usually the most costly step in industrial applications.

5.2 Catalytic activity of the LPMCM-41 series C_2-PAMAM dendrimers for the hydroformylation of olefins.

The catalytic properties of G(0)-G(2) materials were investigated using the hydroformylation of olefins as a test reaction. Among other substrates, a long chain linear olefin was used for the hydroformylation test reaction due to the specific separation challenges facing industrial processes of these olefins. The separation becomes challenging due to the high boiling point of long chain aldehyde products and homogeneous catalysts of these olefins should not only be temperature stable but very robust as distillation is usually used to separate catalyst and product streams. A simple separation by filtration would have significant impact on the hydroformylation of these olefins. 1-Octene was selected as the olefin of choice and remarkable activity was observed with the current catalysts.

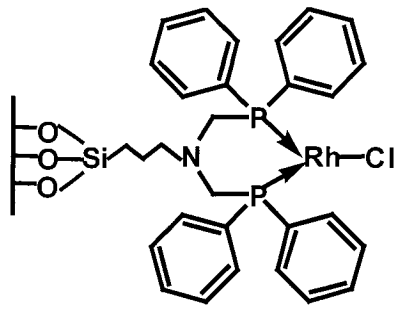

Figure 5-1. The Rh-G(0) catalyst.

The G(0) catalyst (Figure 5-1) gave a turnover frequency (TOF) of over 1800 h^{-1} at 70 °C with a total turnover number (TON) of 21000. The TOF of this catalyst is significantly higher than previous results (200 h^{-1}) where the TOF for styrene hydroformylation was determined at 70 °C over an amorphous silica supported dendrimer catalyst (styrene is usually more reactive than 1-octene for the hydroformylation reaction).[3] In contrast, the selectivity to linear aldehyde was below expectations, with the best results giving a L:B selectivity of around 1.6 (Table 5-1).

Table 5-1. Comparison of the Activity for the Hydroformylation of 1-Octene of Rh-Complexed MCM-41 Supported Dendrimers with Different Generations.

Entry	Generation	Time (h)	Conversion (%)	B:L	TOF[a] (h^{-1})
1	0	8	>99	1:1.6	1800
2	1	22	>99	1:1.7	1430
3	2	20	trace	-	-

Conditions: 50 mg catalyst, 100 mmol 1-octene, 70 °C, 1000 psi H_2:CO 1:1 in cyclohexane (90 ml) (a) TOF refers to average turnover frequency.

However, it was possible to recycle the catalysts three times before the amount of collected catalyst became too small to carry out further reaction cycles (Table 5-2).

Table 5-2. Recycle Study of Rh-Complexed LPMCM-41 Supported G(0) catalyst.

Entry	Substrate	Cycle	Conversion (%)	B:L	TOF (h^{-1})
1	1-octene	1	>99	1:1.5	486
2	1-octene	2	>99	1:1.6	486[b]
3	1-octene	3	>99	1:1.4	486[b]

Conditions: 22h, 30 mg catalyst, 50 mmol substrate, 70 °C, 1000 psi H_2:CO 1:1 in cyclohexane (90 ml) . (a) TON = 11000. (b) Refers to maximum TOF as Rh content could not be determined.

Moreover, several solvent systems were tested, and cyclohexane was found to be the best solvent to use in the recycle reactions. The G(1) catalyst was less active due to the lower levels of rhodium and from G(2), the incorporation of the metal was too low to give significant activity (Table 5-1). As shown in Table 5-3, the best catalyst G(0), was also tested with other substrates and gave good results with styrene and vinyl acetate, particularly at 70-75 °C.

Table 5-3. Activity of the Rh-Complexed MCM-41 Supported G(0) catalyst for the Hydroformylation Reaction.

Entry	Substrate	Amount (mmol)	T (°C)	Conversion (%)[d]	B:L[e]	TOF (h^{-1})
1	styrene	10	75	99	9	345
2	styrene	10	60	40	12	138
3	styrene	10	50	25	15	86
4	vinyl acetate	5	80	57	11	98
5	vinyl acetate	10	75	60	12	206
6	vinyl acetate	10	60	50	11	173
7	vinyl acetate	10	50	trace	nd	-
8	vinyl acetate	10[a]	25	trace	nd	-
9	phenylvinyl sulphone	1	75	25	f	-
10	1-octene	100[b]	70	99	1: 1.4	896[c]

All reaction times 22 h, 10 mg catalyst (1.3 μmol Rh) in CH_2Cl_2, 1000 psi H_2:CO 1:1. (a) 48 h, 25 mg catalyst. (b) 35 mg catalyst (5 μmol Rh), 24 h (c) TON 21400. (d) determined by GC (e) branched to linear aldehyde, determined by ^1H NMR and GC. (f) no linear aldehyde detected.

5.3 Catalytic activity of the Davisil series C_2-PAMAM dendrimers for the hydroformylation of olefins.

As for the LPMCM-41 series catalysts, the Davisil series catalysts were also tested with 1-octene as the substrate. However, contrary to the LPMCM-41 series, we found that the Davisil series showed significant activity up to the third generation. (Figure 5-2)

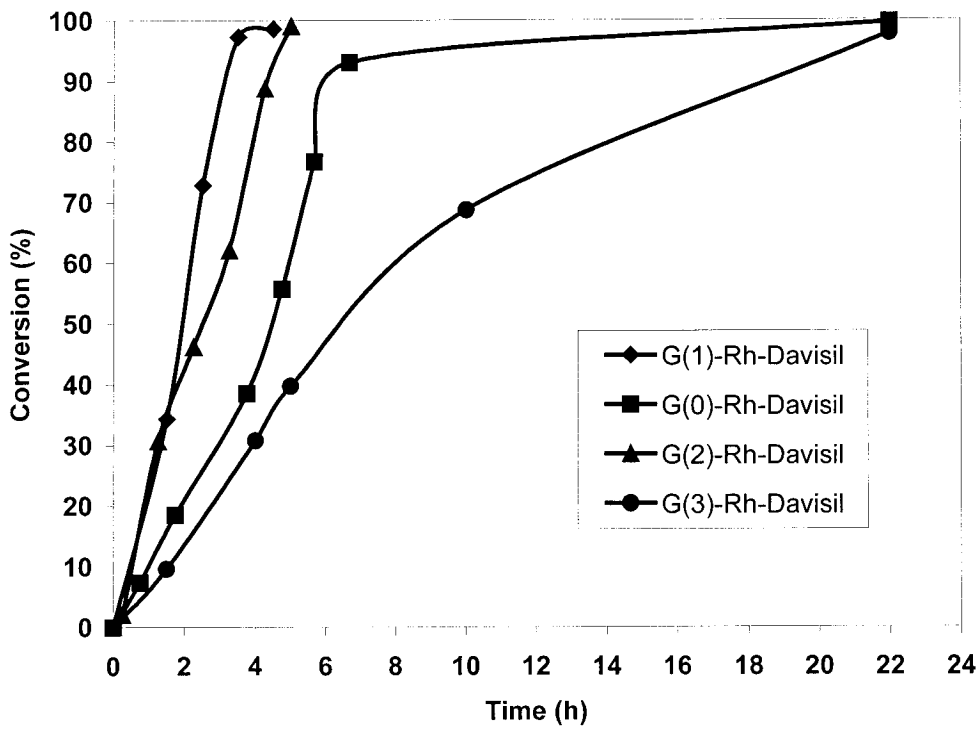

Conditions: 50 mg catalyst, 100 mmol 1-octene, 70 °C, 1000 psi H_2:CO 1:1 in cyclohexane (90 ml).

Figure 5-2. Graphical representation of the conversion vs. time for the G(0)-G(3) Davisil series dendrimer catalysts.

Table 5-4. Comparison of the Activity for the Hydroformylation of 1-Octene of Rh-Complexed Davisil Supported Dendrimers with Different Generations.

Entry	Generation	Time (h)	Conversion (%)	L :B	TOF[a] (h^{-1})
1	0	6.67	93	1.93	1700
2	1	4.5	99	1.65	1600
3	2	5	99	1.8	1360
4	3	22	98	1.70	300

Conditions: 50 mg catalyst, 100 mmol 1-octene, 70 °C, 1000 psi H_2:CO 1:1 in cyclohexane (90 ml) (a) TOF refers to average turnover frequency.

It is clear from Table 5-4 that the activity of the catalysts decreases with increasing generation, but the generation three catalysts still shows activity comparable to previously reported systems. As the rhodium content of the catalysts differ it is difficult to control the concentration of the active sites, and therefore the activity at 50 % conversion was compared. In Figure 5-3 the activity as a function of catalyst mass is compared with the activity as a function of rhodium content. It is interesting to note that the activity of the G(1) catalyst is in both cases the highest and the other generations are normalized using this value. It is however very important to note that the G(1) catalyst has higher activity than the G(0). This is completely different from the LPMCM-41 series, and shows that the support plays an important role in the success of the catalysts.

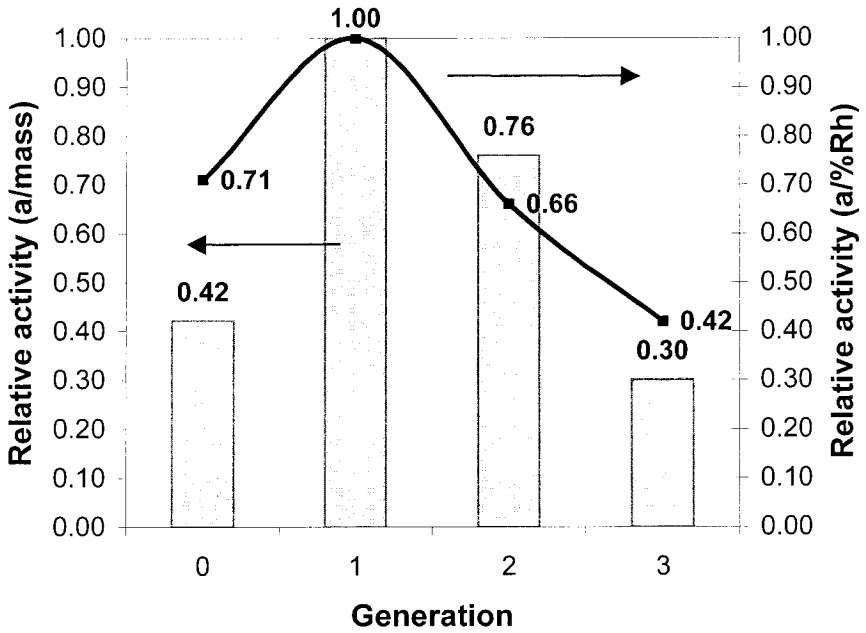

Figure 5-3. Graphical representation of the relative activity of G(0)-G(3) Davisil series dendrimer catalysts taken at 50% conversion.

The G(1) catalyst was then tested for activity with various other substrates. Vinyl acetate, vinyl benzoate and styrene were selected because these substrates are commonly used in industry. All reactions were affected at 70 °C as the LPMCM-41 substrates showed the best activity at this temperature.

Table 5-5. Activity for the Hydroformylation Reaction of Rh-Complexed Davisil supported G(1) dendrimer.

Entry	Substrate	Amount (mmol	T (°C)	Conversion (%)	B:L[c]	TOF (h^{-1})
1	styrene	40	70	99	8	325
2	vinyl acetate	40	70	80	14	261
3	vinyl benzoate	40	70	99	26	325
4	1-octene	100[a]	70	99	1: 1.9	1600

Reaction times, 22 h, 20 mg catalyst (5.4 µmol Rh) in CH_2Cl_2, 1000 psi H_2:CO 1:1. (a) 50 mg catalyst (1.4 µmol Rh) 6.67 h (b) determined by GC (c) branched to linear aldehyde, determined by ^1H NMR and GC.

The catalysts were tested for recyclability, but none of the generations could be recycled. This is surprising as the LPMCM-41 catalysts could be recycled without much loss of activity. It therefore appears that the pore structure also has a significant effect on the success of the recyclability.

5.4 Conclusions:

Dendrimers of generations 0, 1 and 2 supported on LPMCM-41 were phosphinomethylated and complexed with rhodium. The G(0) and G(1) materials were found to be excellent recyclable catalysts for olefin hydroformylation. A

turnover frequency (TOF) as high as 1800 h^{-1} was obtained for the hydroformylation of 1-octene at 70 °C.

Generations 0, 1, 2 and 3 dendrimers supported on Davisil were phosphinomethylated and complexed with rhodium. These catalysts also showed excellent activity for the hydroformylation reaction, with a maximum turnover frequency of 1700 h^{-1} observed for the hydroformylation of 1-octene. The G(1) catalysts was identified as the most active at 50 % conversion.

The Davisil supported catalysts could however not be recycled.

5.5 References for Chapter 5

1. (a) O. Roelen, German Patent 849,548, **1938**. (b) O. Roelen, U. S. Patent 2,327,066, **1943**. (c) Adkins H., Kresek, *J. Am. Chem. Soc.,* **1949**, 71, 3051.
2. (a) Botteghi C., Marchetti M., Paganelli S., in Beller M., Bolm C., *Transition Metals for Organic Synthesis Volume 1*, Wiley-VCH, Weinheim, **1998**, p 25. (b) Green C. R., U. S. Patent 3,278,612, **1966**. (c) Hughes O.R., Hillman M., U. S. Patent 3,821,311, **1974**. (d) Pruett R. L., *Advances in Organometallic Chemistry*, **1979**, Vol. 17, 1.
3. Bourque, S. C., Alper, H., Manzer, L. E., Arya, P., *J. Am. Chem. Soc.,* **2000**, *122*, 956.

Chapter 6. *Experimental Section*

6.1 General considerations: Section A.

All olefins were purchased from Aldrich or Fluka chemical companies and used as received or percolated through a short column of activated alumina.

All solvents were dried, distilled and in some cases degassed before use. All other chemicals were used as received without further purification.

All reactions were carried out under an atmosphere of nitrogen or argon, in the case of very air sensitive compounds. All manipulations of air-sensitive compounds or materials were carried out using standard Schlenk techniques.

Hewlett-Packard series 5890 and 6890 gas chromatographs were used for the quantification of reaction products.

A Brucker 300 MHz NMR instrument was used for the ^{1}H, and ^{13}C, analyses of reagents and products operating at 300.13 MHz and 75.48 Mhz respectively. ^{13}C and ^{31}P CP/MAS solid-state NMR spectra were obtained on a Bruker ASX-200 instrument operating at 50.32 and 80.99 MHz, respectively with a spinning rate of 5.0 – 6.0 kHz and with a contact time of 2 ms. $[MeP^{+}Ph_3]Br^{-}$ was used as internal standard for the ^{31}P NMR experiments to characterize the supported dendrimers.

Phosphorus and palladium ICP-MS was done by Galbraith laboratories, Knoxville, TN.

TGA and BET surface characterization was done at Sastech R&D laboratories in Sasolburg, South Africa.

High-pressure reactions were conducted in stainless steel autoclaves manufactured by the Parr Instrument Company. Reactions with carbon monoxide were carried out in a fume hood fitted with CO detectors and high flow capacity.

6.1.1 General experimental procedure for the preparation of C_6-PAMAM dendrimers on aminopropylsilica gel:

C_6-Polyamidoamide (PAMAM) dendrimers, up to the 4th generation, on commercial aminopropyl silica gel (0.9 mmol ±0.1 amine groups/g), were prepared using literature methods.[1]

Procedure: Step1: G(0)-G(0.5) aminopropyl silica gel (20g, 0.018 mol amine groups) and methylacrylate (0.18 mol, 15.65g) were stirred at 50 °C in dry methanol (300ml) under a nitrogen atmosphere for 5 days. The mixture was cooled and filtered through a medium pore frit under nitrogen flow and washed with dry methanol (3 X 50 ml). The residual solvent was removed in vacuo, affording the G(0.5) dendrimer supported on silica.

Step 2: G(0.5) - G(1). G(0.5) (20g, 0.032 mol ester groups) was added to 1,6-diaminohexane (40 g, 0.35 mol) in dry methanol (300 ml) under a nitrogen atmosphere. The reaction was stirred for 5 days and the resulting G(1) dendrimer supported on silica was isolated by filtration through a medium pore frit. The solid was washed with dry methanol (3 X 50 ml). The residual solvent was removed in vacuo. The higher generations were prepared by repetition of step 1 and 2 with modification for the increasing end groups.

G(1), **27.** Yield from G(0) (TGA): 60 %, ^{13}C CP/MAS NMR (50.32 MHz, solid-state) δ (ppm) 10.2, 22.2, 26.8, 32.5, 40.2, 50.1, 173.1(C=O). S_{BET}= 248.06 m^2/g, Vp = 0.51 cm^3/g, *w* = 7.04 nm.

G(2), Yield from G(0) (TGA): 35%, ^{13}C CP/MAS NMR (50.32 MHz, solid-state) δ (ppm) 10.8, 27.9, 34.6, 41.7, 50.7, 173.1(C=O). S_{BET}= 225.16 m^2/g, Vp = 0.46 cm^3/g, *w* = 7.05 nm.

G(3), Yield from G(0) (TGA): 32%, ^{13}C CP/MAS NMR (50.32 MHz, solid-state) δ (ppm) 10.8, 27.9, 34.6, 41.7, 50.8, 173.2(C=O). S_{BET}= 190.32 m^2/g, Vp = 0.39 cm^3/g, *w* = 6.90 nm.

G(4), Yield from G(0) (TGA): 30%, ^{13}C CP/MAS NMR (50.32 MHz, solid-state) δ (ppm) 10.7, 28.2, 32.5, 39.6, 44.6, 51.5, 173.3(C=O). S_{BET}= 147.92 m^2/g, Vp = 0.33 cm^3/g, *w* = 6.98 nm.

6.1.2 Phosphinomethylation of dendrimers.

The dendrimers were phosphonated using diphenylphosphine and paraformaldehyde by modification of literature methods.[6] The double phosphinomethylation of the terminal amine groups of the dendrimers was achieved by reacting the dendrimers with diphenylphosphinomethanol prepared in situ from diphenylphosphine and paraformaldehyde in toluene (110 °C, 48 h). The resulting phosphonated dendrimers were characterized by solid-state ^{31}P and ^{13}C NMR, e g a chemical shift of ca. –27 ppm in the ^{31}P NMR spectrum compares well with previously reported systems.[1]

Procedure: To a stirred suspension of paraformaldehyde (0.9 eq, 1.36g) in dry toluene (20 ml) under argon was added diphenylphosphine (10 g, 0.0504 mol). The resulting mixture was heated to reflux (110 °C) and stirred for 2h until the mixture became clear. At this stage aminopropyl silica gel (2g, 0.018 mol NH_2,) was added and the resulting suspension was stirred under argon at reflux (110 °C) for 48 h. The phosphinomethylated aminopropyl silica gel was isolated by filtration through a medium pore frit under a flow of argon and the resulting light yellow solid was washed with toluene (2 X 20 ml). The residual solvent was removed in vacuo. The procedure was modified for the preparation of the higher generations, by increasing the reagents to accommodate the increasing end groups of the dendrimers.

G(0)-$(PPh_2)_2$, **28**, Yield (TGA and ICP-MS): 27 %, ^{31}P CP/MAS NMR (80.99 MHz, solid-state) δ (ppm) –28.1. ^{13}C CP/MAS NMR (50.32 MHz, solid-state) δ (ppm) 9.7, 19.5, 44.6,61.1, 128.8, 133.3. 1.11% P (ICP-MS)

G(1)-$(PPh_2)_2$, **30,** Yield (TGA and ICP-MS): 27 %, ^{31}P CP/MAS NMR (80.99 MHz, solid-state) δ (ppm) –28.8. ^{13}C CP/MAS NMR (50.32 MHz, solid-state) δ (ppm) 9.8, 19.5, 44.6, 51.7, 61.1, 132.0, 173.1(C=O).1.57% P (ICP-MS).

G(2)-$(PPh_2)_2$, **31,** Yield (TGA and ICP-MS): 33 %, ^{31}P CP/MAS NMR (80.99 MHz, solid-state) δ (ppm) –28.65. ^{13}C CP/MAS NMR (50.32 MHz, solid-state) δ (ppm) 9.7, 20.7, 27.4, 51.5, 130.3,169.7(C=O).1.38 % P (ICP-MS).

G(3)-$(PPh_2)_2$, **32,** Yield (TGA and ICP-MS): 44 %, ^{31}P CP/MAS NMR (80.99 MHz, solid-state) δ (ppm) –27.93. ^{13}C CP/MAS NMR (50.32 MHz, solid-state) δ (ppm) 9.3, 20.7, 27.3, 40.7, 51.2 128.5, 132.7, 169.5(C=O).1.96 % P (ICP-MS).

G(4)-$(PPh_2)_2$, **33,** Yield (TGA and ICP-MS): 41 %, ^{31}P CP/MAS NMR (80.99 MHz, solid-state) δ (ppm) –28.2. ^{13}C CP/MAS NMR (50.32 MHz, solid-state) δ (ppm) 9.7, 21.5, 27.5, 40.0, 51.7, 130.2, 132.9, 172.7(C=O).1.96 % P (ICP-MS). 1.90% P (ICP-MS).

6.1.3 Complexation of phosphinomethylated dendrimers.

The phosphinomethylated dendrimers were readily complexed on treatment with the appropriate palladium complexes in toluene (rt., 1-2h under argon). The silica would turn deep orange to blood red and decoloration of the supernatant solvent was used as an indication of the extent of complexation.

Procedure: Phosphinomethylated dendrimers (1g, 0.82 mmol PPh_2) and PdL_2X_2 (0.204 mmol, L = labile ligand, X = non-labile ligand) were stirred under argon for 2h in dry toluene (20ml). The mixture was filtered through a medium pore frit under argon flow and washed with toluene (2 X 20 ml). The residual solvent was removed in vacuo to yield the product. The complex is stored under argon. The procedure was modified for the preparation of complexes of the higher generations, by taking into consideration the phosphorus contents of the phosphomethylated species.

G(0)-$(PPh_2)_2PdCl_2$, **34**, ^{31}P CP/MAS NMR (80.99 MHz, solid-state) δ (ppm) 13.0, 28,0. ^{13}C CP/MAS NMR (50.32 MHz, solid-state) δ (ppm) 11.3, 21.7, 44.6, 52.2, 131.4. 0.96% Pd (ICP-MS).

G(0)-$(PPh_2)_2Pd(OAc)_2$, **35**, ^{31}P CP/MAS NMR (80.99 MHz, solid-state) δ (ppm) – 27.7,15.8, 28.0. ^{13}C CP/MAS NMR (50.32 MHz, solid-state) δ (ppm) 10.7, 20.4, 43.0, 60.8, 129.0, 1.49% Pd (ICP-MS).

G(0)-$(PPh_2)_2Pd(dba)_{0.5}$, **36**, ^{31}P CP/MAS NMR (80.99 MHz, solid-state) δ (ppm) 28.0. ^{13}C CP/MAS NMR (50.32 MHz, solid-state) δ (ppm) 10.4, 21.4, 43.0, 51.3, 131.1, 211.7. 1.47% Pd (ICP-MS) 2.23% P (ICP-MS).

G(0)-$(PPh_2)_2Pd(PPh_3)_2$, **29**, Yield (ICP-MS): 75% ^{31}P CP/MAS NMR (80.99 MHz, solid-state) δ (ppm) 27.7*, 7.5, -26.1. ^{13}C CP/MAS NMR (50.32 MHz, solid-state) δ (ppm) 10.2, 20.1, 44.9, 53.0, 60.5, 130.8, 0.96% Pd (ICP-MS) 1.11% P (ICP-MS).

G(1)-$(PPh_2)_2Pd(PPh_3)_2$, **29a,** Yield (ICP-MS): 94%, ^{31}P CP/MAS NMR (80.99 MHz, solid-state) δ (ppm) 26.2*, 10.3, -26.2. ^{13}C CP/MAS NMR (50.32 MHz, solid-state) δ (ppm) 10.2, 16.9, 26.7, 49.8, 60.5, 130.5, 170.7 (C=O). 0.74% Pd (ICP-MS) 1.72% P (ICP-MS).

G(2)-$(PPh_2)_2Pd(PPh_3)_2$, **29b**, Yield (ICP-MS): 73%,^{31}P CP/MAS NMR (80.99 MHz, solid-state) δ (ppm) 25.9*, 8.7, -27.4 ^{13}C CP/MAS NMR (50.32 MHz, solid-state) δ (ppm) 9.8, 26.8, 38.8, 51.5, 129.6, 172.5 (C=O). 0.96% Pd (ICP-MS) 1.39% P (ICP-MS).

G(3)-$(PPh_2)_2Pd(PPh_3)_2$, **29c**, Yield (ICP-MS): 75%, ^{31}P CP/MAS NMR (80.99 MHz, solid-state) δ (ppm) 27.7*, 13.6, -25.3 ^{13}C CP/MAS NMR (50.32 MHz, solid-state) δ (ppm) 10.41, 19.9, 27.1, 39.9, 44.6, 50.9, 128.3, 171.0 (C=O). 0.99% Pd (ICP-MS) 1.85% P (ICP-MS).

G(4)-$(PPh_2)_2Pd(PPh_3)_2$, **29d**, Yield (ICP-MS): 68%, ^{31}P CP/MAS NMR (80.99 MHz, solid-state) δ (ppm) 28.51*, 11.3, -29.0, ^{13}C CP/MAS NMR (50.32 MHz, solid-state) δ (ppm) 9.3, 20.0, 26.6, 38.8, 50.4, 127.8, 171.4 (C=O). 0.88% Pd (ICP-MS) 1.77% P (ICP-MS).

6.1.4 General experimental procedure for the hydroesterification of olefins with methanol:

To a 50 ml stainless steel autoclave equipped with a pressure gauge, a glass liner and a stirring bar were added 20 mg of a palladium containing catalyst (4.0 μmol Pd), a toluene:methanol mixture (1:1 v:v, 5ml), 25 eq. PPh_3, 35 eq. acid and 1000 eq. of olefin. The autoclave was flushed 3 times with carbon monoxide and pressurized to 150 psi and placed in a pre-heated oil bath at 115 °C. The reaction was left for 22 h under vigorous stirring and after cooling, ether (2ml) was added and the contents were filtered through 0.45 μm membrane filter and washed with ether. The conversion and the branched to linear ratio was determined by GC. Please refer to the tables for exact conditions of the optimization reactions.

6.2 General considerations: Section B:

Same as Section A.

6.2.1 Characterization.

X-ray powder diffraction (XRD) patterns were collected on a Scintag X_2 Advanced Diffraction System using Cu Kα radiation with 0.15418 nm wavelength, a step size of 0.02° 2θ, and a counting time per step of 4.0 s over a 0.7° < 2θ < 8° range.

Nitrogen adsorption experiments were performed at 77 K using a Coulter Omnisorp 100 gas analyzer. The specific surface area, S_{BET}, was determined from the linear part of the BET plot (P/P_0 = 0.05 – 0.15). The pore size distribution (PSD) was calculated from the adsorption branch using the KJS (Kruk, Jaroniec, Sayari) method.[4] The pore wall thickness (b) was calculated using b = a – w_{KJS} where a and w_{KJS} are the unit cell dimension and pore size, respectively.

Quantitative elemental analysis of N, C and H was carried out on a Carlo Erba EA1100 CHNS Elemental Analyzer.

^{13}C and ^{31}P CP/MAS solid-state NMR spectra were obtained on a Bruker ASX-200 instrument operating at 50.32 and 80.99 MHz, respectively with a spinning

rate of 5.0 – 6.0 kHz and with a contact time of 2 ms. $[MeP^{+}Ph_3]Br^{-}$ was used as internal standard. ^{29}Si CP/MAS solid-state NMR spectra were also recorded on the same instrument operating at 39.75 MHz with a spinning rate of 5.0 – 6.0 kHz and with a contact time of 2 ms.

Fourier transform infrared spectra were obtained using a Shimadzu FTIR-8400s spectrometer equipped with a Specac Silver Gate (ZnSe-crystal) single reflection attenuated total reflectance (ATR) system. Spectra were recorded from 600 cm^{-1}-4000 cm^{-1} using a resolution of 4 cm^{-1} and 150 scans.

Thermal analysis experiments were carried out on a combined DSC-TGA (SDT 2960) from TA Instruments. Simultaneous DSC-TGA measurements were obtained under air flow (100 ml min^{-1}) at a uniform heating rate of 20 °C min^{-1} from 25 °C to 1000 °C. Approximately 10-20 mg of sample was used for each experiment.

Phosphorus and rhodium ICP-MS was done by Galbraith laboratories, Knoxville TN.

6.2.2 General procedure for the hydroformylation reaction of 1-octene.

To a 300ml stainless steel, stirred tank Parr reactor equipped with a pressure

transducer and temperature control was added 50 mg of the rhodium containing catalyst (9.7 μmol Rh), cyclohexane (90ml), 1-octene (0.1 mol, 11.2 g) and m-xylene (11.2 g) as internal standard. The reactor was sealed and flushed 3 times with carbon monoxide and then pressurized to 500 psi with carbon monoxide. The reactor was then further pressurized to 1000 psi with hydrogen to give a 1:1 ratio of CO/H_2 with a total pressure of 1000 psi. The reactor was stirred at 600 rpm at 70 °C. Samples were routinely taken and analyzed by means of GC (with m-xylene as internal standard) and NMR.

6.2.3 Synthesis of large pore MCM-41.

Large pore MCM-41 samples were prepared by Dr. Yong Yang by the following procedure: In the presence of cetyltrimethylammonium bromide (CTAB) via the pore expansion method that was first reported by Khushalani *et al.*[1] and further developed by the group of Sayari.[2,3,4,5] The synthesis mixture had the following molar composition 1 SiO_2 : 0.33 TMAOH : 0.17 CTAB : 0.17 NH_4OH : 17 H_2O. Fumed Cab-O-Sil M-5 silica (36 g) was suspended in water (60 g) under vigorous stirring, and then 61.6 g of 25 wt % tetramethylammonium hydroxide (TMAOH) was added. Independently, 36.5 g of CTAB was dissolved in 65.6 g of water, and subsequently 11.7 g of 30 wt % NH_4OH was introduced. The mixtures containing the silica and CTAB were stirred together for ca. 30 min, then transferred into a Teflon-lined autoclave, and treated under autogenous pressure without stirring at 343 K for 3 days. The autoclave was transferred in another oven preheated at

150 °C and kept for 24 h. The obtained material was filtered, washed, dried, and calcined at 540 °C for 5 h under flowing air (6 L/h).

6.2.4 Propylamine Grafting.

This was performed in a three-necked round flask under nitrogen. Calcined silica (10 g) was first dried at 120 °C for 2 h to remove surface humidity and then added into 200 ml of boiling anhydrous toluene. After 1 h of stirring and refluxing, 4.82 g of 3-aminopropyltriethoxysilane was added to this mixture, which was then stirred and refluxed at 110 °C for 5 h. The white amine-functionalized silica was separated by filtration, thoroughly washed with toluene and dried in ambient condition.

LPMCM-41 S_{BET}= 585 m^2/g, Vp = 0.77 cm^3/g, *w* = 6.5 nm. *a*= 7.8 ± 0.1 nm *b* = 0.68. ^{29}Si CP/MAS NMR (39.75 MHz solid-state) δ (ppm) –110 (Q_4), -100.6 (Q_3)

LPMCM-41 G(0), **41.** Yield (EA/TGA): 98%. S_{BET}= 409 m^2/g, Vp = 0.51 cm^3/g, *w* = 5.6 nm. *a*= 7.8 ± 0.1 nm *b* = 2.25. ^{29}Si CP/MAS NMR (39.75 MHz solid-state) δ (ppm) –109.6 (Q_4), -101.0 (Q_3),-64.6 (T_2), -58.5 (T_1). ^{13}C CP/MAS NMR (50.32 MHz, solid-state) δ (ppm) 8.76, 25.34, 43.35. EA (%) N = 1.72, C = 4.59, H = 1.67. TGA mass loss (corrected %) = 7.00.

SBA-15. S_{BET}= 767 m^2/g, Vp = 0.82 cm^3/g, Vm = 0.11 cm^3/g *w* = 8.5 nm. ^{29}Si CP/MAS NMR (39.75 MHz solid-state) δ (ppm) –110.2 (Q_4), -101.2 (Q_3)

SBA-15-G(0). Yield (EA/TGA): 98% S_{BET}= 360 m^2/g, Vp = 0.50 cm^3/g, *w* = 7.7 nm. ^{29}Si CP/MAS NMR (39.75 MHz solid-state) δ (ppm) –108.3 (Q_4), -103.3 (Q_3),-65.9 (T_2), -59.3 (T_1). ^{13}C CP/MAS NMR (50.32 MHz, solid-state) δ (ppm) 8.85, 24.81, 43.16. EA (%) N = 1.65, C = 4.25, H = 1.86. TGA mass loss (corrected %) = 8.46.

Davisil G(0) Yield (EA/TGA): 75 %. S_{BET}= 230 m^2/g, Vp = 0.77 cm^3/g, *w* = 17.5 nm. ^{29}Si CP/MAS NMR (39.75 MHz solid-state) δ (ppm) –110.8 (Q_4), -101.4 (Q_3), -67.3 (T_2), -59.0 (T_1). ^{13}C CP/MAS NMR (50.32 MHz, solid-state) δ (ppm) 9.33, 25.42, 43.26. EA (%) N = 1.23, C = 3.12, H = 1.09. TGA mass loss (corrected %) = 3.84.

LPMCM-41 G(0) Yield (EA/TGA): 99.6%. S_{BET}= 612 m^2/g, Vp = 1.26 cm^3/g, *w* = 8.9 nm. ^{29}Si CP/MAS NMR (39.75 MHz solid-state) δ (ppm) –110.1 (Q_4), -101.3 (Q_3), -67.6 (T_2), -59.3 (T_1). ^{13}C CP/MAS NMR (50.32 MHz, solid-state) δ (ppm) 9.24, 25.60, 43.54. EA (%) N = 2.28, C = 6.33, H = 2.33. TGA mass loss (corrected %) = 9.61.

6.2.5. Preparation and characterization of dendrimers supported on mesoporous materials.

Polyamidoamine (PAMAM) dendrimers, up to the 3rd generation were prepared using a modified procedure based on literature methods, on pore expanded MCM-41.

Procedure:

Step1: G(0)-G(0.5) Aminopropyl functionalized LPMCM-41 (6.9 mmol NH_2, 6g) and methylacrylate (0.14 mol, 11.82g) were stirred at 50 °C in dry methanol (300ml) under a nitrogen atmosphere for 5 days. The mixture was cooled and filtered through a medium pore frit under nitrogen flow and washed with dry methanol (3 X 50 ml). The residual solvent was removed in vacuo, affording methyl propylaminopropionate functionalized LPMCM-41 in 98 % yield.

Step 2: G(0.5) - G(1). Methyl propylaminopropionate functionalized LPMCM-41 (0.13 mol ester groups, 6g) was added to ethylenediamine (65 ml) in dry methanol (300 ml) under a nitrogen atmosphere. The reaction was stirred for 5 days and the resulting G(1) dendrimer supported on LPMCM-41 was isolated by filtration through a medium pore frit. The solid was washed with dry methanol (3 X 50 ml). The residual solvent was removed in vacuo. The higher generations were prepared by repetition of step 1 and 2 with modification or the increasing

end groups. Dendrimers were synthesized on Davisil and LPMCM-41 by similar procedures, taking into account the amine loading on these supports.

LPMCM-41 series dendrimers.

LPMCM-41 G(0.5), **45.** Yield from G(0) (EA/TGA): 90 %. S_{BET}= 271 m^2/g, Vp = 0.34 cm^3/g, *w* = 5.0 nm. *a*= 7.8 ± 0.1 nm *b* = 2.97. ^{29}Si CP/MAS NMR (39.75 MHz solid-state) δ (ppm) –109.4 (Q_4), -101.4 (Q_3), -65.2 (T_2), -58.3 (T_1). ^{13}C CP/MAS NMR (50.32 MHz, solid-state) δ (ppm) 9.37, 20.87, 32.42, 50.07, 173.27(C=O). EA (%) N = 1.45, C = 11.49, H = 2.18. TGA mass loss (corrected %) = 20.94. IR (ATR, cm-1) 1740.

LPMCM-41 G(1) ,**42**. Yield from G(0) (EA/TGA): 77%. S_{BET}= 265 m^2/g, Vp = 0.33 cm^3/g, *w* = 5.0 nm. *a*= 7.8 ± 0.1 nm *b* = 2.79. ^{29}Si CP/MAS NMR (39.75 MHz solid-state) δ (ppm) –109.1 (Q_4), -100.7 (Q_3), -65.0 (T_2), -58.0 (T_1). ^{13}C CP/MAS NMR (50.32 MHz, solid-state) δ (ppm) 10.26, 21.62, 33.67, 40.69, 50.52, 173.23(C=O). EA (%) N = 4.03, C = 11.73, H = 2.60. TGA mass loss (corrected %) = 21.22. IR (ATR, cm-1) 3277, 2951, 2824, 1740, 1643, 1547.

LPMCM-41 G(1.5). Yield from G(0) (EA/TGA): 68 %. S_{BET}= 157 m^2/g, Vp = 0.18 cm^3/g, *w* = 4.3 nm. *a*= 7.8 ± 0.1 nm *b* = 3.49. ^{29}Si CP/MAS NMR (39.75 MHz solid-state) δ (ppm) –109.3 (Q_4), -101.1 (Q_3), -65.1 (T_2), -58.2 (T_1). ^{13}C CP/MAS NMR (50.32 MHz, solid-state) δ (ppm) 10.20, 22.23, 32.88, 50.61, 172.79 (C=O).

EA (%) N = 3.31, C = 16.55, H = 2.88. TGA mass loss (corrected %) = 30.81. IR (ATR, cm-1) 3277, 2951, 2824, 1740, 1643, 1547.

LPMCM-41 G(2), **43**. Yield from G(0) (EA/TGA): 62 %. S_{BET}= 145 m^2/g, Vp = 0.16 cm^3/g, *w* = 4.2 nm. *a*= 7.8 ± 0.1 nm *b* = 3.59. ^{29}Si CP/MAS NMR (39.75 MHz solid-state) δ (ppm) –109.4 (Q_4), -100.9 (Q_3), -65.2 (T_2), -58.1 (T_1). ^{13}C CP/MAS NMR (50.32 MHz, solid-state) δ (ppm) 10.41, 21.43, 38.75, 50.97, 173.67 (C=O). EA (%) N = 5.7, C = 16.98, H = 3.71. TGA mass loss (corrected %) = 30.63. IR (ATR, cm-1) 3277, 2951, 2824, 1643, 1547.

LPMCM-41 G(2.5). Yield from G(0) (EA/TGA): 58 %. S_{BET}= 0 m^2/g, Vp = 0 cm^3/g, *w* = - nm. *a*= 7.8 ± 0.1 nm *b* = -. ^{29}Si CP/MAS NMR (39.75 MHz solid-state) δ (ppm) –109.9 (Q_4), -101.2 (Q_3), -65.4 (T_2), -57.7 (T_1). ^{13}C CP/MAS NMR (50.32 MHz, solid-state) δ (ppm) 9.69, 20.68, 32.87, 50.43, 173.27 (C=O). EA (%) N = 5.28, C = 21.1, H = 3.96. TGA mass loss (corrected %) = 37.99. IR (ATR, cm-1) 3277, 2951, 2824, 1740, 1643, 1547.

LPMCM-41 G(3), **44**. Yield from G(0) (EA/TGA): 55 %. S_{BET}= 0 m^2/g, Vp = 0 cm^3/g, *w* = - nm. *a*= 7.8 ± 0.1 nm *b* = -nm. ^{29}Si CP/MAS NMR (39.75 MHz solid-state) δ (ppm) –109.3 (Q_4), -101.5 (Q_3), -65.2 (T_2), -58.1 (T_1). ^{13}C CP/MAS NMR (50.32 MHz, solid-state) δ (ppm) 10.58, 21.98, 39.45, 51.74, 173.51 (C=O). EA (%) N = 7.36, C = 19.59, H = 4.32. TGA mass loss (corrected %) = 37.95. IR (ATR, cm-1) 3277, 2951, 2824, 1643, 1547.

Davisil series dendrimers.

G(0.5), Yield from G(0) (EA/TGA): 82 %. S_{BET}= 169 m^2/g, Vp = 0.60 cm^3/g, *w* = 15.5 nm. ^{29}Si CP/MAS NMR (39.75 MHz solid-state) δ (ppm) –111.5 (Q_4), -101.2 (Q_3), -66.7 (T_2), -56.6 (T_1). ^{13}C CP/MAS NMR (50.32 MHz, solid-state) δ (ppm) 10.27, 20.71, 32.44, 49.84, 56.47, 173.22 (C=O). EA (%) N = 1.16, C = 8.93, H = 1.94. TGA mass loss (corrected %) = 14.48. IR (ATR, cm-1) 1740.

G(1), Yield from G(0) (EA/TGA): 76 %. S_{BET}= 163 m^2/g, Vp = 0.59 cm^3/g, *w* = 14.4 nm. ^{29}Si CP/MAS NMR (39.75 MHz solid-state) δ (ppm) –110.4 (Q_4), -101.5 (Q_3), -67.0 (T_2), -60.0 (T_1). ^{13}C CP/MAS NMR (50.32 MHz, solid-state) δ (ppm) 11.05, 21.64, 35.14, 40.94, 49.96, 173.40 (C=O). EA (%) N = 3.22, C = 9.76, H = 2.15. TGA mass loss (corrected %) = 15.83. IR (ATR, cm-1) 3277, 2951, 2824, 1643, 1547.

G(1.5), Yield from G(0) (EA/TGA): 63 %. S_{BET}= 133 m^2/g, Vp = 0.52 cm^3/g, *w* = 13.4 nm. ^{29}Si CP/MAS NMR (39.75 MHz solid-state) δ (ppm) –110.8 (Q_4), -101.2 (Q_3), -65.3 (T_2), -57.9 (T_1). ^{13}C CP/MAS NMR (50.32 MHz, solid-state) δ (ppm) 10.64, 21.24, 32.61, 50.51, 172.96 (C=O). EA (%) N = 2.90, C = 13.51, H = 2.51. TGA mass loss (corrected %) = 23.35. IR (ATR, cm-1) 3277, 2951, 2824, 1740, 1643, 1547.

G(2), Yield from G(0) (EA/TGA): 58 %. S_{BET}= 132 m^2/g, Vp = 0.50 cm^3/g, *w* = 13.5 nm. ^{29}Si CP/MAS NMR (39.75 MHz solid-state) δ (ppm) –110.6 (Q_4), -101.4 (Q_3), -66.5 (T_2), -58.9 (T_1). ^{13}C CP/MAS NMR (50.32 MHz, solid-state) δ (ppm) 11.78, 22.47, 38.73, 50.49, 172.93 (C=O). EA (%) N = 4.67, C = 13.74, H = 2.70. TGA mass loss (corrected %) = 23.77. IR (ATR, cm-1) 3277, 2951, 2824, 1643, 1547.

G(2.5), Yield from G(0) (EA/TGA): 54 %. S_{BET}= 130 m^2/g, Vp = 0.48 cm^3/g, *w* = 11.1 nm. ^{29}Si CP/MAS NMR (39.75 MHz solid-state) δ (ppm) –110.6 (Q_4), -103.1 (Q_3), -65.2 (T_2), -58.1 (T_1). ^{13}C CP/MAS NMR (50.32 MHz, solid-state) δ (ppm) 11.30, 19.98, 32.57, 50.19, 172.78 (C=O). EA (%) N = 4.20, C = 17.08, H = 3.03. TGA mass loss (corrected %) = 30.96. IR (ATR, cm-1) 3277, 2951, 2824, 1740, 1643, 1547.

G(3) Yield from G(0) (EA/TGA): 51 %. S_{BET}= 126 m^2/g, Vp = 0.50 cm^3/g, *w* = 11.9 nm. ^{29}Si CP/MAS NMR (39.75 MHz solid-state) δ (ppm) –111.1 (Q_4), -101.9 (Q_3), -65.8 (T_2), -58.7 (T_1). ^{13}C CP/MAS NMR (50.32 MHz, solid-state) δ (ppm) 10.09, 23.02, 38.04, 51.56, 173.91 (C=O). EA (%) N = 5.93, C = 17.00, H = 3.23. TGA mass loss (corrected %) = 31.04. IR (ATR, cm-1) 3277, 2951, 2824, 1643, 1547.

PEMCM-41 series dendrimers.

G(0.5), **26.** Yield from G(0) (EA/TGA): 96 %. S_{BET}= 457 m^2/g, Vp = 0.88 cm^3/g, *w* = 8.1 nm. ^{29}Si CP/MAS NMR (39.75 MHz solid-state) δ (ppm) –109.8 (Q_4), -102.5 (Q_3), -66.1 (T_2), -57.7 (T_1). ^{13}C CP/MAS NMR (50.32 MHz, solid-state) δ (ppm) 8.81, 20.76, 32.57, 49.86, 56,39, 172.75. EA (%) N = 1.89, C = 15.19, H = 2.86. TGA mass loss (corrected %) = 28.02. IR (ATR, cm-1) 1740.

G(1) ,**27.** Yield from G(0) (EA/TGA): 86 %. S_{BET}= 385 m^2/g, Vp = 0.77 cm^3/g, *w* = 7.7 nm. ^{29}Si CP/MAS NMR (39.75 MHz solid-state) δ (ppm) –109.8 (Q_4), -101.3 (Q_3), -65.6 (T_2), -58.4 (T_1). ^{13}C CP/MAS NMR (50.32 MHz, solid-state) δ (ppm) 11.81, 22.38, 41.56, 51.18, 57.76, 173.38 (C=O). EA (%) N = 7.42, C = 16.28, H = 4.11. TGA mass loss (corrected %) = 29.27. IR (ATR, cm-1) 3277, 2951, 2824, 1643, 1547.

G(1.5), Yield from G(0) (EA/TGA): 81 %. S_{BET}= 286 m^2/g, Vp = 0.54 cm^3/g, *w* = 7.0 nm. ^{29}Si CP/MAS NMR (39.75 MHz solid-state) δ (ppm) –109.8 (Q_4), -102.2 (Q_3), -64.7 (T_2), -58.5 (T_1). ^{13}C CP/MAS NMR (50.32 MHz, solid-state) δ (ppm) 9.77, 20.73, 32.65, 50.41, 172.73. EA (%) N = 4.91, C = 22.83, H = 4.06. TGA mass loss (corrected %) = 43.31. IR (ATR, cm-1) 3277, 2951, 2824, 1740, 1643, 1547.

G(2), Yield from G(0) (EA/TGA): 73%. S_{BET}= 215 m^2/g, Vp = 0.40 cm^3/g, *w* = 6.8 nm. ^{29}Si CP/MAS NMR (39.75 MHz solid-state) δ (ppm) –109.2 (Q_4), -100.5 (Q_3),

-65.1 (T_2), -60.4 (T_1). ^{13}C CP/MAS NMR (50.32 MHz, solid-state) δ (ppm) 11.34, 21.11, 41.71, 51.39, 173.50 (C=O). EA (%) N = 9.90, C = 22.58, H = 5.28. TGA mass loss (corrected %) = 41.63. IR (ATR, cm-1) 3277, 2951, 2824, 1643, 1547.

G(2.5), Yield from G(0) (EA/TGA): 76 %. S_{BET}= 119 m^2/g, Vp = 0.20 cm^3/g, *w* = 5.8 nm. ^{29}Si CP/MAS NMR (39.75 MHz solid-state) δ (ppm) –110.6 (Q_4), -102.4 (Q_3), -64.5 (T_2), -57.9 (T_1). ^{13}C CP/MAS NMR (50.32 MHz, solid-state) δ (ppm) 9.80, 20.75, 33.21, 51.01, 173.08. EA (%) N = 7.42, C = 28.15, H = 5.13. TGA mass loss (corrected %) = 54.96. IR (ATR, cm-1) 3277, 2951, 2824, 1740, 1643, 1547.

G(3), Yield from G(0) (EA/TGA): 71 %. S_{BET}= 13 m^2/g, Vp = 0.03 cm^3/g, *w* = 5.6 nm. ^{29}Si CP/MAS NMR (39.75 MHz solid-state) δ (ppm) –110.2 (Q_4), -101.5 (Q_3), -65.3 (T_2), -58.8 (T_1). ^{13}C CP/MAS NMR (50.32 MHz, solid-state) δ (ppm) 43.01, 51.61, 173.82 (C=O). EA (%) N = 11.59, C = 27.11, H = 5.90. TGA mass loss (corrected %) = 53.49. IR (ATR, cm-1) 3277, 2951, 2824, 1643, 1547.

G(3.5), Yield from G(0) (EA/TGA): 72 %. S_{BET}= 0 m^2/g, Vp = 0 cm^3/g, *w* = - nm. ^{29}Si CP/MAS NMR (39.75 MHz solid-state) δ (ppm) –110.3 (Q_4), -102.2 (Q_3), -64.1 (T_2), -58.2 (T_1). ^{13}C CP/MAS NMR (50.32 MHz, solid-state) δ (ppm) 11.02, 22.24, 38.96, 51.63, 173.00. EA (%) N = 9,59, C = 31.28, H = 5.83. TGA mass

loss (corrected %) = 60.97. IR (ATR, cm-1) 3277, 2951, 2824, 1740, 1643, 1547.

G(4), Yield from G(0) (EA/TGA): 71 %. S_{BET}= 0 m^2/g, Vp = 0 cm^3/g, *w* = - nm. ^{29}Si CP/MAS NMR (39.75 MHz solid-state) δ (ppm) –110.5 (Q_4), -101.5 (Q_3), -65.3 (T_2), -58.8 (T_1). ^{13}C CP/MAS NMR (50.32 MHz, solid-state) δ (ppm) 38.05, 51.15, 173.15 (C=O). EA (%) N = 13.03, C = 32.03, H = 6.50. TGA mass loss (corrected %) = 61.59. IR (ATR, cm-1) 3277, 2951, 2824, 1643, 1547.

6.2.6 Phosphinomethylation of dendrimers.

The dendrimers were phosphinomethylated using diphenylphosphine and paraformaldehyde under modified literature methods.[6] The double phosphinomethylation of the terminal amine groups of the dendrimers was achieved by reacting the dendrimers with diphenylphosphinomethanol prepared in situ from diphenylphosphine and paraformaldehyde in toluene (110 °C, 48 h). The resulting phosphinomethylated dendrimers were characterized by solid state ^{31}P and ^{13}C NMR, e g a chemical shift of –27 ppm in the ^{31}P NMR spectrum compares well with previously reported systems.

Procedure: To a stirred suspension of paraformaldehyde (0.9 eq, 1.36g) in dry toluene (20ml) under argon was added diphenylphosphine (0.0504 mol, 10 g). The resulting mixture was heated to reflux (110 °C) and stirred for 2h until the mixture became clear. At this stage aminopropyl functionalized MCM-41 (2.9

mmol NH_2, 2.5g) was added and the resulting suspension was stirred under argon at reflux (110 °C) for 48 h. The phosphinomethylated aminopropyl functionalized MCM-41 was isolated by filtration through a medium pore frit under a flow of argon and the resulting light yellow solid was washed with toluene (2 X 20 ml). The residual solvent was removed in vacuo. The procedure was modified for the higher generations, taking into account the amount of end groups for each generation. The same procedure was used for the Davisil series dendrimers.

LPMCM-41 series dendrimers.

G(0), ^{31}P CP/MAS NMR (80.99 MHz, solid-state) δ (ppm) –28.44. ^{13}C CP/MAS NMR (50.32 MHz, solid-state) δ (ppm) 9.68, 20.14, 60.25, 129.79. ^{29}Si CP/MAS NMR (39.75 MHz solid-state) δ (ppm) –109.8 (Q_4), -101.1 (Q_3), -64.6 (T_2), -58.1 (T_1). 2.41% P (ICP-MS)

G(1), ^{31}P CP/MAS NMR (80.99 MHz, solid-state) δ (ppm) –28.44. ^{13}C CP/MAS NMR (50.32 MHz, solid-state) δ (ppm) 9.81, 20.48, 51.77, 56.97, 131.11, 172.8 (C=O). ^{29}Si CP/MAS NMR (39.75 MHz solid-state) δ (ppm) –110.1 (Q_4), -101.1 (Q_3), -64.6 (T_2), -58.2 (T_1). 1.90% P (ICP-MS)

G(2), ^{31}P CP/MAS NMR (80.99 MHz, solid-state) δ (ppm) –28.04. ^{13}C CP/MAS NMR (50.32 MHz, solid-state) δ (ppm) 10.08, 20.10, 37.15, 50.56, 130.04, 172.15 (C=O). ^{29}Si CP/MAS NMR (39.75 MHz solid-state) δ (ppm) –108.6 (Q_4), -101.4 (Q_3), -64.8 (T_2), -58.3 (T_1). 2.12% P (ICP-MS)

G(3), ^{31}P CP/MAS NMR (80.99 MHz, solid-state) δ (ppm) –28.0. ^{13}C CP/MAS NMR (50.32 MHz, solid-state) δ (ppm) -. ^{29}Si CP/MAS NMR (39.75 MHz solid-state) δ (ppm) –110.2 (Q_4), -100.0 (Q_3), -65.7 (T_2), -58.3 (T_1). 0.37 % P (ICP-MS)

Davisil series dendrimers.

G(0), ^{31}P CP/MAS NMR (80.99 MHz, solid-state) δ (ppm) –28.0. ^{13}C CP/MAS NMR (50.32 MHz, solid-state) δ (ppm) 10.11, 19.64, 42.27, 60.45, 128.95, 131.0. ^{29}Si CP/MAS NMR (39.75 MHz solid-state) δ (ppm) –110.2 (Q_4), -101.1 (Q_3), -67.7 (T_2), -57.7 (T_1). 1.99% P (ICP-MS)

G(1), ^{31}P CP/MAS NMR (80.99 MHz, solid-state) δ (ppm) –27.6. ^{13}C CP/MAS NMR (50.32 MHz, solid-state) δ (ppm) 10.77, 19.10, 43.90, 60.50, 128.97, 171.08 (C=O). ^{29}Si CP/MAS NMR (39.75 MHz solid-state) δ (ppm) –110.1 (Q_4), -101.2 (Q_3), -67.5 (T_2), -57.8(T_1). 1.86% P (ICP-MS)

G(2), ^{31}P CP/MAS NMR (80.99 MHz, solid-state) δ (ppm) –27.67. ^{13}C CP/MAS NMR (50.32 MHz, solid-state) δ (ppm) 10.14, 21.83, 27.48, 38.00, 50.52, 128.52, 171.79 (C=O). ^{29}Si CP/MAS NMR (39.75 MHz solid-state) δ (ppm) –110.5 (Q_4), -101.5 (Q_3), -67.6 (T_2), -56.7(T_1). 1.99% P (ICP-MS)

G(3), ^{31}P CP/MAS NMR (80.99 MHz, solid-state) δ (ppm) –27.78. ^{13}C CP/MAS NMR (50.32 MHz, solid-state) δ (ppm) 10.16, 29.48, 39.40, 51.64, 129.55, 172.69 (C=O). ^{29}Si CP/MAS NMR (39.75 MHz solid-state) δ (ppm) –110.0 (Q_4), -102.0

(Q_3), -65.3 (T_2), -59.5 (T_1). 2.87% P (ICP-MS)

6.2.7 Complexation of the phosphinomethylated dendrimers.

The phosphinomethylated dendrimers were readily complexed on treatment with the appropriate rhodium complexes in toluene (rt., 1-2h under argon). The support would turn yellow and decolorization of the supernatant solvent was used as an indication of the extent of complexation.

Procedure: Phosphinomethylated aminopropyl functionalized LPMCM-41 (0.82 mmol PPh_2, 1g) and $[Rh(COD)Cl]_2$ (0.204 mmol, 0.1006 g) were stirred under argon for 2h in dry toluene (20ml). The mixture was filtered through a medium pore frit under argon flow and washed with toluene (2 X 20 ml). The residual solvent was removed in vacuo to yield the product. The complex is stored under argon. Similar procedures were used for the higher generations taking into account the phosphine content of the phosphomethylated dendrimers. Similar procedures were also used for the preparation of the Davisil series dendrimers.

LPMCM-41 series dendrimers.

G(0.), Rh, Yield (TGA and ICP-MS): 43 %, ^{31}P CP/MAS NMR (80.99 MHz, solid-state) δ (ppm) –28.20, +24.05. ^{13}C CP/MAS NMR (50.32 MHz, solid-state) δ (ppm) 9.99, 21.00, 54.99, 59.63, 130.27. ^{29}Si CP/MAS NMR (39.75 MHz solid-state) δ (ppm) –109.55 (Q_4), -101.6 (Q_3), -65.88 (T_2), -52.05 (T_1). 1.65 % P, 1.81 % Rh (ICP-MS)

G(1), Rh, Yield (TGA and ICP-MS): 10 %, ^{31}P CP/MAS NMR (80.99 MHz, solid-state) δ (ppm) –27.90, +26.96. ^{13}C CP/MAS NMR (50.32 MHz, solid-state) δ (ppm) 10.82, 21.49, 34.69, 52.37, 129.60, 170.88 (C=O). ^{29}Si CP/MAS NMR (39.75 MHz solid-state) δ (ppm) –109.8 (Q_4), -101.4 (Q_3), -65. 8 (T_2), -57.6 (T_1). 2.02 % P, 0.83 % Rh (ICP-MS).

G(2), Rh, Yield (TGA and ICP-MS): 31 %, ^{31}P CP/MAS NMR (80.99 MHz, solid-state) δ (ppm) –27.31, +28.15. ^{13}C CP/MAS NMR (50.32 MHz, solid-state) δ (ppm) 10.44, 20.97, 36.42, 44.88, 51.17, 129.07, 172.42 (C=O). ^{29}Si CP/MAS NMR (39.75 MHz solid-state) δ (ppm) –110.2 (Q_4), -100.6 (Q_3), -65. 6 (T_2), -57.7 (T_1). 1.812 % P, 0.619 % Rh (ICP-MS).

Davisil series dendrimers.

G(0) Rh, Yield (TGA and ICP-MS): 40 %, ^{31}P CP/MAS NMR (80.99 MHz, solid-state) δ (ppm) +24.9. ^{13}C CP/MAS NMR (50.32 MHz, solid-state) δ (ppm) 11.19, 17.79, 42.36, 59.52, 131.49. ^{29}Si CP/MAS NMR (39.75 MHz solid-state) δ (ppm) –110.3 (Q_4), -101.5 (Q_3), -65.9 (T_2), -58.1 (T_1). 2.43 % P, 1.70 % Rh (ICP-MS)

G(1) Rh , Yield (TGA and ICP-MS): 67 %, ^{31}P CP/MAS NMR (80.99 MHz, solid-state) δ (ppm) –27.8,+24.8. ^{13}C CP/MAS NMR (50.32 MHz, solid-state) δ (ppm) 10.22, 21.31, 30.11, 39.91, 52.40, 130.47, 171.55 (C=O). ^{29}Si CP/MAS NMR

(39.75 MHz solid-state) δ (ppm) –110.3 (Q_4), -101.4 (Q_3), -66.0 (T_2), -58.4 (T_1). 1.50 % P, 2.87 % Rh (ICP-MS)

G(2) Rh , Yield (TGA and ICP-MS): 80 %, ^{31}P CP/MAS NMR (80.99 MHz, solid-state) δ (ppm) –25.4,+24.2. ^{13}C CP/MAS NMR (50.32 MHz, solid-state) δ (ppm) 10.55, 21.35, 38.14, 50.95, 129.94, 172.15 (C=O). ^{29}Si CP/MAS NMR (39.75 MHz solid-state) δ (ppm) –110.4 (Q_4), -101.6 (Q_3), -66.9 (T_2), -59.0 (T_1). 2.02 % P, 3.30 % Rh (ICP-MS)

G(3) Rh , Yield (TGA and ICP-MS): 45 %, ^{31}P CP/MAS NMR (80.99 MHz, solid-state) δ (ppm) –25.96,+24.8. ^{13}C CP/MAS NMR (50.32 MHz, solid-state) δ (ppm) 10.60, 30.54, 36. 43, 50.55, 130.17, 173.18 (C=O). ^{29}Si CP/MAS NMR (39.75 MHz solid-state) δ (ppm) –110.2 (Q_4), -101.7 (Q_3), -61.6 (T_2), -59.4 (T_1). 2.10 % P, 2.03 % Rh (ICP-MS)

6.3 References for Chapter 6:

1. Khushalani, D., Kuperman, A., Ozin, G. A., Tanaka, K., Garces, J., Olken, J. J., Coombs, N., *Adv. Mater.* **1995**, *7*, 842.

2. Sayari, A., Liu, P., Kruk, M., Jaroniec, M., *Chem. Mater.* **1997**, *9*, 2499.

3. Kruk, M., Jaroniec, M., Sayari, A., *J. Phys. Chem. B.* **1999**, *103*, 4590.

4. Kruk, M., Jaroniec, M., Sayari, A., *Langmuir* **1997**, *13*, 6267.

5. Kruk, M., Jaroniec, M., Sayari, A., *Microporous Mesoporous Mater.* **1997**, *27*, 217.

6. Reetz, M. T., Lohmer, G., Schwickardi, R., *Angew. Chem. Int. Ed. Engl.* **1997**, *36*, 1526.

Chapter 7. *Concluding Remarks*

Polyamidoamine (PAMAM) dendrimers were grown on various supports including two different mesoporous amorphous silicas and two periodic mesoporous silicas. C_6-PAMAM dendrimers up to the fourth generation were synthesized on commercial aminopropyl silica gel (7.0 nm) and C_2-PAMAM dendrimers up to the third generation were grown for the first time inside the channels of LPMCM-41 (6.5 nm) and on the outside surface of Davisil (18 nm) silica. C_2-PAMAM dendrimers up to the fourth generation were also grown for the first time inside the channels of PEMCM-41 (10.6 nm) silica. Various methods (^{13}C CP/MAS NMR, ^{31}P CP/MAS NMR, ICP, TGA and nitrogen adsorption methods) were used to characterize the silica supported C_6-PAMAM dendrimers and the metal complexes attached to the periphery of the dendrimers. All the quantitative methods showed average yields per reaction in excess of 97%. For the C_2-PAMAM dendrimers all the above mentioned characterization methods were also used and ^{29}Si CP/MAS NMR, DSC, EA and FTIR were added to complement the other methods.

For the C_6-PAMAM dendrimers the nitrogen adsorption study revealed that the BET surface area of the support significantly decreases with increase in generation from around 300 m^2/g for G(0) to around 150 m^2/g for G(4). The pore volume also decreases from 0.70 cm^3/g at G(0) to 0.33 cm^3/g at G(4). This is taken as evidence that significant dendrimer growth takes place inside the pores

of the support.

The C_6-PAMAM dendrimers were phosphomethylated and complexed with palladium and these complexes were used as new recyclable catalysts for the hydroesterification of olefins. The catalysts show high activity for styrene derivatives and linear long chain olefins (TON of up to 1200) and favor the linear product of the reaction even for styrene. The catalysts can be recycled up to 6 times by simple filtration in air.

For the C_2-PAMAM dendrimers supported on LPMCM-41 the nitrogen adsorption study revealed that the third generation dendrimer almost completely filled the pore system, whereas the generation three dendrimers on the Davisil support still adsorb nitrogen and are less affected by steric interactions than the dendrimers on LPMCM-41. The dendrimers on the PEMCM-41 reach pore saturation at one generation higher (G(4)) than LPMCM-41, but the overall yield for these dendrimers are significantly higher than anticipated (71% at G(4)). This translates to a yield per reaction of over 99%. Dendrimers of generations 0, 1 and 2 on LPMCM-41 were phosphinomethylated and complexed with rhodium and dendrimers of generations 0, 1, 2 and 3 on Davisil were phosphinomethylated and complexed with rhodium.

It is clear that the pore geometry is very important in determining the size of the dendrimer that can be constructed on the support. The MCM-41 supports, where

the dendrimers are grown on the inside surface are subject to significant steric encumbrance. The dendrimers grown on the Davisil support are less prone to steric encumbrance, and dendrimers up to generation three can be easily constructed, phosphomethylated and complexed. Although the PEMCM-41 has significantly larger pores, the threshold in the growth of the dendrimers is reached at G(4) instead of G(3) for the LPMCM-41. This was disappointing and the PEMCM-41 was not phosphomethylated or complexed.

The generations 0 and 1 rhodium complexed phosphomethylated C_2-PAMAM dendrimers supported on LPMCM-41 are excellent recyclable catalysts for olefin hydroformylation. A turnover frequency (TOF) as high as 1800 h^{-1} was observed for the hydroformylation of 1-octene at 70 °C.

Generations 0, 1, 2 and 3 rhodium complexed phosphomethylated C_2-PAMAM dendrimers supported on Davisil showed excellent activity for the hydroformylation reaction, with a maximum turnover frequency of 1700 h^{-1} observed for the hydroformylation of 1-octene. The G(1) catalyst was identified as the most active at 50 % conversion. The Davisil supported catalysts could unfortunately not be recycled.

The characterization results for the C_6-PAMAM and C_2-PAMAM dendrimers show that the size of the dendrimer, the pore geometry and the surface area greatly affect the success of the dendrimer synthesis. These factors then also affect the

phosphomethylation, complexation and the activity of the catalysts. The characterization methods developed in this thesis allow for the evaluation of supports for various grafting reactions, and could be used to explain why some grafting experiments fail or give less than optimum results.

Claims to Original Research

1. The first synthesis and comprehensive characterization of a series of recyclable, supported, polyamidoamine (PAMAM) dendrimer-based catalysts for the hydroesterification reaction of olefins.

2. The first synthesis and comprehensive characterization of PAMAM dendrimers inside the channels of periodic mesoporous materials (both LPMCM-41 and PEMCM-41) and on the outside surface of large pore amorphous silica (Davisl)

3. The first synthesis of rhodium catalysts based on these PAMAM dendrimers supported inside the channels of mesoporous materials and on the outside surface of large pore amorphous silica, and their use as, in some cases recyclable catalysts for the hydroformylation of olefins.

List of publications:

1. Reynhardt, J. P. K.; Alper, H., *Hydroesterification Reactions with Palladium-Complexed PAMAM-Dendrimers Immobilized on Silica*, *J. Org. Chem.* **2003**, *68*, 8353.

2. Reynhardt, J. P. K., Yang Y., Sayari, A., Alper, H., *Periodic Mesoporous, Silica Supported Recyclable Rhodium Complexed Dendrimer Catalysts, Chem. Mater,* **2004**,.16(21), 4095.

3. Reynhardt, J. P. K., Yang Y., Sayari, A., Alper, H., *Rhodium Complexed C_2-PAMAM Dendrimers Supported on Davisil as Catalysts for the Hydroformylation of Olefins*, Submitted to *Advanced Synthesis and Catalysis,* in press.

4. Reynhardt, J. P. K., Yang Y., Sayari, A., Alper, H., *C_2-PAMAM Dendrimers Prepared inside the channels of Pore Expanded Periodic Mesoporous Silica*, Submitted to *Advanced Materials,* in press.